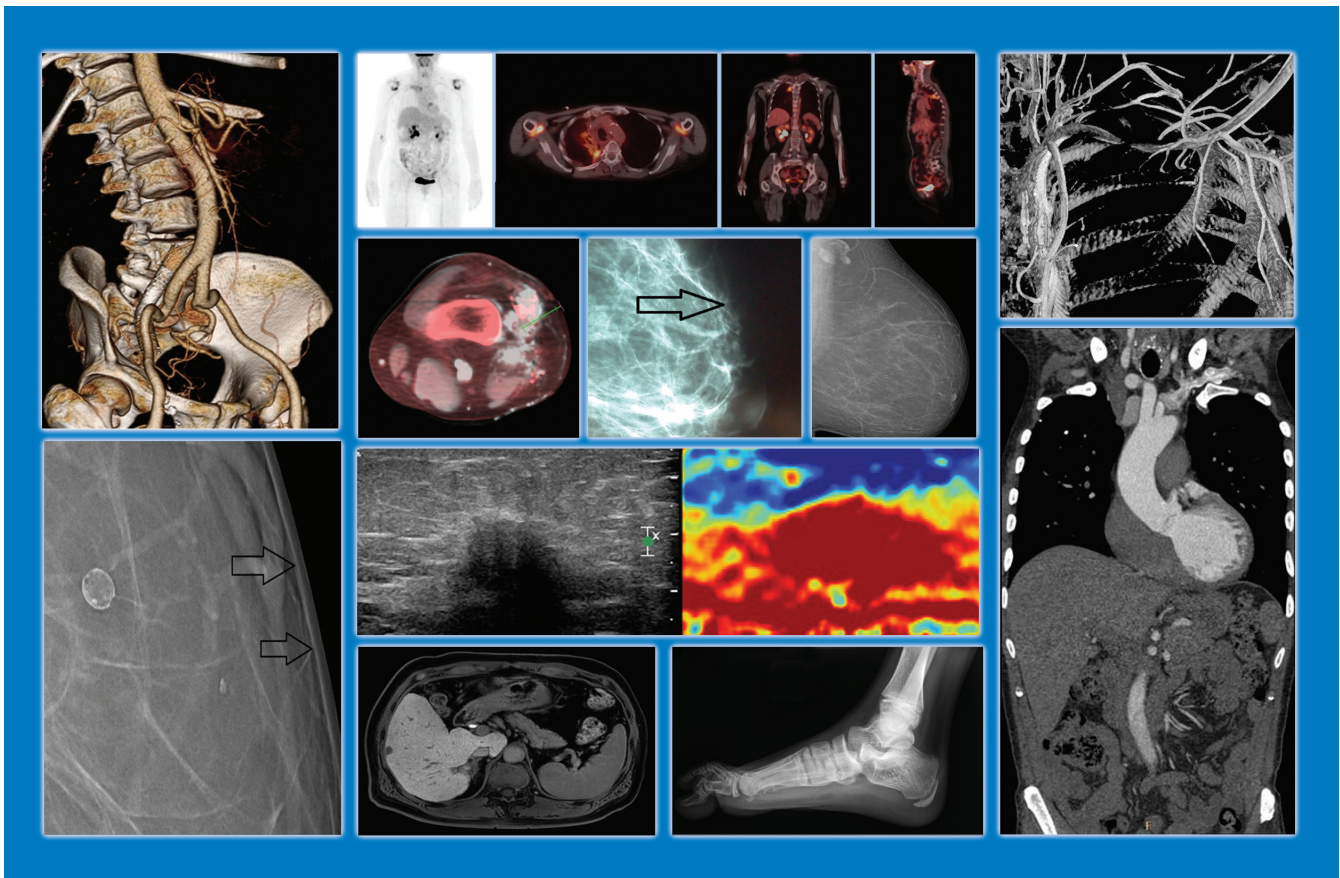


SUPPLEMENT TO
DECEMBER 2012

APPLIED RADIOLOGY®

THE JOURNAL OF PRACTICAL MEDICAL IMAGING AND MANAGEMENT



Transforming Patient Care Through Patient Focus,
Improved Productivity and Improved Clinical Outcomes

Sponsored by

PHILIPS



Strategies, solutions, success.

Healthcare is in a state of transformation. Some only see the challenges. Philips Healthcare Consulting sees the opportunities. We have helped many clients achieve improved performance and can do the same with you. Our consultants can help you drive growth, solve complex workflow challenges, and deliver a quality healthcare experience. We provide objective, expert management advice and work with you to plan, create, and implement comprehensive strategies for managing ongoing change. We draw on our extensive real-world experiences everyday and can help you develop the strategic and operational initiatives you need to succeed. Let us help you achieve new levels of financial and operational performance, visit www.philips.com/healthcareconsulting.

PHILIPS
sense and simplicity

Low dose and high quality: A delicate balance



Larry Dentice

Better patient care is one of the driving forces behind what we do.

Low radiation dose and high diagnostic image quality—it's the delicate balance we all try to strike in radiology to provide the best possible care and improve patient outcomes. At Philips, we continue to make advances in establishing just the right balance in all of our products as we carry on our Imaging 2.0 vision, based on clinical integration and collaboration, patient focus, and improved economic value.

We incorporate the principle of keeping radiation dose as low as reasonably achievable in every product we create. A prime example is our BrightView XCT, which provides high-quality images with less radiation dose than computed tomography (CT) scanners that lack Philips' dose-reduction tools, while boosting reporting speed and accuracy. Additionally, our innovative iDose⁴ iterative reconstruction technique for Philips Ingenuity CT systems allows radiologists to manage dose without sacrificing image quality. Even for electrophysiology and angio procedures, which traditionally require high levels of radiation, Philips is constantly looking at ways to develop low-dose interventional X-ray systems that advance patient care. We are incredibly excited about these products and how they are advancing the science of achieving the ideal balance of low radiation dose and high diagnostic image quality.

At the same time, there is increasing pressure in the industry to improve productivity and keep healthcare costs down. Increased workflow demands on clinicians require the ability to diagnose and collaborate virtually anytime, anywhere. That's the principle behind Philips' IntelliSpace Portal, a powerful thin-client solution for advanced image review and analysis offering a clinical solution that's multi-specialty, multi-modality and multi-vendor—and accessible through iPad[®]*, laptop or smartphone*.

Better patient care is one of the driving forces behind what we do across the healthcare field, and these technologies offer enhanced diagnostic confidence to deliver improved care. The following pages detail nine perspectives from experienced clinicians in various specialties, reflecting how they are achieving better patient care in their specialty areas. Our hope is that their insights will inspire you with new ideas about the exciting possibilities within our field.

We would like to extend Philips' thanks for the collaboration and insights of all the physicians included in this special supplement to *Applied Radiology* as we work together to create the future of healthcare and save lives.

Larry Dentice
Senior Vice President, Imaging Systems Sales and Marketing
Philips Healthcare North America

**Note: Images are not for diagnosis except when using cleared software for mobile application.*

Introduction

- 1.....Low dose and high quality: A delicate balance
Larry Dentice

DXR

- 9.....The impact of digital radiography on the pediatric patient
Richard Towbin, MD, and James Owen
- 12.....Clinical Case: Isolated non-osseous navicular-medial cuneiform tarsal coalition
Seth Vatsky, MD, and Richard Towbin, MD

IXR

- 14.....3D imaging in the angiography suite advances interventional patient care
David Siegel, MD, FSIR
- 18.....Clinical Case: Treating recurrent pelvic congestion
David Siegel, MD, FSIR

Ambient Experience

- 20.....Ambient Experience for PET/CT: Reducing patient anxiety, improving the clinical process
Joseph Jalkiewicz

MR

- 22.....3T MR imaging protocol for characterization of renal masses
Gaurav Khatri, MD, and Ivan M. Pedrosa, MD
- 27.....Clinical Case: Metastatic workup of a morbidly obese patient with colorectal cancer
Julia Grossman, MD, Gaurav Khatri, MD, and Ivan M. Pedrosa, MD

IntelliSpace Portal

- 30.....IntelliSpace streamlines the continuum of care
Cristen Bolan

PET

- 32.....Striking a balance in PET imaging transforms patient care
Medhat M. Osman, MD, PhD
- 36.....Clinical Case: Recurrent lymphoma in the left acetabulum
Razi Muzaffar, DO, and Medhat M. Osman, MD, PhD

SPECT

- 39.....Low-dose, high-quality SPECT/CT imaging transforms patient care
Medhat M. Osman, MD, PhD
- 46.....Clinical Case: Osteomyelitis with associated fracture in the toe as seen on high-resolution SPECT/CT
Razi Muzaffar, DO, and Medhat M. Osman, MD, PhD

Ultrasound

- 49.....Improving patient outcomes with ultrasound elastography
Richard G. Barr, MD, PhD, FACR
- 53.....Clinical Case: Elastography in evaluation of musculoskeletal abnormalities
Richard G. Barr, MD, PhD, FACR

Women's Health

- 56.....Transformation from film-screen to MicroDose digital mammography: Selection challenges, opportunity, and value
Raymond Tu, MD, Riad Charafeddine, MD, Theodore Williams, MA, RT(R), and Steven Rothenberg
- 60.....Clinical Case: Breast cyst and dermal calcification
Raymond Tu, MD

APPLIED RADIOLOGY

THE JOURNAL OF PRACTICAL MEDICAL IMAGING AND MANAGEMENT

Publisher

O. Oliver Anderson

Associate Publisher

Kieran Anderson

Executive Editor

Cristen Bolan

Contributing Editor

Joseph Jalkiewicz

Art Director and Production

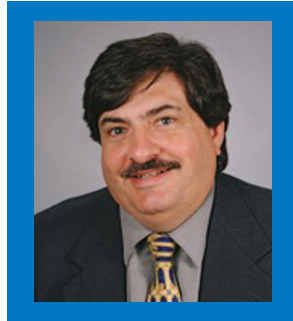
Barbara A. Shopiro

Applied Radiology and this supplement, *Transforming Patient Care Through Patient Focus, Improved Productivity and Improved Clinical Outcomes*, are published by Anderson Publishing, Ltd. The journal does not warrant the expertise of any author in a particular field, nor is it responsible for any statements by such authors. The opinions expressed in this supplement are those of the authors. They do not imply endorsement of advertised products and do not necessarily reflect the opinions or recommendations of our sponsors or the editors and staff of *Applied Radiology*.

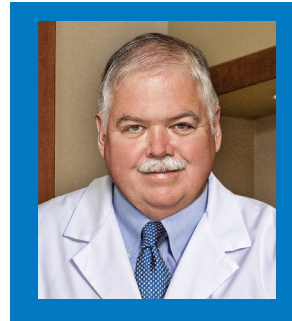
Copyright © 2012 by
Anderson Publishing, Ltd.,
180 Glenside Avenue,
Scotch Plains, NJ 07076.

All rights reserved.

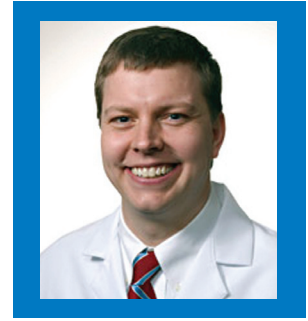
Contributing Faculty



Richard G. Barr, MD, PhD, FACR, Professor of Radiology, Northeastern Ohio Medical University, and a Diagnostic Radiologist at Radiology Consultants Inc., Youngstown, OH



Bruce A. Cross, MD, Radiation Oncologist, Sparks Health System, Fort Smith, AR



Andrew J. Mullinix, MD, Diagnostic Radiologist, Franciscan St. Francis Health, Indianapolis, IN



Medhat M. Osman, MD, PhD, Program Director of the Division of Nuclear Medicine, Department of Radiology, Saint Louis University Hospital, St. Louis, MO



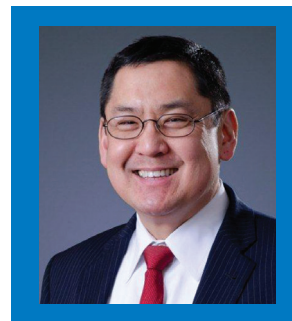
Ivan M. Pedrosa, MD, Chief-of-MRI, Associate Professor of Radiology, Department of Radiology, University of Texas Southwestern Medical Center, Advanced Imaging Research Center, Dallas, TX



David Siegel, MD, FSIR, System Chief, Interventional Radiology Services, North Shore LIJ Health System, and Associate Professor of Radiology, Hofstra North Shore LIJ School of Medicine, New Hyde Park, NY



Richard Towbin, MD, Radiologist-in-Chief, Department of Radiology, Phoenix Children's Hospital, Phoenix, AZ



Raymond Tu, MD, Chairman, Department of Radiology, United Medical Center and Clinical Associate Professor of Radiology, The George Washington University School of Medicine and Health Sciences, Washington, DC

Introduction

- 1.....Low dose and high quality: A delicate balance
Larry Dentice

DXR

- 9.....The impact of digital radiography on the pediatric patient
Richard Towbin, MD, and James Owen
- 12.....Clinical Case: Isolated non-osseous navicular-medial cuneiform tarsal coalition
Seth Vatsky, MD, and Richard Towbin, MD

IXR

- 14.....3D imaging in the angiography suite advances interventional patient care
David Siegel, MD, FSIR
- 18.....Clinical Case: Treating recurrent pelvic congestion
David Siegel, MD, FSIR

Ambient Experience

- 20.....Ambient Experience for PET/CT: Reducing patient anxiety, improving the clinical process
Joseph Jalkiewicz

MR

- 22.....3T MR imaging protocol for characterization of renal masses
Gaurav Khatri, MD, and Ivan M. Pedrosa, MD
- 27.....Clinical Case: Metastatic workup of a morbidly obese patient with colorectal cancer
Julia Grossman, MD, Gaurav Khatri, MD, and Ivan M. Pedrosa, MD

IntelliSpace Portal

- 30.....IntelliSpace streamlines the continuum of care
Cristen Bolan

PET

- 32.....Striking a balance in PET imaging transforms patient care
Medhat M. Osman, MD, PhD
- 36.....Clinical Case: Recurrent lymphoma in the left acetabulum
Razi Muzaffar, DO, and Medhat M. Osman, MD, PhD

SPECT

- 39.....Low-dose, high-quality SPECT/CT imaging transforms patient care
Medhat M. Osman, MD, PhD
- 46.....Clinical Case: Osteomyelitis with associated fracture in the toe as seen on high-resolution SPECT/CT
Razi Muzaffar, DO, and Medhat M. Osman, MD, PhD

Ultrasound

- 49.....Improving patient outcomes with ultrasound elastography
Richard G. Barr, MD, PhD, FACR
- 53.....Clinical Case: Elastography in evaluation of musculoskeletal abnormalities
Richard G. Barr, MD, PhD, FACR

Women's Health

- 56.....Transformation from film-screen to MicroDose digital mammography: Selection challenges, opportunity, and value
Raymond Tu, MD, Riad Charafeddine, MD, Theodore Williams, MA, RT(R), and Steven Rothenberg
- 60.....Clinical Case: Breast cyst and dermal calcification
Raymond Tu, MD

Low dose and high quality: A delicate balance



Larry Dentice

Better patient care is one of the driving forces behind what we do.

Low radiation dose and high diagnostic image quality—it's the delicate balance we all try to strike in radiology to provide the best possible care and improve patient outcomes. At Philips, we continue to make advances in establishing just the right balance in all of our products as we carry on our Imaging 2.0 vision, based on clinical integration and collaboration, patient focus, and improved economic value.

We incorporate the principle of keeping radiation dose as low as reasonably achievable in every product we create. A prime example is our BrightView XCT, which provides high-quality images with less radiation dose than computed tomography (CT) scanners that lack Philips' dose-reduction tools, while boosting reporting speed and accuracy. Additionally, our innovative iDose⁴ iterative reconstruction technique for Philips Ingenuity CT systems allows radiologists to manage dose without sacrificing image quality. Even for electrophysiology and angio procedures, which traditionally require high levels of radiation, Philips is constantly looking at ways to develop low-dose interventional X-ray systems that advance patient care. We are incredibly excited about these products and how they are advancing the science of achieving the ideal balance of low radiation dose and high diagnostic image quality.

At the same time, there is increasing pressure in the industry to improve productivity and keep healthcare costs down. Increased workflow demands on clinicians require the ability to diagnose and collaborate virtually anytime, anywhere. That's the principle behind Philips' IntelliSpace Portal, a powerful thin-client solution for advanced image review and analysis offering a clinical solution that's multi-specialty, multi-modality and multi-vendor—and accessible through iPad[®]*, laptop or smartphone*.

Better patient care is one of the driving forces behind what we do across the healthcare field, and these technologies offer enhanced diagnostic confidence to deliver improved care. The following pages detail nine perspectives from experienced clinicians in various specialties, reflecting how they are achieving better patient care in their specialty areas. Our hope is that their insights will inspire you with new ideas about the exciting possibilities within our field.

We would like to extend Philips' thanks for the collaboration and insights of all the physicians included in this special supplement to *Applied Radiology* as we work together to create the future of healthcare and save lives.

Larry Dentice
Senior Vice President, Imaging Systems Sales and Marketing
Philips Healthcare North America

**Note: Images are not for diagnosis except when using cleared software for mobile application.*

Introduction

- 1.....Low dose and high quality: A delicate balance
Larry Dentice

DXR

- 9.....The impact of digital radiography on the pediatric patient
Richard Towbin, MD, and James Owen
- 12.....Clinical Case: Isolated non-osseous navicular-medial cuneiform tarsal coalition
Seth Vatsky, MD, and Richard Towbin, MD

IXR

- 14.....3D imaging in the angiography suite advances interventional patient care
David Siegel, MD, FSIR
- 18.....Clinical Case: Treating recurrent pelvic congestion
David Siegel, MD, FSIR

Ambient Experience

- 20.....Ambient Experience for PET/CT: Reducing patient anxiety, improving the clinical process
Joseph Jalkiewicz

MR

- 22.....3T MR imaging protocol for characterization of renal masses
Gaurav Khatri, MD, and Ivan M. Pedrosa, MD
- 27.....Clinical Case: Metastatic workup of a morbidly obese patient with colorectal cancer
Julia Grossman, MD, Gaurav Khatri, MD, and Ivan M. Pedrosa, MD

IntelliSpace Portal

- 30.....IntelliSpace streamlines the continuum of care
Cristen Bolan

PET

- 32.....Striking a balance in PET imaging transforms patient care
Medhat M. Osman, MD, PhD
- 36.....Clinical Case: Recurrent lymphoma in the left acetabulum
Razi Muzaffar, DO, and Medhat M. Osman, MD, PhD

SPECT

- 39.....Low-dose, high-quality SPECT/CT imaging transforms patient care
Medhat M. Osman, MD, PhD
- 46.....Clinical Case: Osteomyelitis with associated fracture in the toe as seen on high-resolution SPECT/CT
Razi Muzaffar, DO, and Medhat M. Osman, MD, PhD

Ultrasound

- 49.....Improving patient outcomes with ultrasound elastography
Richard G. Barr, MD, PhD, FACR
- 53.....Clinical Case: Elastography in evaluation of musculoskeletal abnormalities
Richard G. Barr, MD, PhD, FACR

Women's Health

- 56.....Transformation from film-screen to MicroDose digital mammography: Selection challenges, opportunity, and value
Raymond Tu, MD, Riad Charafeddine, MD, Theodore Williams, MA, RT(R), and Steven Rothenberg
- 60.....Clinical Case: Breast cyst and dermal calcification
Raymond Tu, MD

Low dose and high quality: A delicate balance



Larry Dentice

Better patient care is one of the driving forces behind what we do.

Low radiation dose and high diagnostic image quality—it's the delicate balance we all try to strike in radiology to provide the best possible care and improve patient outcomes. At Philips, we continue to make advances in establishing just the right balance in all of our products as we carry on our Imaging 2.0 vision, based on clinical integration and collaboration, patient focus, and improved economic value.

We incorporate the principle of keeping radiation dose as low as reasonably achievable in every product we create. A prime example is our BrightView XCT, which provides high-quality images with less radiation dose than computed tomography (CT) scanners that lack Philips' dose-reduction tools, while boosting reporting speed and accuracy. Additionally, our innovative iDose⁴ iterative reconstruction technique for Philips Ingenuity CT systems allows radiologists to manage dose without sacrificing image quality. Even for electrophysiology and angio procedures, which traditionally require high levels of radiation, Philips is constantly looking at ways to develop low-dose interventional X-ray systems that advance patient care. We are incredibly excited about these products and how they are advancing the science of achieving the ideal balance of low radiation dose and high diagnostic image quality.

At the same time, there is increasing pressure in the industry to improve productivity and keep healthcare costs down. Increased workflow demands on clinicians require the ability to diagnose and collaborate virtually anytime, anywhere. That's the principle behind Philips' IntelliSpace Portal, a powerful thin-client solution for advanced image review and analysis offering a clinical solution that's multi-specialty, multi-modality and multi-vendor—and accessible through iPad[®]*, laptop or smartphone*.

Better patient care is one of the driving forces behind what we do across the healthcare field, and these technologies offer enhanced diagnostic confidence to deliver improved care. The following pages detail nine perspectives from experienced clinicians in various specialties, reflecting how they are achieving better patient care in their specialty areas. Our hope is that their insights will inspire you with new ideas about the exciting possibilities within our field.

We would like to extend Philips' thanks for the collaboration and insights of all the physicians included in this special supplement to *Applied Radiology* as we work together to create the future of healthcare and save lives.

Larry Dentice
Senior Vice President, Imaging Systems Sales and Marketing
Philips Healthcare North America

**Note: Images are not for diagnosis except when using cleared software for mobile application.*

Introduction

- 1.....Low dose and high quality: A delicate balance
Larry Dentice

CT

- 4.....Low iodine contrast combined with low radiation dose doubles the benefit in abdominal CT imaging for vascular mapping
Barry Daly, MD, FRCR, and Barton F. Lane, MD
- 7.....Clinical Case: Low kVp vascular imaging with iDose⁴ on the iCT scanner for diagnosis of an unusual aortic endograft leak in a patient with renal compromise
Barton F. Lane, MD, and Barry Daly, MD, FRCR

DXR

- 9.....The impact of digital radiography on the pediatric patient
Richard Towbin, MD, and James Owen
- 12.....Clinical Case: Isolated non-osseous navicular-medial cuneiform tarsal coalition
Seth Vatsky, MD, and Richard Towbin, MD

IXR

- 14.....3D imaging in the angiography suite advances interventional patient care
David Siegel, MD, FSIR
- 18.....Clinical Case: Treating recurrent pelvic congestion
David Siegel, MD, FSIR

Ambient Experience

- 20.....Ambient Experience for PET/CT: Reducing patient anxiety, improving the clinical process
Joseph Jalkiewicz

MR

- 22.....3T MR imaging protocol for characterization of renal masses
Gaurav Khatri, MD, and Ivan M. Pedrosa, MD
- 27.....Clinical Case: Metastatic workup of a morbidly obese patient with colorectal cancer
Julia Grossman, MD, Gaurav Khatri, MD, and Ivan M. Pedrosa, MD

IntelliSpace Portal

- 30.....IntelliSpace streamlines the continuum of care
Cristen Bolan

PET

- 32.....Striking a balance in PET imaging transforms patient care
Medhat M. Osman, MD, PhD
- 36.....Clinical Case: Recurrent lymphoma in the left acetabulum
Razi Muzaffar, DO, and Medhat M. Osman, MD, PhD

SPECT

- 39.....Low-dose, high-quality SPECT/CT imaging transforms patient care
Medhat M. Osman, MD, PhD
- 46.....Clinical Case: Osteomyelitis with associated fracture in the toe as seen on high-resolution SPECT/CT
Razi Muzaffar, DO, and Medhat M. Osman, MD, PhD

Ultrasound

- 49.....Improving patient outcomes with ultrasound elastography
Richard G. Barr, MD, PhD, FACR
- 53.....Clinical Case: Elastography in evaluation of musculoskeletal abnormalities
Richard G. Barr, MD, PhD, FACR

Women's Health

- 56.....Transformation from film-screen to MicroDose digital mammography: Selection challenges, opportunity, and value
Raymond Tu, MD, Riad Charafeddine, MD, Theodore Williams, MA, RT(R), and Steven Rothenberg
- 60.....Clinical Case: Breast cyst and dermal calcification
Raymond Tu, MD

APPLIED RADIOLOGY

THE JOURNAL OF PRACTICAL MEDICAL IMAGING AND MANAGEMENT

Publisher

O. Oliver Anderson

Associate Publisher

Kieran Anderson

Executive Editor

Cristen Bolan

Contributing Editor

Joseph Jalkiewicz

Art Director and Production

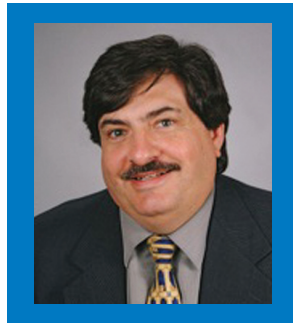
Barbara A. Shopiro

Applied Radiology and this supplement, *Transforming Patient Care Through Patient Focus, Improved Productivity and Improved Clinical Outcomes*, are published by Anderson Publishing, Ltd. The journal does not warrant the expertise of any author in a particular field, nor is it responsible for any statements by such authors. The opinions expressed in this supplement are those of the authors. They do not imply endorsement of advertised products and do not necessarily reflect the opinions or recommendations of our sponsors or the editors and staff of *Applied Radiology*.

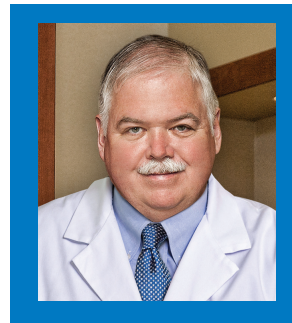
Copyright © 2012 by
Anderson Publishing, Ltd.,
180 Glenside Avenue,
Scotch Plains, NJ 07076.

All rights reserved.

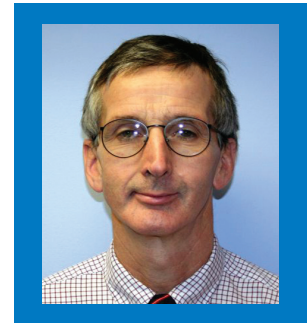
Contributing Faculty



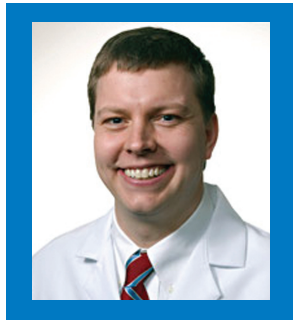
Richard G. Barr, MD, PhD, FACR, Professor of Radiology, Northeastern Ohio Medical University, and a Diagnostic Radiologist at Radiology Consultants Inc., Youngstown, OH



Bruce A. Cross, MD, Radiation Oncologist, Sparks Health System, Fort Smith, AR



Barry Daly, MD, FRCR, Professor of Radiology, University of Maryland School of Medicine, Section of Abdominal Imaging, Department of Diagnostic Radiology, University of Maryland Medical Center and School of Medicine, Baltimore, MD



Andrew J. Mullinix, MD, Diagnostic Radiologist, Franciscan St. Francis Health, Indianapolis, IN



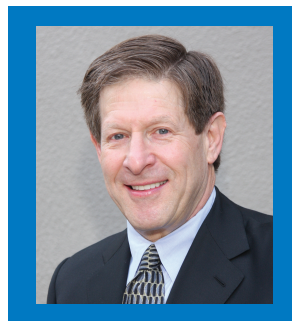
Medhat M. Osman, MD, PhD, Program Director of the Division of Nuclear Medicine, Department of Radiology, Saint Louis University Hospital, St. Louis, MO



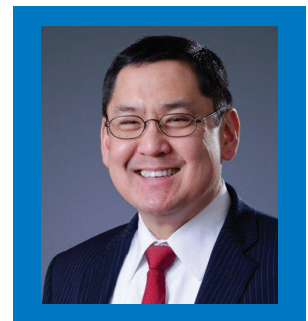
Ivan M. Pedrosa, MD, Chief-of-MRI, Associate Professor of Radiology, Department of Radiology, University of Texas Southwestern Medical Center, Advanced Imaging Research Center, Dallas, TX



David Siegel, MD, FSIR, System Chief, Interventional Radiology Services, North Shore LIJ Health System, and Associate Professor of Radiology, Hofstra North Shore LIJ School of Medicine, New Hyde Park, NY



Richard Towbin, MD, Radiologist-in-Chief, Department of Radiology, Phoenix Children's Hospital, Phoenix, AZ



Raymond Tu, MD, Chairman, Department of Radiology, United Medical Center and Clinical Associate Professor of Radiology, The George Washington University School of Medicine and Health Sciences, Washington, DC

Low iodine contrast combined with low radiation dose doubles the benefit in abdominal CT imaging for vascular mapping

Dr. Daly is a Professor of Radiology, and **Dr. Lane** is an Assistant Professor of Radiology, University of Maryland School of Medicine, Section of Abdominal Imaging, Department of Diagnostic Radiology, University of Maryland Medical Center and School of Medicine, Baltimore, MD.

Barry Daly, MD, FRCR, and Barton F. Lane, MD



Barry Daly, MD, FRCR

The low tube potential 80 kVp technique allows for improved vascular enhancement with decreases in both contrast dose and radiation dose.

The high and increasing prevalence of chronic renal failure in the United States has led to concerns among radiologists, referring physicians, and patients about the potential nephrotoxic side effects of intravenous iodinated contrast. In our practice, an increasing number of computed tomography (CT) studies are now done without intravenous (IV) contrast. Enhanced CT imaging may be declined when the serum creatinine level is raised, even where it is the best available test for the evaluation of vascular disease or preoperative vascular mapping. However, in such cases, optimized iodine contrast dose can diminish concerns and make patients with decreased renal function eligible for CT evaluation of vascular disease.

In this paper, we address CT imaging of the abdomen and pelvis on the iCT scanner, utilizing both a) low tube potential (80 kVp) to optimize the required volume of iodinated contrast dose and b) iDose⁴ iterative reconstruction to manage required radiation dose.

The increased power of x-ray generators and tolerance of x-ray tubes for higher and longer sustained milliamperage in the latest generation CT scanners, such as the iCT, now allows CT to be performed at lower kilovoltage potential (kVp) levels than previously possible. As noted in recent publications^{2,3} and in phantom studies at our institution,⁴ imaging with an 80-kVp x-ray tube potential improves the x-ray attenuation of iodine by almost a factor of 2 when compared to 120 kVp due to increased photoelectric absorption. For a given dose of intravenous contrast,

the blood vessels will be much “brighter” at 80 kVp than at 120 kVp, and this facilitates the use of lower doses of iodinated contrast.

However, dropping the kVp decreases the x-ray photon flux in a logarithmic fashion, such that imaging at 80 kVp will result in a much lower radiation dose than at 120 kVp, if all other scan parameters are kept the same. This translates into less tissue penetration and increased image noise. To overcome this limitation, the tube current (mAs) must in theory be increased by a factor of 2.75 at 80 kVp in order to obtain the same image quality as at 120 kVp. In general, only recent generation CT scanners, such as the iCT, are capable of performing such scans, especially in large patients. However, an important and helpful development in this setting is the introduction of iterative reconstruction techniques that compensate for this increased mAs requirement and allow for a major overall reduction in the required radiation dose. In this paper, we will provide clinical examples where the expected rise in mAs was reduced, facilitating the use of this “double low dose” technique, which provides major savings in both iodine contrast and radiation dose.

In our practice, we have utilized the technique described above to offer CT abdominal imaging to patients with decreased renal function. Typically the patients require investigation of vascular disease in the abdomen and pelvis. The sample studies included here were performed on an iCT 256-channel multidetector CT scanner at the University of Maryland Medical Center. This scanner has a selection

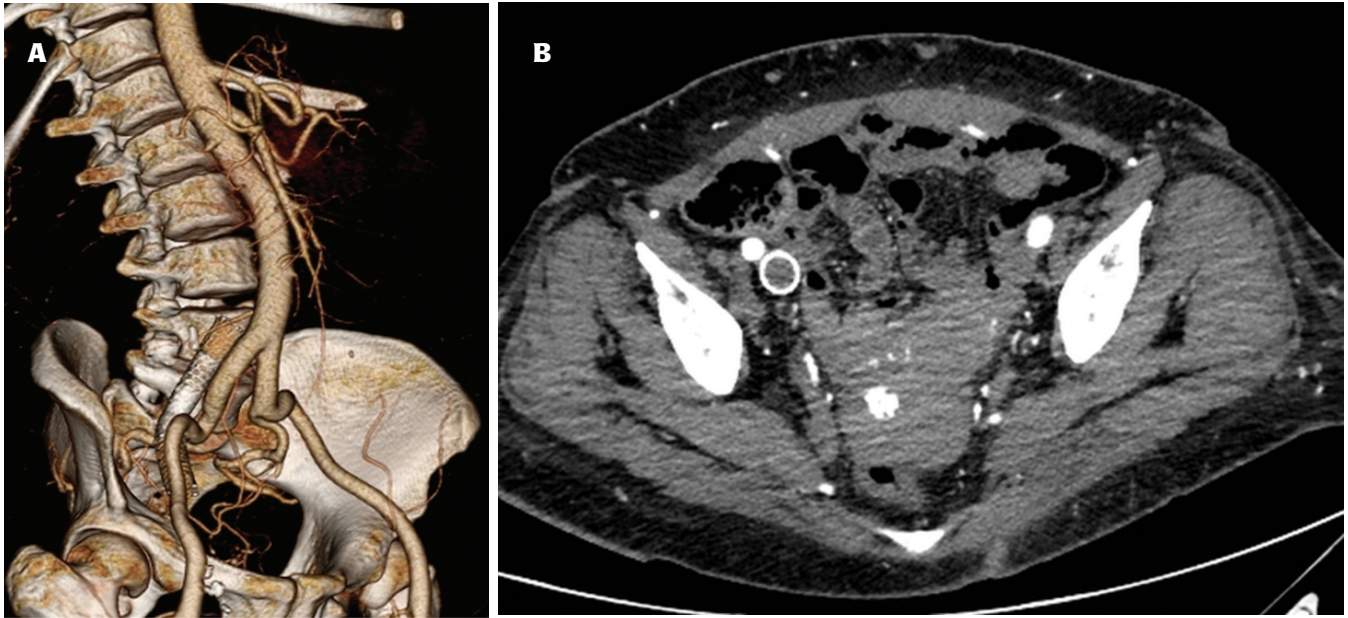


FIGURE 1. A 3-dimensional (3D) volume rendered reconstruction (A) utilizing low iodine and low radiation dose techniques demonstrates a tortuous aorta and major iliac branches without evidence of arterial stenosis or aneurysm. An incidental thrombosed right iliac vein stent is noted. An axial image (B) through the pelvis utilizing low iodine and low radiation dose techniques demonstrates satisfactory image quality and arterial contrast density (>400 HU) in both external iliac arteries. The thrombosed right iliac vein stent is also noted.

of optional kVp settings from 80 to 140, and both a large 120 kW generator and an effective 30 MHU x-ray tube, which allows the higher mAs required for the low kVp technique. The iCT also has iDose⁴, a fourth generation iterative reconstruction technology allowing for radiation dose reduction while maintaining image quality. While the iCT could generate the required high mAs for the low kVp technique without the need for iDose⁴, we believe in using iDose⁴ in every case possible in order to decrease radiation doses as low as reasonably achievable. The iodine dose used is typically 35 mL to 50 mL of 350 mg/mL concentration of low osmolar contrast for abdomen and pelvic scanning.

Example 1. A 38-year-old patient presents with chronic renal failure and pelvic pain. Suspicion of pulsatile mass in right iliac fossa was noted on clinical exam in the emergency room.

Abdominal CT was performed after injection of 50 mL of 350 mg/mL iodinated contrast at 4 mL/second utilizing 80 kVp technique (Figure 1). The patient body mass index (BMI) was 23. The mAs was 320 using level 5 iDose⁴ iterative reconstruction. CTDI_{vol} was 6.1 mGy with DLP of 290 mGy-cm and dose equivalent of 4.3 mSv.

Example 2. A 47-year-old patient presents with chronic renal failure secondary to polycystic disease. CT was obtained for pretransplant vascular evaluation.

A CT abdominal scan was performed utilizing low iodine and low radiation dose with injection of 50 mL of 350 mg/mL iodinated contrast at 4 mL/second utilizing 80 kVp technique (Figure 2). The patient's BMI was 29. The mAs was 373 using level 5 iDose⁴ iterative reconstruction. CTDI_{vol} was 7.0 mGy with DLP of 352 mGy-cm and dose equivalent of 5.3 mSv.

Of note in both cases is very satisfactory image quality, reflecting the ability of iodinated contrast to effectively "double absorb" x-rays at 80 kVp. Of additional value is the remarkably low mAs utilized and the subsequent absorbed dose and dose equivalent (4.3 mSv and 5.3 mSv, respectively). As noted above, in theory the 80-kVp technique requires mAs levels 2.75 times greater than the equivalent needed at 120 kVp. This should be in the range of 500 mAs or greater, but in practice lower mAs (and lower absorbed dose and dose equivalent) may be possible for several reasons. These include the use of a higher level of iDose⁴ (level 5 in this case), which is particularly useful

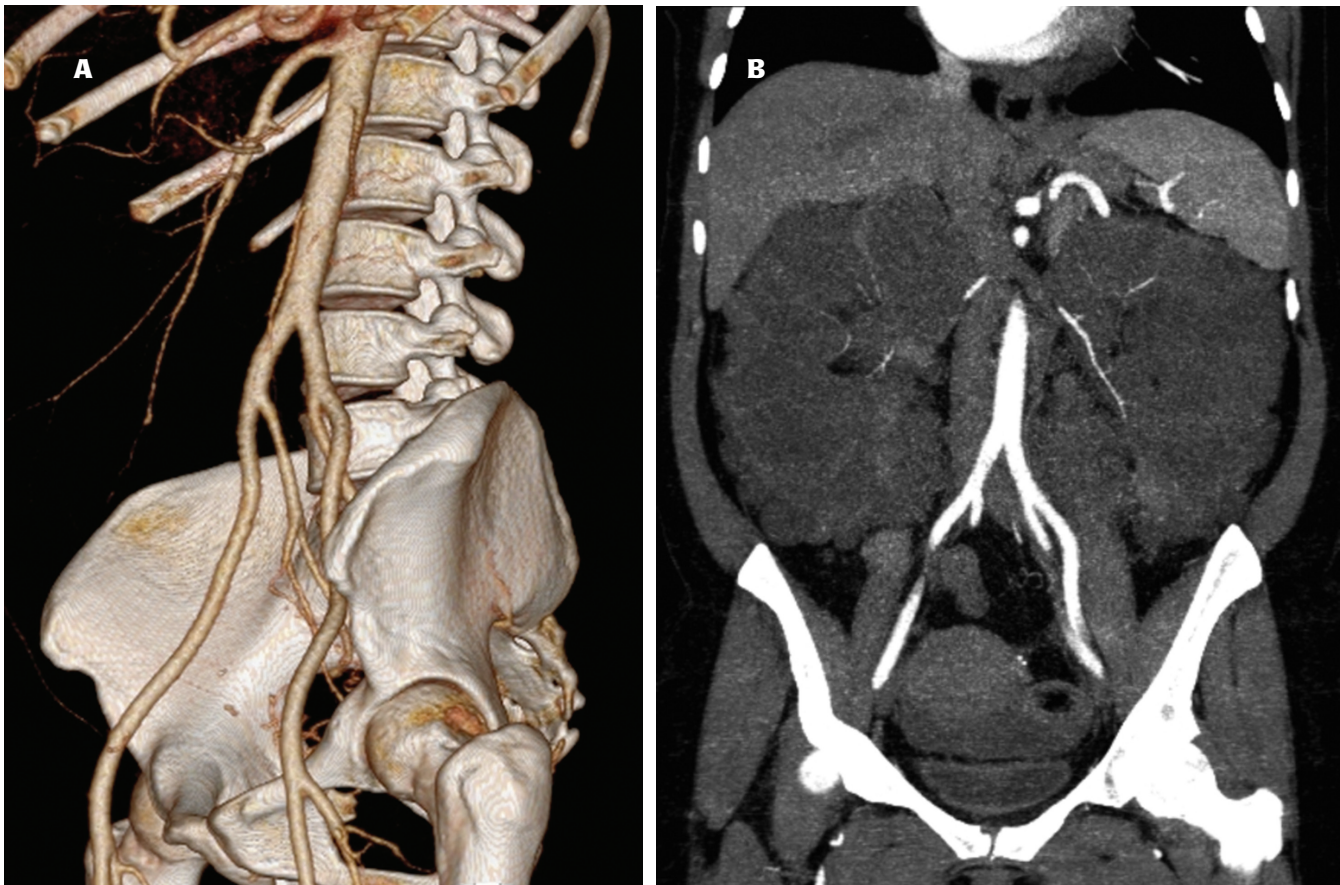


FIGURE 2. 3D-volume rendered reconstruction (A) utilizing low iodine and low radiation dose techniques demonstrates normal aorta and major iliac branches without evidence of arterial calcification or stenosis. A maximum intensity projection (MIP) coronal image utilizing low iodine and low radiation dose techniques (B) demonstrates satisfactory contrast density (386 HU) and image quality. Bilateral enlarged polycystic kidneys are present.

for optimized dose reduction in vascular imaging. In addition, arterial imaging is an inherently “high contrast” type of examination where image noise is of less importance than in “low contrast” exams (such as in nonenhanced brain or liver imaging).

In conclusion, the utilization of the low tube potential 80 kVp technique allows for improved vascular enhancement with decreases in both contrast dose and radiation dose. The ability to reduce the iodine dose by at least 50% compared with current standard doses may allow many patients with chronic renal failure to become candidates for this procedure. The use of this technique is likely to become more widespread with the growing availability of the latest

generation of CT scanners, such as the iCT, and innovative iterative reconstruction techniques, such as iDose⁴.

References

1. Coresh J, Selvin E, Stevens LA, et al. Prevalence of chronic kidney disease in the United States. *JAMA*. 2007;298:2038-2047.
2. Nakayama Y, Awai K, Funama Y, et al. Abdominal CT with low tube voltage: Preliminary observations about radiation dose, contrast enhancement, image quality, and noise. *Radiology*. 2005;237:945-951.
3. Kalva SP, Sahani DV, Hahn PF, Saini S. Using the K-edge to improve contrast conspicuity and to lower radiation dose with a 16-MDCT: A phantom and human study. *J Comput Assist Tomogr*. 2006;30:391-397.
4. Lane BF, Daly BD, Yang Z, Read K. Low iodinated contrast dose CT angiography of the abdomen and pelvis utilizing 80 kVp technique. (Abstract) RSNA 2010.

Clinical Case

Low kVp vascular imaging with iDose⁴ on the iCT scanner for diagnosis of an unusual aortic endograft leak in a patient with renal compromise

Barton F. Lane, MD, and Barry Daly, MD, FRCR

Case summary

A 59-year-old moderately obese male patient presented to the emergency department with back pain lasting 24 hours. He had a history of abdominal aortic aneurysm repair with placement of a vascular endograft 3 months earlier. He also had a history of chronic renal dysfunction with elevated serum creatinine.

Imaging findings

Imaging was obtained on an iCT 256-channel multidetector computed tomography (CT) scanner. An abdominal CT scan was performed utilizing low 80 kVp technique and 50 mL of 350 mg/mL iodinated contrast dose and iDose⁴ iterative reconstruction technique. The study demonstrated a type 2 endograft leak (Figures 1A and B) due to retrograde blood flow into the aneurysm sac via an accessory right renal artery (Figure 1C). The aneurysm was stable in size since an initial post-endograft placement CT scan.

Diagnosis

Aortic endograft with type II endoleak through an accessory right renal artery

Discussion

Endograft repair of thoracic and abdominal aortic aneurysms was first introduced over 20 years ago as an alternative to open surgical repair. In this procedure, a covered stent is placed across the aneurysm, with the proximal and distal ends of the graft anchored to

nonaneurysmal segments of the artery above and below the aneurysm. The graft serves as a conduit for arterial blood flow, excluding the surrounding aneurysm sac from the pulsatile high-pressure arterial blood flow.¹

The most important complication unique to endograft repair is an endograft leak, of which 5 types have been described, based upon the source of blood flow into the aneurysm sac:

Type I — Incomplete seal at either the proximal (type IA) or distal (type IB) end of the graft. This is the most common leak associated with thoracic aneurysm repair. If an abdominal graft involves a unilateral iliac component, with an occlusion device or coil embolization of the contralateral common iliac artery (such as with a femoral-femoral bypass), this represents an additional potential site of leak (type IC) via incomplete occlusion.

Type II — Retrograde filling of the aneurysm sac via small aortic branch arteries, typically lumbar arteries or the inferior mesenteric artery. This can be the result of one (type IIA) or multiple (type IIB) arteries. This is the most common leak associated with abdominal aneurysm repair.

Type III — Structural failure of the graft device, with leak either through a separation of components (type IIIA) or a hole in the wall of the device (type IIIB).

Type IV — Porosity of the graft with a slow leak across the graft material, without a discrete break or hole. This is uncommon with modern endograft devices.

Dr. Lane is an Assistant Professor of Radiology, and **Dr. Daly** is a Professor of Radiology, University of Maryland School of Medicine, Section of Abdominal Imaging, Department of Diagnostic Radiology, University of Maryland Medical Center and School of Medicine, Baltimore, MD.



FIGURE 1A. An axial CT scan through the lower abdomen shows abnormal enhancement within the excluded aneurysm sac with contrast opacification noted anterior to and between the two limbs of the endograft (arrow).



FIGURE 1B. A sagittal volume-rendered 3D image also shows enhanced blood flow outside the endograft. This simulates the appearance of a patent inferior mesenteric artery, but on Figure 1A it is clearly shown to lie within the aneurysm sac (arrow).



FIGURE 1C. Coronal multiplanar reconstruction (MPR) image shows a small accessory right renal artery (arrow) that communicated through retrograde blood flow with the excluded aortic aneurysm lumen noted on Figures 1A and 1B.

Type V — Suspected leak, with continued enlargement of the aneurysm sac with the site of the leak not identified. Post-operative evaluation of endoleaks is most commonly obtained with abdominal CT imaging, which is more sensitive for detection of leaks than is digital subtraction angiography.² A multiphase protocol, including arterial- and venous-phase imaging, is essential for evaluation, as leaks may have different flow rates and may be visible on only the arterial or venous phase.^{3,4}

The type II leak in this case represents the most common type of leak following abdominal aortic endograft repair. Most commonly retrograde flow occurs via a lumbar artery or the inferior mesenteric artery, but this case represents a rare instance of flow via an accessory renal artery that was not recognized preoperatively. The treatment of type II endoleaks is somewhat controversial, as many of these will resolve, or show stable or decreased size of the aneurysm sac over time.⁵

Conclusion

In this case, conservative management resulted in spontaneous resolution of the leak

over time. The patient's back pain was attributed to a musculoskeletal etiology. Low kVp imaging with iDose⁴ on the iCT scanner and allowed immediate detailed evaluation of the complex aortic endograft leak with consideration to iodinated contrast injected in this obese patient with decreased renal function.

References

1. Stavropoulos SW, Charagundla SR. Imaging techniques for detection and management of endoleaks after endovascular aortic aneurysm repair. *Radiology*. 2007;243:641-655.
2. Armerding MD, Rubin GD, Beaulieu CF, et al. Aortic aneurysmal disease: Assessment of stent-graft treatment-CT versus conventional angiography. *Radiology*. 2000;215:138-146.
3. Macari M, Chandarana H, Schmidt B, Lee J, et al. Abdominal aortic aneurysm: Can the arterial phase at CT evaluation after endovascular repair be eliminated to reduce radiation dose? *Radiology*. 2006;241:908-914.
4. Iezzi R, Cotroneo AF, Filippone A, et al. Multidetector CT in abdominal aortic aneurysm treated with endovascular repair: Are unenhanced and delayed phase enhanced images effective for endoleak detection? *Radiology*. 2006;241:915-921.
5. Tolia AJ, Landis R, Lamparello P, et al. Type II endoleaks after endovascular repair of abdominal aortic aneurysms: Natural history. *Radiology*. 2005;235:683-686.

The impact of digital radiography on the pediatric patient

Richard Towbin, MD, and James Owen

In the past three decades, the practice of radiology in general, and pediatric radiology in particular, has been transformed by imaging technology. Ultrasound, computed tomography (CT), and magnetic resonance imaging (MRI) have all contributed immensely to the care of children and led to a deeper understanding of both normal anatomy and disease processes. However, there has been no greater impact on pediatric radiology than the development of digital radiography (DR).

Plain radiography has evolved considerably over the past 20 years. Film screen radiography was the standard—the diagnostic centerpiece—of radiology departments for decades. By today's standards, the technology was not too expensive and was able to create diagnostic images of good to excellent quality. But as technology advanced it became clear that there were several issues, including the need for film processing with the associated processing equipment, a dark room, chemicals and dedicated darkroom personnel. As a result, throughput was slow, repeat rates at times exceeded 10%, and the pressure was on the technologists to restrain, position, and make exposures that minimized motion artifacts in children who could be crying and/or unwilling to cooperate.

In 1985, computed radiography (CR) was introduced, providing an alternative to film-screen radiography. CR was able to use existing x-ray equipment to create and retain an image on a phosphor plate. Once exposed, the CR cassette was put into a reader, where a laser scanned the plate and converted the analog (A) image into a digital (D) format. This A-to-D conversion changed plain film radiography. The digital image could be fed into a computer and displayed

on a PACS for review and interpretation. This simplified and decreased the expense of the entire process, since no photographic development was needed; film processors, dark rooms and associated personnel also were no longer necessary. This technology was widely accepted and utilized by radiology departments around the world. Once in a digital format, the images could be post-processed in a variety of ways to improve the diagnostic abilities of the radiologist and to promote rapid distribution of the imaging study to be immediately available to local and wide-area networks. In addition, once digitized, the images were immediately available on PACS and could be reviewed by the pediatric radiologist, who could assist the technologist with difficult cases and more rapidly provide a final reading to physicians caring for the child. The shortened turnaround time from image production to final reading improved patient care and radiology workflow, leading to customer satisfaction and potentially increased business.

Definitions of "DR"

The term 'DR' has two meanings in medical imaging. The first is "digital radiography," which includes all methods of image acquisition, resulting in an image that can be displayed in a digital format. The hierarchy of digital radiography is divided into two major categories usually abbreviated as 'CR' and 'DR'. This second use of the abbreviation 'DR' refers to 'direct radiography,' and it includes any system in which the image is created directly from a receptor. In direct radiography systems, the image is sent directly from the receptor for processing. Computed radiography is also referred to as indirect radiography because the image is read off the imaging plate through a

Dr. Towbin is Radiologist-in-Chief, and **Mr. Owen** is PACS Administrator, Department of Radiology, Phoenix Children's Hospital, Phoenix, AZ.



Richard Towbin, MD

Digital radiography has had a substantial positive impact on pediatric imaging by reducing radiation dose, imaging costs, and patient turnaround times.

Table 1. Pros and cons of DR and CR

DR	CR
Greater ease of use	Unlimited manipulation and positioning of the image receptor for cross-table projections – useful in trauma cases.
Elimination of cassette handling	(-) Repetitive motion injuries b/c of long-term cassette handling
Enhanced patient throughput	(-) Slower, more complex workflow
Potential for better IQ with lower radiation dose	(-) Greater maintenance cost
Faster workflow	(-) More dose required
Shorter turnaround time for viewing images	Lower acquisition cost
(-) Higher cost	(-) Less integration to x-ray system
Less patient movement	(-) Need to move patient before viewing image
Larger imaging area	
More latitude during image review	
More customizable imaging parameters	
Wireless transmission possible	
Ability for rapid exposures (multiple frames per second)	
Can track and QA images easier as well as exposure details	
(-) Higher start-up costs	

Key: (-) = cons

discrete acquisition process. Generally speaking, techniques used in CR imaging can be compared to a 200 speed film/screen system while DR techniques may be compared to a 400 speed or higher film/screen system.^{1,5} Essentially, a DR system requires approximately 50% or less technique than a CR system to produce a comparable image.

Direct radiography was introduced in the late 1990s. The substantial impact of DR on daily practice is multifaceted, and related in part to the high percentage of case volume represented by plain radiography. In our practice, and that of most departments, plain film radiography accounts for more than 50% of total imaging volume. As a result, this section of the department employs the most technologists. The high efficiency and rapid turnaround time [TAT] of digital radiography often lead to a reduction in the number of technologists by significantly increasing the number of studies performed per technologist. To better understand the effect of direct radiography in the pediatric radiology setting, we did a time-motion study that contrasted film screen radiography (FSR) and DR. We found that the average TAT for a 3-view skeletal examination was approximately 12 minutes for FSR and 3 minutes for DR. The effect on exam completion was more dramatic when all or part of an examination needed to be repeated. Other

authors have documented similar experiences. An unanticipated outcome of the faster TAT was demonstrated in the relationship between radiology and clinical services. For example, with FSR or CR, the TAT was too slow to keep up with a busy orthopedic clinic, resulting in tension between the two groups. In contrast, with DR, the TAT is fast enough to keep up with the demands of “herd-type” scheduling and multiple orthopedists seeing patients simultaneously. This has dramatically improved relations between the two groups.

The Phoenix Children’s experience

DR may be configured using single or dual detector systems. While both configurations work well and add efficiency at lower radiation doses, the technologists in our department prefer the dual-detector configuration because it is easier to position patients and requires fewer steps to complete a study with >2 views. However, this is not always a practical solution, since it is more costly—about \$100,000. In 2011 Phoenix Children’s Hospital opened a new hospital building that included a new radiology department fitted with Philips imaging equipment. We made a commitment to use DR only and installed three DR units, one with a dual-detector system and two with

single detectors. In addition, our satellites feature combination RF/DR rooms with single detectors.

As a children's hospital, our facility is a strong advocate of the Image Gently® movement with the goal of producing diagnostic studies at the lowest possible radiation dose. Our DR equipment supports these efforts by using lower mAs in most studies¹ and reducing the repeat rate. Other positive features of DR include faster TAT, more flexibility of the imaging device making it easier for the technologist to position the child resulting in shorter imaging times in our experience and that reported in the literature.^{2,3} Compared to film/screen imaging, digital imaging systems are very forgiving of both under- and overexposure. Severely underexposed digital images can be grainy and unacceptable even after post-processing. In contrast, overexposed digital images can appear as if a correct technique had been used. This is a double-edged sword, since it eliminates a second exposure but may lead to exposure creep, one of the major problems of DR. Exposure creep is a tendency to increase technique to ensure that all images are diagnostic. Studies have shown DR images with exposure rates of 500% to 1000% can still produce a diagnostic quality image.⁴ Thus, a quality-assurance program that regularly monitors the technical output of DR to ensure the highest-quality imaging at the lowest possible dose is very important.

At Phoenix Children's, the prevention of exposure creep has been addressed through two simple but effective measures: Technique charts and a film review program. Technique charts that build in substantive reductions in dose are employed in all our imaging systems. Coupled with the technique charts is a regular review of randomly selected studies to ensure compliance with the charts. A few examples of DR techniques include: a neonatal chest radiograph was typically obtained with CR using 58 Kvp and 2.0 mAs. With DR, the same examination is performed using 56 Kvp and 1.0-1.25 mAs. A 3-view ankle scan on a teenager (15-19 years old) on a CR system used 60 kVp at 4 mAs. The same study on DR uses 55 kVp at 1.5 mAs. An AP chest technique for a 6-month-old using CR required 70 kVp at 2-3 mAs. The same study on our DR system uses 60 kVp at 0.8 mAs. All

examples show a reduction equal to or greater than 50% of patient dose.

In most CR systems, technique tracking can only be achieved through exposure indicators in the DICOM header. There is not an accurate way to track kVp, mA, or time. This is because a CR cassette has no connectivity to the x-ray generator. Consequently, there is no way to transfer study information from the x-ray generator to the CR cassette. CR system exposure indicators can be problematic. Every CR system manufacturer has a different methodology and scale to designate exposure indicator values. In addition, exposure indicators are a reference value representing the relative amount of radiation hitting the plate. Direct radiography systems do have the ability to track technique factors. With DR, the x-ray generator and receptor are part of a single, fully integrated system. Technique factors [mA, kVp, time] from the x-ray generator component of the DR system are included in the DICOM header. Patient and study information from the work list also becomes part of the DICOM header.

The pros and cons of DR and CR are summarized in Table 1.

In conclusion, DR has had a substantial positive impact on pediatric imaging by reducing radiation dose, imaging costs, and patient turnaround times. As a result of the image-acquisition advantages, post-processing toolbox, and cost savings, we anticipate that over time, DR will replace all other forms of plain film pediatric imaging.

References

1. Seibert JA. *Medical Radiation Exposure Requirements for Digital Radiography*. Presented: Digital Imaging Summit and Workshop for Veterinary Radiologists. San Luis Obispo, Calif. May 29-31, 2008.
2. Hermann T. Computed radiography and digital radiography: A comparison of technology, functionality, patient dose, and image quality. eRadimaging.com <http://www.eradimaging.com/site/article.cfm?ID=535>. Accessed September 1, 2012.
3. Reiner Bruce I, et al. Multi-institutional analysis of computed and direct radiography: Part I. Technologist, Productivity, *Radiology*. 2005;236:413-419. Epub 2005 Jun 21.
4. Siebert J. The standardized exposure index for digital radiography: An opportunity for optimization of radiation dose to the pediatric population. *Pediatr Radiol*. 2011;41: 573-581. Published online 2011 April 14. doi: 10.1007/s00247-010-1954-6.
5. Willis, C. Computed radiography: A higher dose? SPR Seminar in Radiation Dose Reduction 2002. *Ped Radiol*. 2002;32:745-750.

Clinical Case

Isolated non-osseous navicular-medial cuneiform tarsal coalition

Seth Vatsky, MD, and Richard Towbin, MD

Dr. Vatsky is a Fellow, and **Dr. Towbin** is Radiologist-in-Chief, Department of Radiology, Phoenix Children's Hospital, Phoenix, AZ.

Case summary

An 11-year-old boy presented to an outpatient orthopedics office for chronic foot pain. The otherwise healthy child was experiencing progressive right foot pain, localized to the proximal medial aspect of the first metatarsal base, over the previous 8 months.

The child had been regularly participating in physical activity with a recreational baseball team. His symptoms had progressively gotten worse throughout the baseball season. His pain was unresponsive to thermal treatment and the regular use of orthotic inserts. His pain at presentation was rated 6/10. On exam there was localized swelling over the medial aspect of the right foot. The area was focally tender on palpation. A bilateral flexible pes planus foot deformity was present. However, both his range of motion and strength were intact bilaterally. Initial treatment was instituted with the application of a walking boot for a period of 4 weeks. Radiographs were obtained to evaluate for underlying osseous abnormality (Figure 1).

Imaging findings

Radiographic examination of the right foot demonstrated sclerosis and irregular narrowing of the inferior joint space at the articulation between the navicular and medial-cuneiform. There was no evidence of mineralized bridging crossing the joint or early degenerative change. The remainder of the examination was normal.

Diagnosis

Isolated non-osseous coalition of the navicular-medial cuneiform

Discussion

Tarsal coalition is an uncommon cause of foot pain, most frequently seen involving the talo-calcaneal and calcaneo-navicular joint.¹ Symptoms typically present in late childhood or early adolescence, depending on the level of activity of the individual. Frequently, there is involvement of multiple joints in the same foot or involvement of both feet (50% to 60%). The most extreme forms of coalition are associated with syndromes such as Apert's, where the coalitions result in the classic "mitten hand" or "stocking feet" appearance. Because of the difficulty of making the diagnosis on plain film radiographs, multiple radiographic signs have been investigated and documented to assist diagnosis.^{2,3} There has also been increased utilization of magnetic resonance and computer tomography imaging to assist in diagnosis and surgical planning.⁴

The frequency of tarsal coalition in the general population has been reported to range from 1% to 6%.⁵ There have been isolated reports of an autosomal dominant inheritance with variable penetration.⁶ Navicular-medial cuneiform tarsal coalition is a rarely described anomaly,⁷ but it is likely underreported in the literature.⁵ Traditionally, symptoms are treated

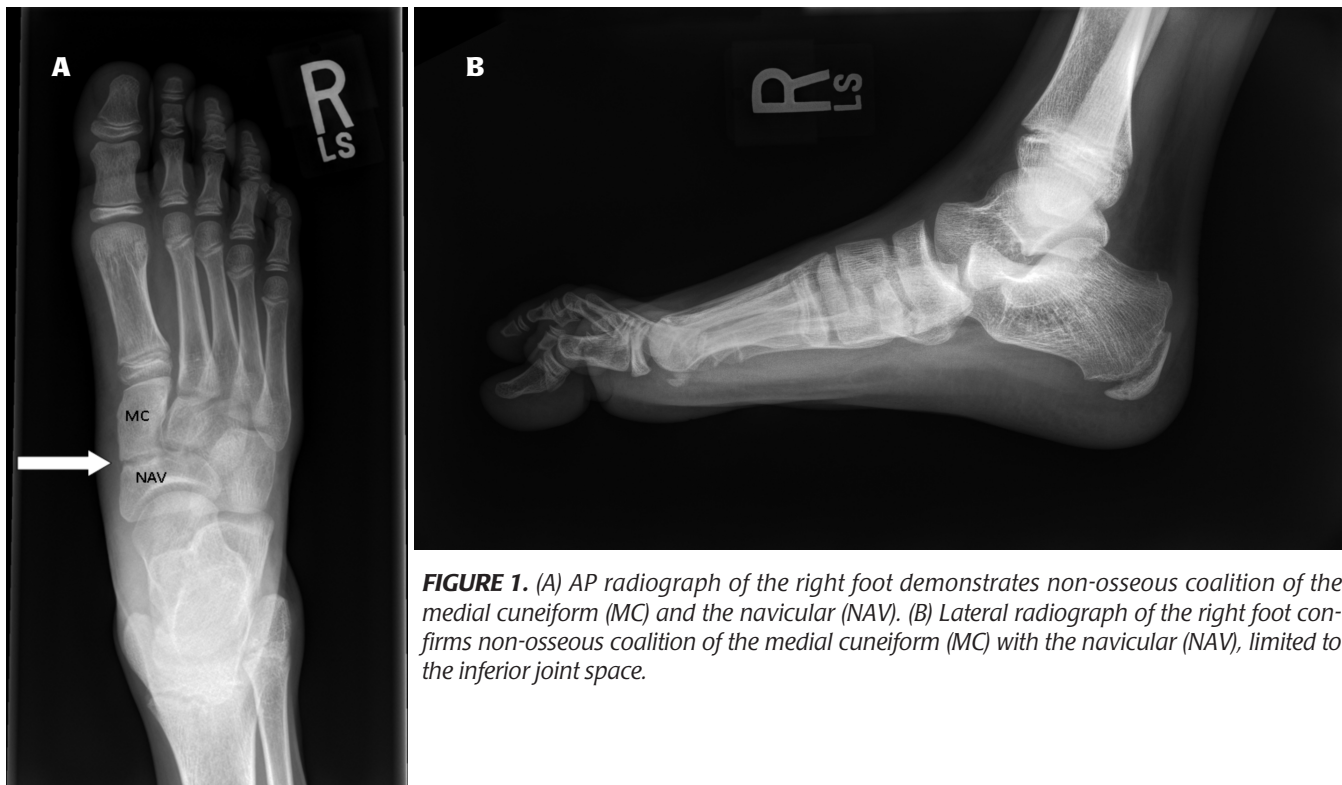


FIGURE 1. (A) AP radiograph of the right foot demonstrates non-osseous coalition of the medial cuneiform (MC) and the navicular (NAV). (B) Lateral radiograph of the right foot confirms non-osseous coalition of the medial cuneiform (MC) with the navicular (NAV), limited to the inferior joint space.

initially with conservative immobilization with graded return to activity through participation in a physical therapy program. Failure to respond to these measures may result in surgical intervention, either fusing the joint or resecting the coalition with fat interposition to prevent recurrence.^{5,7}

The overall rarity of this form of tarsal coalition in the population requires a high level of suspicion and knowledge of the radiographic findings of coalitions in this anatomically complex region. While the visualization of joint change at the navicular-medial cuneiform is relatively simple and unobscured on AP radiographs, the more common subtalar and calcaneal navicular coalitions can be challenging to identify because of the complex anatomy. The radiographic signs seen on conventional views: continuous C sign, talar beaking, absent middle facet, anteatler, and reverse anteatler sign, have variable sensitivity and specificity, but their presence must be suspected by the interpreting radiologist, to expedite further evaluation with cross-sectional imaging.^{3,4}

Conclusion

The child's pain responded well to conservative treatment. Physical therapy was initiated 2 weeks after initial presentation. He was pain free after 4 weeks. While surgical consultation was obtained, surgical intervention was indefinitely postponed, since the current interventions were effective in relieving symptoms.

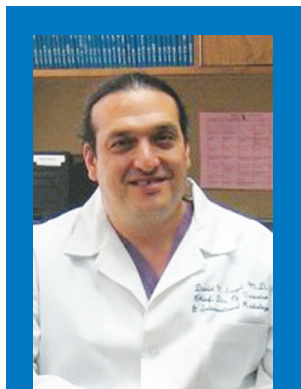
References

1. Helms C. *Fundamentals of Skeletal Radiology* 3rd edition. Elsevier Saunders 2005.
2. Crim J. Imaging of tarsal coalition. *Radiology Clinics of North America*. 2008;46:1017-1026.
3. Crim J, Kjeldsberg KM. Radiographic diagnosis of tarsal coalition. *AJR Am J Roentgenol*. 2004;182:323-328.
4. Newman JS, Newberg AH. Congenital tarsal coalition: Multimodality evaluation with emphasis on CT and MR imaging. *Radiographics*. 2000;20:321-332.
5. Morrissy RT, Weinstein SL. *Tarsal Coalitions in Lovell & Winter's Pediatric Orthopaedics*, 6th Edition. Pittsburgh, PA: Lippincott Williams & Wilkins 2006.
6. Leonard MA. The inheritance of tarsal coalition and its relationship to spastic flat foot. *J Bone Joint Surgery*. 1974 56B:520-525.
7. Ross JR, Dobbs MB. Isolated navicular-medial cuneiform tarsal coalition revisited: A case report. *J Pediatric Orthopaedics*. 2011;31:e85-e88.

3D imaging in the angiography suite advances interventional patient care

David Siegel, MD, FSIR

Dr. Siegel is System Chief, Interventional Radiology Services, North Shore LIJ Health System, and Associate Professor of Radiology, Hofstra North Shore LIJ School of Medicine, New Hyde Park, NY.



David Siegel, MD, FSIR

3D angiographic and CT imaging with needle-guidance software brings us one step closer to the full-service, image-guided procedure suite.

Interventional radiology has evolved rapidly over the last two to three decades, primarily due to refinements in catheters and catheter-based devices. These technological advances have allowed for the development of new techniques and applications of interventional therapy in territories previously not reachable. While image quality has improved and digital technology has been used to its full advantage over time in the evolution of angiography and interventional radiology suites, until recently little had really changed with respect to the way imaging has been utilized to guide these interventional procedures.

Cone-beam computed tomography (CT), developed several years ago, has revolutionized the way we guide procedures by allowing for soft-tissue imaging in the angiography suite that can be used with fluoroscopy. While rotating C-arms and 3-dimensional (3D) acquisition techniques were developed nearly 20 years ago, current technology adds the ability to image soft tissue with CT, along with improvements in fluoroscopic and angiographic imaging of contrast-filled vessels and other structures. Techniques for software reconstruction, manipulation, and analysis continue to be refined, and they now aid the interventional radiologist in guiding both vascular and nonvascular procedures in ways unimaginable as recently as 5 to 7 years ago.

At the forefront of the development of this technology is Philips Healthcare, whose flagship interventional suite is the Allura Xper FD 20 system. Besides providing the high-quality fluoroscopy and digital x-ray acquisition systems now customary in modern interventional suites, the ceiling-suspended C-arm of the Allura Xper FD 20 system can perform high-speed rotational scanning with or without simultaneous contrast

injection, depending on the situation. This digital image dataset is then processed in seconds; depending on the technique utilized, the dataset provides interventionalists with a 3D vascular or soft-tissue image for diagnosis and 3D road mapping. Using the dedicated XperGuide software, this dataset also can be used to guide percutaneous interventions with the aid of interactive needle-path planning and guidance software. This sophisticated software overlays a preplanned needle path, which the operator designs at an integrated workstation. Previously acquired CT scans and images from other modalities, such as magnetic resonance imaging (MRI) and MR angiography, can also be imported and superimposed on a fluoroscopic image.

This article reviews the different abilities of the 3D tools available in newer interventional suites and provides an overview of their various clinical applications.

3D rotational angiography and road mapping

Rotational angiography takes advantage of the C-arm's ability to rotate rapidly around the patient and acquire angiographic images at numerous oblique projections around its arch. Contrast injection volume and duration must be coordinated with the rotation speed and the desired images. Angiographers understand that the ability to see a vessel's origination or the exact point and angle of branching is essential to planning procedures that require selective catheterization and precise endovascular therapy. The 3D reconstructed angiogram can also be used for 3D road mapping. The 3D image can be superimposed on the live fluoroscopic image and manipulated together with the live

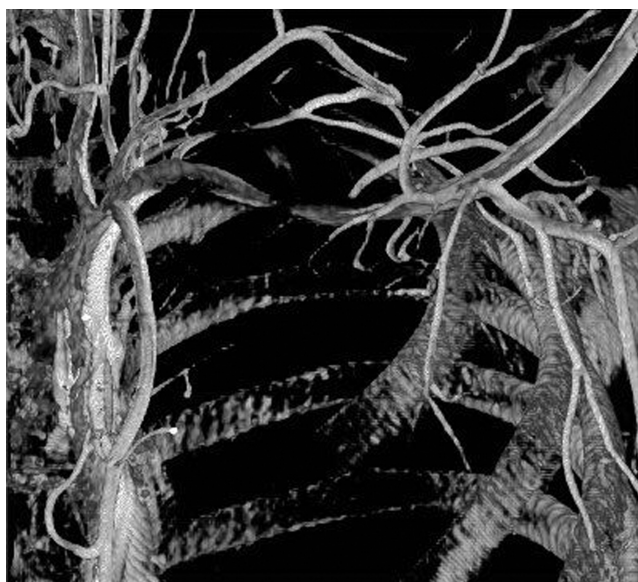


Figure 1. 3D image demonstrating compression of the subclavian artery consistent with Paget-Schroetter syndrome. This cone-beam CT reconstruction was created from a single rotational acquisition with contrast injection via 5-French catheter positioned at the origin of the subclavian artery. Note: The clavicle has been manually removed from the image so that the critical narrowing can be seen.

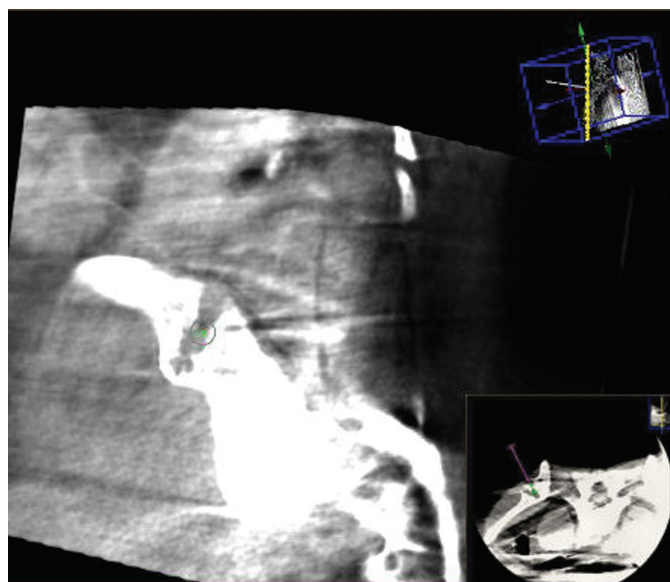


Figure 2. An XperGuide "target view" for a biopsy of a lesion in the iliac bone. Note the green circle over the lesion on the reconstructed image. This is superimposed on the live fluoroscopic image, indicating where the operator should place the needle. The insert in the right lower corner is one of several axial images used to plan the needle path.

fluoroscopic image. Oblique angles can be obtained, the patient can be moved, and the image can be magnified during endovascular manipulations and interventions. Previously, numerous stationary oblique "runs" were required, using trial and error; once the appropriate projection was determined, it was then employed for treatment planning and guidance.

With practice, interventionalists gain an understanding of when the added time, contrast, and radiation of these rotational acquisitions will ultimately lead to lower cumulative procedural time, contrast use, and exposure.

Cone-beam CT

Cone-beam CT employs image acquisition similar to that of rotational angiography. Computer software then performs a sophisticated 3D reconstruction, resulting in images that can be viewed as a multiplanar reconstruction. These images can be manipulated, rotated and zoomed; adjustments in window and level also can be made. Imaging soft tissue simultaneously with opacified vessels can be essential to appreciating the relationship of these structures and

understanding the blood supply and drainage of various organs. In interventional oncological procedures, when caustic chemotherapeutic preparations or radioactive particles are to be introduced into the liver vessels, confining the materials within the liver is essential, as non-target embolization can be catastrophic, especially when it involves the GI tract. If a vessel is opacified during such a procedure and its vascular territory is uncertain, XperCT can be performed during contrast injection, and the vascular distribution identified on that soft-tissue imaging. These techniques can be utilized outside the liver, as well. We often utilize cone-beam CT before embolization to evaluate the potential distribution of the embolic. Following embolization procedures, XperCT can assess the precise territory embolized, making it clear whether further embolization is necessary.¹

Understanding the relationship of vessels to surrounding structures can be essential to diagnosing different vascular conditions. Paget-Schroetter syndrome, or thoracic outlet syndrome, is a condition where the subclavian vessels are crushed between the first rib and the clavicle

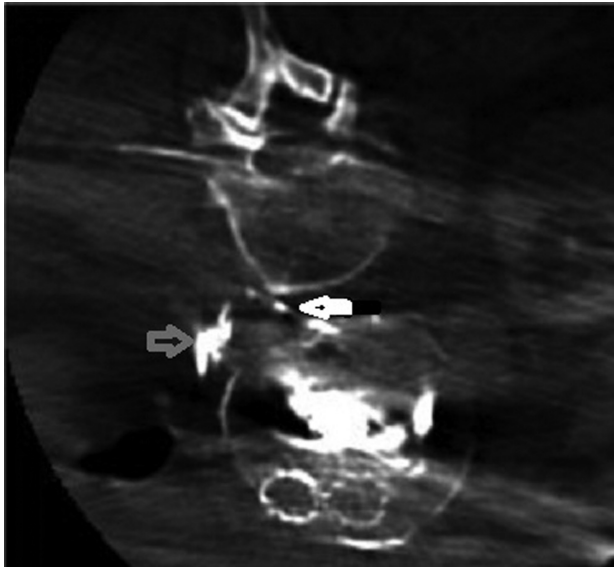


Figure 3. XperCT image following endoleak embolization with metallic coils, a vascular plug, and glue. Note the metallic coils and high-density tissue acrylic in the aneurysm sac, the back disc of a vascular plug (grey arrow) used to seal the puncture site in the aneurysm sac, and the radiopaque glue (white arrow) used to embolize the lumbar vessels seen supplying the type 2 endoleak.

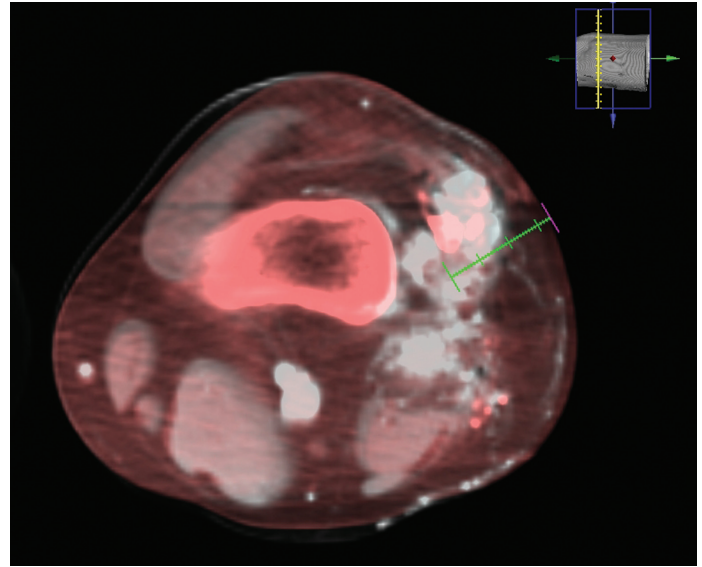


Figure 4. Intraprocedural XperCT with MR overlay during injection sclerotherapy for treatment of a recurrent symptomatic left lower extremity venous malformation. Note the needle path designed with XperGuide to guide puncture of a previously suboptimally treated portion of the lesion.

and confined by the scalene muscles between those bony structures. This generally occurs when the affected arm is abducted and extended. Figure 1 is a cone-beam CT image that demonstrates Paget-Schroetter syndrome. On this image, compression of the subclavian artery by the surrounding structures is beautifully depicted.

XperCT can also be employed during interventional procedures to locate and evaluate devices. We have used cone-beam CT imaging to guide filter placement in patients with severe contrast allergies or renal failure, to guide fenestration of aortic dissections by locating the appropriate point for flap puncture, and to evaluate the course of catheters or guide wires when it is unclear if the true lumen of an occluded vessel was traversed or if a collateral vessel that would be dangerous to dilate was catheterized. The applications for this technology continue to expand.

Interventional tools for needle guidance

The 3D image dataset obtained by the cone-beam CT acquisition of the Philips FD20 Allura Xper unit can be used with the dedicated needle-guidance software to plan a needle path

and then to aid the operator in precisely placing the needle during a variety of interventional procedures. The 3D CT image is first used to design the course of a needle or multiple needles that do not traverse any significant vascular or other dangerous structures. The unit will then assume the necessary compound oblique positions based on calculated coordinates. Initially, the C-arm will assume a “down the barrel” projection, or target view, and superimpose a circle on the fluoroscopic field where the needle should be placed. After fluoroscopically guided placement of the needle, so that only a point is seen, the C-arm is then turned to an orthogonal view to monitor progress of the advancing needle. When the unit is turned to this orthogonal view, or to any position, the 3D soft-tissue image and needle path remain superimposed on the fluoroscopic image. Biopsies and other procedures requiring needle access can be performed more accurately and reliably, translating into fewer needle passes and lower complication rates, especially when related to bleeding and post-procedure discomfort. Figure 2 is a target view for a biopsy of a 19-year-old man with a benign cartilaginous lesion of the iliac bone.

Radiation dose

Radiation exposure to the patient is certainly a factor in deciding how and when cone-beam CT and/or 3D angiography should be utilized in interventional practice. While rotational C-arm imaging techniques certainly deliver a greater radiation dose to the patient than does conventional fluoroscopy, in many situations, this technology can actually dramatically decrease the total fluoroscopy time and number of individual digital acquisitions—therefore decreasing overall radiation exposure.

When a needle can be advanced under real-time fluoroscopic guidance after a single cone-beam CT acquisition, the need for interval CT scanning during manipulations and needle passes is eliminated. Even with the addition of an extra CT scan to confirm needle position, cumulative radiation dose to a patient during a complex biopsy or other procedure requiring CT guidance is usually decreased. For these situations, the Philips Allura Xper FD20 system allows for a lower-dose cone-beam CT acquisition. This will produce an image of somewhat lower quality, but it can be used to determine needle position accurately. The overall decrease in radiation to patients during biopsy procedures has been validated in several published studies.²

Complex interventional procedures

We now use XperGuide in many clinical situations where accurate CT-needle guidance placement is needed in conjunction with additional vascular or nonvascular catheter and guide wire-based procedures. The combination of soft-tissue CT imaging, needle-guidance software, and 3D angiographic imaging can often simplify what would be relatively complex or cumbersome procedures; at times, it eliminates the need to move a patient from one suite to another where these different modalities are available. There are several reports of translumbar endoleak embolization utilizing cone-beam CT guidance for sac puncture.³ Figure 3 demonstrates an example of XperCT following endoleak embolization using coils, a vascular plug, and tissue acrylic.

We regularly perform nephrostomy placement, biliary drainage, and complex fluid collection drainage with Xper guide. Needle placement can be guided with the accuracy of CT imaging in an environment where subsequent catheter manipulations and exchanges can be performed with high-quality fluoroscopic guidance. Needle guidance has significantly expanded our interventional armamentarium. For example, we have performed puncture and intubation of the pancreatic duct for stenting of a persistent leak. Utilizing overlay of an MR image for targeting the cisterna choli, we were able to access the thoracic duct and then embolize a postoperative leak. Figure 4 demonstrates an intraprocedural XperCT with MR overlay, obtained in a patient with a venous malformation where recurrent symptoms were related to a deeper, previously untreated loculation. This deeper portion of the malformation was targeted and successfully treated with sclerotherapy, resulting in complete symptom relief.

Conclusion

The availability of 3D angiographic and CT imaging with needle-guidance software in the traditional interventional environment brings us one step closer to the full-service, image-guided procedure suite, where interventional radiologists can perform all procedures with the required technology at their disposal. Future developments in this technology should continue to enhance our precision and expand the role of interventional medicine.

Acknowledgement: The author would like to thank his colleague, Igor Lobko, MD, for his collaboration in much of the work discussed in this article.

References

1. Tognolini Alessia, Louie John D., Hwang Gloria L., et al. Utility of C-arm CT in patients with hepatocellular carcinoma undergoing transhepatic arterial chemoembolization. *J Vasc Interv Radiol.* 2010;21: 339-347.
2. Braak Sicco J, Strijen van Marco JL, Es van Hendrik W, et al. Effective dose during needle interventions: Cone-beam CT guidance compared with conventional CT guidance. *J Vasc Interv Radiol.* 2011;22:455-461.
3. Bindsbergen van Lars, Braak Sicco J, Strijen van Marco JL, de Vries Jean-Paul PM. Type II endoleak embolization after endovascular abdominal aortic aneurysm repair with use of real-time three-dimensional fluoroscopic needle guidance. *J Vasc Interv Radiol.* 2010;21:1443-1447.

Clinical Case

Treating recurrent pelvic congestion

David Siegel, MD, FSIR

Dr. Siegel is the System Chief, Interventional Radiology Services, North Shore LIJ Health System, and Associate Professor of Radiology, Hofstra-North Shore LIJ School of Medicine, New Hyde Park, NY.

Case summary

A 39-year-old female patient, SG, presented with painful varices in the lower extremities and pubic region after having several failed saphenous vein procedures. Following consultation and venography, diagnoses of pelvic congestion and iliac vein compression, or May-Thurner Syndrome, were made. The latter was treated successfully with stenting of the iliac vein; the gonadal veins were embolized bilaterally after venographic confirmation of reflux. Over the next 8 years, the patient underwent 11 additional procedures to treat symptomatic recurrences. Although the patient's symptoms completely or nearly completely resolved following each successful procedure, they were rarely in control for more than 6 to 8 months.

Diagnosis

Pelvic congestion syndrome

Imaging findings

As the patient's varicosities recurred, it became increasingly more difficult to obtain access to them and to perform sclerotherapy, especially when they began to develop in the inferior pelvis, causing pain and a burning sensation involving the pelvic floor. Pudendal veins, cross pelvic collateral veins, recanalized portions of the saphenous vein and many unnamed veins were accessed and/or treated in subsequent sessions. An example is seen in Figure 1, a venogram from one of those procedures. Injection of contrast is being performed via microcatheter, which was manipulated into the visualized pelvic floor veins via the vein of Giacomini. This was then used

for sclerotherapy. Figure 2 demonstrates a direct puncture through the perineum, which was used for access to some of the deep pelvic varices at a subsequent procedure.

In this circumstance, direct access to a sizable pelvic vein for sclerotherapy would be quite advantageous, but the issue is safely guiding a needle to the mid-pelvis accurately and reliably to avoid traversing any unwanted or dangerous pelvic structures. Figure 3, obtained at the last procedure, is a venogram obtained by direct puncture of a posterior division branch of the left hypogastric vein using the planning functionality of XperCT and XperGuide. Contrast injection beautifully demonstrates the symptomatic pelvic venous plexi, including the periterine/periovarian plexus and the dilated veins surrounding the urinary bladder, communicating with the deep peroneal veins. Following this venogram, 3% sodium tetradecyl was injected through the needle and allowed to dwell in place with the patient in the semi-upright position for 25 minutes. This procedure was performed about 1 year prior to the preparation of this case report and the patient has remained asymptomatic during that time, which is her longest symptom-free interval since presentation.

Discussion

Pelvic congestion syndrome, or ovarian venous incompetence, was originally described in 1958¹ and the name pelvic congestion syndrome first appeared in the literature in 1976.² For many years, this was a misunderstood and underdiagnosed entity. The confusion is primarily due to the variable clinical presentations and the wide

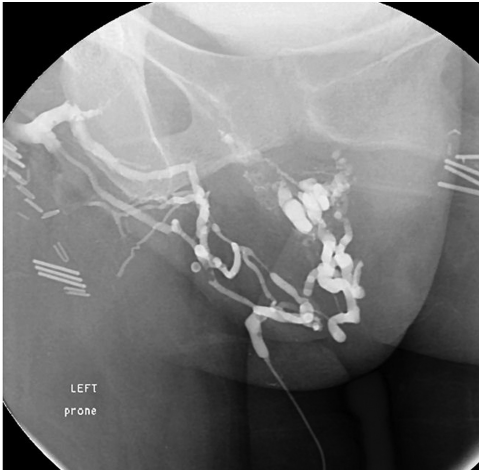


FIGURE 1. Contrast injection via microcatheter, which was manipulated into the visualized pelvic floor veins via the vein of Giacomini. This was then used for sclerotherapy.

variations in response to endovascular therapy. As there are a myriad of etiologies for pelvic pain and many patients are asymptomatic with respect to their pelvic varices, treatment failures are not uncommon. Additionally, many patients have simple ovarian vein incompetence with involvement of one or both ovarian veins, while others have some contribution from the internal iliac system.³ The latter situation can lead to treatment failures or incomplete symptom resolution following gonadal vein embolization alone.

Conclusion

Pelvic congestion syndrome is a complex condition, the hallmark of which is ovarian vein reflux and symptomatic pelvic varices. This case of recurrent pelvic varices after embolotherapy illustrates how XperCT and XperGuide can support direct access for sclerotherapy after numerous procedures have essentially eliminated the conventional vascular access routes. While this specific situation is quite rare, it is the author's hope that practitioners will consider cone-beam CT and dedicated needle guidance when faced with other situations where direct deep vascular access would be advantageous.

References

1. Topolanski-Sierra R. Pelvic phlebography. *Am J Obstet Gynecol.* 1958;76:44-45.
2. Hobbs JT. The pelvic congestion syndrome. *Practitioner.* 1976; 41:41-46.
3. Ignacio EA, Dua R, Sarin S, et al. Pelvic congestion syndrome: Diagnosis and treatment. *Semin Intervent Radiol.* 2008;25:361-368.



FIGURE 2. Venogram performed through a trocar needle placed through the perineum using fluoroscopic landmarks only. Note the opacified deep pelvic varices and some extravasation of contrast from the prior nonguided needle passes.



FIGURE 3. Venogram obtained by contrast injection through a needle used to puncture a posterior branch of the left hypogastric vein using XperCT and XperGuide. The varicosities around the uterus, ovaries, bladder and pelvic floor are opacified. This access was then used for injection of a sclerosing agent. The insert in the left upper corner is one of several axial images used to plan the needle path on the workstation.

Ambient Experience for PET/CT: Reducing patient anxiety, improving the clinical process

Joseph Jalkiewicz



“the whole gamut of cancers,” including lymphomas and cancers of the head and neck, lung, and breast.

Patient anxiety: A PET/CT imaging challenge

Yet getting patients' anxiety under control is crucial to the success of PET/CT scanning, which requires injections of ^{18}F fluorodeoxyglucose (^{18}F -FDG) and relies heavily on the patient to remain quiet and still for up to 90 minutes or more. That's a challenging task for anyone, much less a patient dealing with the emotional turmoil accompanying a cancer diagnosis, said Dr. Cross.

“You are asking [patients] to wait while you inject them with radioactive material, and they are already pretty nervous to start with because they have cancer, and on top of that they have to be quiet. That is incredibly difficult for people to do,” he said.

“When you inject the patient with FDG, you want patients to be relaxed so they don't produce false positives in the images, which may be caused by motion, either from humming, talking or just moving about,” he said, explaining that such motion can cause extra dye uptake and metabolism by the muscles, leading to false positive results.

Administering sedatives like diazepam to help patients relax is an option, but various studies have produced mixed results on their effectiveness, in addition to other drawbacks, such as the inability of outpatients to drive home and potential interactions with other drugs.²

Radiation oncologists like Dr. Cross use a variety of techniques to relax patients and enhance the clinical process.

The Ambient Experience solution

Ambient Experience is Philips' strategy for creating a patient-friendly, soothing environment for those undergoing PET/CT imaging procedures. To calm nervous patients during radiopharmaceutical injection, the walls of

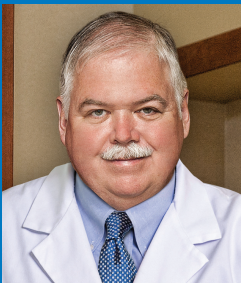
Few words strike fear into a person like the words, “You have cancer.”

An estimated 1.64 million people will hear those words this year as they receive a diagnosis of breast cancer, prostate cancer, head/neck cancer, or any one of the many other forms of the second-leading cause of death in the United States.¹

As part of their treatment, many of these patients will undergo positron emission tomography and computed tomography (PET/CT) scanning, one of the most powerful and effective imaging technologies available to help radiation oncologists diagnose, stage, and monitor cancerous lesions and their response to treatment.

“PET scanning has revolutionized scanning for treatment of cancer,” said Bruce Cross, MD, citing head/neck cancer as just one example. “Before, we had assumed that if you had a large lymph node, you had to treat the entire lymph node. With PET scanning, you can distinguish which lymph nodes are involved and which ones are not. We have been able to tailor our treatment fields to [target] only the areas involved and to protect, for example, the salivary glands.”

As a radiation oncologist in the Sparks Health System in Fort Smith, AR, Dr. Cross said he uses PET/CT to help treat adults with



Bruce A. Cross, MD

We do a better job here at Sparks in part because of Ambient Experience.

the uptake room are bathed in a warm-colored glow, and patients are provided with a comfortable chair. Patients entering the exam room, meanwhile, can select from several different room themes by using a touchscreen tablet PC. The selected theme is reflected in immediate changes to the room environment, including colored lighting from a skylight and animated projected images accompanied by soothing music and other sounds.

An Ambient Experience suite is also designed to promote operational efficiency that, combined with more relaxed patients, helps improve patient compliance and streamlines PET/CT examinations by reducing patient anxiety.³

**Audiovisual intervention:
A sound solution**

A recent study concluded that “audiovisual intervention” can help to reduce patient anxiety in the PET uptake room and reduce false positive 18F-FDG uptake in brown adipose tissue (BAT) “without the disadvantages associated with pharmacologic interventions.”²

“Throughout the stay in the uptake room, a significant decrease in overall anxiety was found, together with several other significant changes in patient physiology. In the cohort with audiovisual intervention, however, the decrease in patient anxiety was significantly larger. The cohort with intervention also showed significantly lower 18F-FDG uptake in BAT, but not in muscles,” the researchers reported.²

The results of the study of 101 patients were published in the June 2012 issue of the *Journal of Nuclear Medicine Technology*.*

The study results are no surprise to Medhat M. Osman, MD, ScM, PhD, Associate Professor and Medical Director of the Division of Nuclear Medicine and PET/CT, Saint Louis University School of Medicine, St. Louis, Mo.

“Strategies such as Ambient Experience can lead to improved patient management because calmer patients are better able to cooperate, which can impact many aspects of the clinical process,” Dr. Osman said. “And that means happier referring physicians.”

In the opinion of Dr. Cross, the value of Ambient Experience lies in delivering a more successful PET/CT examination because you have a calm, relaxed, and cooperative patient.

“The fact that we have provided [patients] with a distraction or entertainment ... to take their mind off the radioactive agent is a really positive thing,” he said. “It gives them something else to focus on.”

He also said the tropical beach scenes are especially popular with his adult patients. “The beach, with palm trees and the ocean, is a classic mental getaway for adults. If the only thing available were cartoon characters, not many adults would want to see them. That’s why the choice [that the Ambient Experience] offers makes them very happy,” he said.

Dr. Cross said he is “convinced that we do a better job here” at Sparks in part because of Ambient Experience.

“I’ve been very impressed that Sparks went all out on with the Ambient Experience. I am convinced, from my 25 years of experience reading PET scans, that we do a better job here. How much of that is patient cooperation or the excellent algorithms in the technology is hard to tell, but I feel very secure that we’re doing a better job.”

**It is important to note that this study was performed with a prototype configuration that is not commercially available. Ambient Experience as a product service has not been designed nor has it been approved by Philips to have capability to provide the effect described in the study.*

References

1. American Cancer Society. Cancer facts and figures 2012: Leading new cancer cases and deaths-2012 estimates. <http://www.cancer.org/acs/groups/content/@epidemiology-surveillance/documents/document/acspc-032012.pdf>. Last accessed Aug. 28, 2012.
2. Vogel, Wouter V, Valdes Olmos Renato A, Tijs Tim JW, et al. “Intervention to lower anxiety of 18F-FDG PET/CT patients by use of audiovisual imagery during the uptake phase before imaging.” *J Nucl Med Technol*. 2012;40;1-7.
3. Philips Website. Ambient Experience. PET/CT. http://www.healthcare.philips.com/us_en/products/ambient_experience/clinical_solutions/pet_ct/index.wpd. Accessed Aug. 28, 2012.



Ambient Experience can help anxious, unsure patients feel a sense of ease and relaxation in a welcoming environment that soothes and calms.

3T MR imaging protocol for characterization of renal masses

Gaurav Khatri, MD, and Ivan M. Pedrosa, MD

Renal cell carcinoma (RCC) is the third most common genitourinary tumor and seventh most common cancer in the United States. Radical or partial nephrectomy has historically been the standard treatment; however, given the trend towards earlier diagnosis, less invasive treatment options are feasible in appropriate cases.¹ Imaging plays a vital role in detection of renal lesions, in assessing local stage, providing crucial information for planning surgical resection and predicting prognosis, thus contributing to management decision making. Although ultrasonography and computed tomography (CT) have been used for evaluation of renal lesions, magnetic resonance (MR) imaging offers certain advantages over these modalities.

Technology

MR imaging possesses higher inherent contrast resolution than CT or ultrasound. In addition, it has a high sensitivity for detecting tissue enhancement when gadolinium is administered. It is free of known pitfalls, such as pseudoenhancement, seen routinely on CT.²⁻⁴ MR imaging with 3.0 Tesla (3T) systems, high-density phased-array coils, and newly developed sequences, such as multiecho Dixon (mDIXON),⁵ offers robust image quality and excellent spatial resolution. 3T magnets have the advantage of higher signal-to-noise, which can be used to yield shorter acquisition times and/or increased image resolution.² Multiplanar imaging, homogeneous fat suppression, and dynamic contrast-enhanced imaging are also routinely achievable on 3T MR platforms, all of which aid in lesion detection and characterization.

Our institutional 3T renal-mass evaluation protocol is performed with the patient

supine with arms placed above his head using a 16-channel phased-array torso coil. Each sequence is obtained as a breathhold acquisition during patients' end-expiration, which allows for more reproducible anatomic co-registration.² Breath-hold times range from 16 to 22 seconds. Coaching prior to actual image acquisition helps improve breath-hold consistency with resultant successful postprocessing of the subtraction images.² A gadolinium-based contrast agent (GBCA) is administered to patients with baseline estimated glomerular filtration rate (eGFR) >30 mL/min/1.73 m² and without evidence for acute exacerbation of renal disease. The GBCA is administered intravenously via power injector at a dose of 0.1 mmol/Kg or 0.1 mL/Kg followed by a bolus of 20 mL of saline, both at an injection rate of 2 cc/second. The protocol is detailed in Table 1.

T2-weighted sequences

Half-fourier T2-weighted single shot turbo spin echo (SS TSE) images provide excellent image quality due to faster acquisition times than that of conventional multislice echo-train imaging offering a virtual breath-hold independent imaging strategy.² However, breath-hold imaging or respiratory triggering with respiratory bellows (when necessary) is recommended to ensure proper anatomic registration of the images and coverage. Visualization of renal lesions can be optimized by improving the dynamic range when utilizing fat-suppression techniques.

Echo-planar with diffusion-weighted imaging

Echo-planar imaging (EPI) is utilized to obtain diffusion-weighted images (DWI) that allow for detection and characterization of



Ivan M. Pedrosa, MD

Parallel imaging strategies, such as SENSE, with the mDIXON technique, allow for fast volumetric acquisition of the abdomen with decreased motion artifacts due to shorter breath-hold times.

Table 1. 3T MRI protocol for Renal Masses

Sequence	TR (msec)	TE (msec)	Flip Angle (°) (Hz/pix)	Bandwidth Thickness/Gap (mm)	Section	FOV (cm)	Matrix
Coronal T2-weighted SS TSE	960	80	90	652	5/1	40 × 45	312 × 279
Axial T2-weighted fat suppressed SS TSE	920	80	90	543	5/1	40 × 30	304 × 168
Axial DWI	1060	53	90	36.5	7/1	44 × 35	144 × 115
Axial 2D T1-weighted dual echo IP/OP GRE	120	2.3/1.15	55	1215	5/1	40 × 38	400 × 269
Coronal mDIXON	3.8	1.7/2.1	10	1923	3/-1.5	39 × 40	260 × 223
Sagittal mDIXON	3.7	1.32/2.3	10	1568	3/-1.5	30 × 30	248 × 230
Axial mDIXON	3.3	1.16/2.1	10	1852	3/-1.5	38 × 33	252 × 218

lesions based on degree of restriction of water motion. The authors acquire images using respiratory triggering and multiple b values: b0, b50, b400, b800. Apparent diffusion coefficient (ADC) maps are generated based on the diffusion images.

T1-weighted sequences

Pre-contrast T1-weighted images include 2-dimensional (2D) dual echo in-phase (IP) and opposed-phase (OP) gradient-echo (GRE) images acquired in the axial plane.

Although dynamic imaging was traditionally performed utilizing 3-dimensional (3D) T1-weighted fat-saturated spoiled gradient-echo images, recently developed DIXON-based acquisitions, such as the mDIXON sequence, allow for more robust fat saturation (ie, fat-water separation) than traditional sequences that utilize frequency selective fat saturation techniques.^{6,7} The combination of parallel imaging strategies, such as SENSE, with the mDIXON technique allows for a fast volumetric acquisition of the abdomen with decreased motion artifacts due to shorter breath-hold times. Furthermore, the mDIXON technique offers the possibility of reconstructing the acquired data set as T1-weighted IP, OP, and fat-only images (without penalty of added acquisition time) in addition to the water-only

images (ie, fat saturated), which are used for the dynamic contrast-enhanced portion of the study. Pre-contrast mDIXON acquisitions are obtained in oblique sagittal orientation along the long axis of each kidney and also in the coronal plane. Coronal 'fat-saturated' T1-weighted spoiled gradient-echo images (mDIXON) are then acquired during a properly timed corticomedullary phase using a real-time bolus tracking technique (BolusTrack, Philips Healthcare), and then during the early and late nephrographic phase at 40 and 90 seconds after the initiation of the corticomedullary phase. Sagittal oblique mDIXON images are again acquired along the long axis of each kidney during the excretory phase after the coronal dynamic acquisition. Finally, an axial mDIXON acquisition is obtained and 'water only' and 'fat only' image datasets are generated. Subtraction of the pre-contrast images from each of the post-contrast images produce subtracted volumetric image datasets, which are useful for assessing the presence of enhancement in a renal lesion.

Clinical applications

T2-weighted images

Simple cysts appear as homogeneously hyperintense thin-walled structures on T2-weighted images, while septations or solid elements appear hypointense relative to the

Dr. Khatri is an Assistant Professor of Radiology, Body/Body MRI Section, and **Dr. Pedrosa** is Chief of MRI, Associate Professor of Radiology, Department of Radiology, University of Texas Southwestern Medical Center, Advanced Imaging Research Center, Dallas, TX.

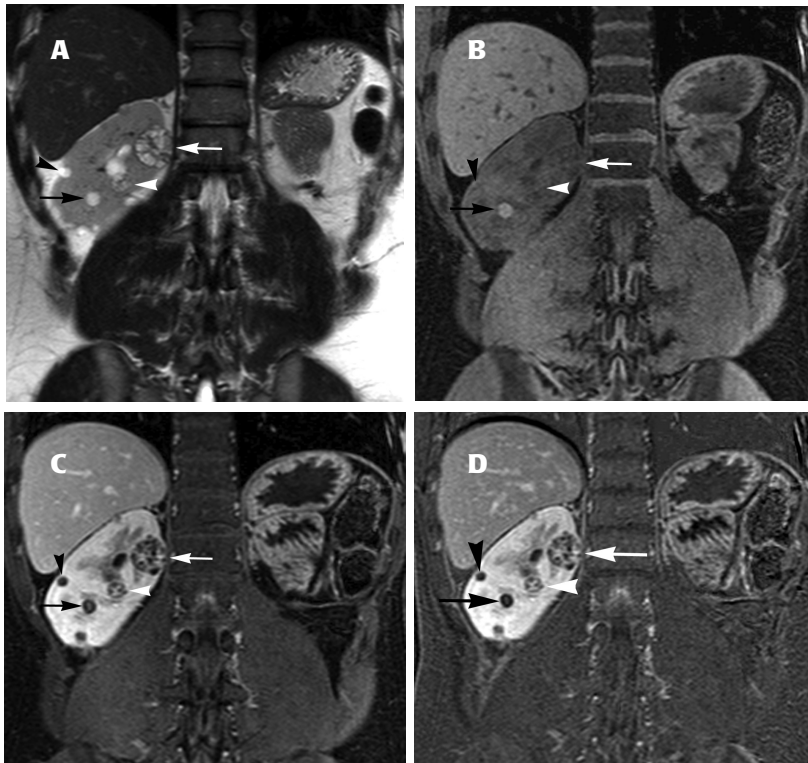


FIGURE 1. Figure 1 demonstrates multiple lesions in the right kidney in a patient with Von-Hippel Lindau (VHL). Two clear-cell renal cell carcinomas (white arrow, white arrowhead) demonstrate predominant hyperintense signal with numerous thick septations on coronal T2-SS TSE image (A), and hypointense signal on coronal mDIXON pre-contrast image (B). The coronal mDIXON post-contrast image (C) shows enhancement of the septations, which is confirmed on the coronal mDIXON subtraction image (D). A smaller lesion in the lower pole (black arrow) is hyperintense on the coronal T2-SS TSE image (A) and hyperintense on coronal mDIXON pre-contrast image (B). Although a majority of the lesion does not appear to enhance on the coronal mDIXON post-contrast image (C), there is a subtle central hyperintense nodule. The coronal mDIXON subtraction image (D) confirms enhancement of this central nodule within a predominantly hemorrhagic lesion. Another small lesion along the lateral cortex (black arrowhead) is hyperintense on the coronal T2-SS TSE image (A), and does not enhance on the coronal mDIXON post-contrast image or on the subtraction image (C and D). This lesion is isointense to the surrounding parenchyma on the coronal mDIXON pre-contrast image (B) and is consistent with a cystic lesion containing hemorrhagic or proteinaceous debris.

hyperintense fluid (Figure 1). Numerous thickened septations increase the likelihood of lesions being malignant.⁸ Hypointense lesions on T2-weighted images may represent solid lesions or cystic lesions with hemorrhagic or proteinaceous contents.⁹ Signal characteristics of solid lesions on T2-weighted images may suggest specific histologic subtyping. Clear-cell RCC, accounting for 65% to 80% of RCC,¹⁰ most

commonly demonstrates increased signal intensity relative to the normal renal parenchyma on T2-weighted images.⁹ Intratumoral necrosis, common in clear cell RCC,¹¹ appears as moderate to high signal intensity on T2-weighted images, although it can occasionally appear hypointense.¹² Intratumoral hemorrhage and fibrosis can be present and exhibits variable signal on T2-weighted images. Clear-cell RCC may present with a capsule or pseudocapsule, which is hypointense on T2-weighted images and discontinuity of the capsule suggests invasion of the perirenal fat and higher grade.^{9,13} Papillary RCC, accounting for approximately 10% to 15% of all RCC,¹⁴ demonstrate homogeneous low signal intensity on T2-weighted images,¹¹ although it may also exhibit foci of hemorrhage and necrosis resulting in a more heterogeneous appearance.⁹ Predominantly fat-containing lesions, such as some angiomyolipomas (AMLs), appear hyperintense on T2-weighted images, and exhibit lower signal on T2-weighted fat-suppressed images. AMLs with minimal fat on the other hand, exhibit homogeneous hypointense signal relative to renal parenchyma on T2-weighted images, but should not demonstrate necrotic elements.⁹

In situations where administration of contrast is contraindicated, T2-weighted images may demonstrate the presence of tumor thrombus in the renal veins and IVC as a filling defect of increased signal intensity against background of dark flow voids.

Diffusion-weighted images

DWI allows for characterization of renal lesions as either solid or cystic based on their degree of restriction of water motion.¹⁵ This may be particularly helpful when intravenous contrast cannot be administered (allergies, renal failure, etc.), precluding evaluation for enhancement. A lesion that remains hyperintense on high b-value images and demonstrates low signal on ADC maps is more indicative of a solid rather than cystic lesion.¹⁵ However, restricted diffusion may be seen in hemorrhagic non-neoplastic contents within a cystic lesion. Although some authors have shown utility of ADC values in differentiation of benign lesions and RCC¹⁶ or between subtypes of RCC,¹⁷

there is considerable overlap in these results, and DWI is not considered as accurate as contrast-enhanced imaging at this time.¹⁶ Although DWI may aid in the detection of lymph nodes, malignant from benign lymph nodes cannot be reliably differentiated based on ADC values.¹⁸

T1-weighted images

Non-contrast T1-weighted dual-phase in-phased (IP) and opposed-phase (OP) gradient refocused echo (GRE) images, a form of chemical shift imaging, are particularly useful when evaluating renal lesions. Intracellular lipids are a relatively common histologic characteristic of clear-cell RCC (approximately 40% of tumors) and can be detected as foci of decreased signal intensity on the OP images when compared to the IP images.^{11,19} Low signal on OP images relative to IP images can be also seen in the setting of AMLs that contain only trace amounts of fat, however, those lesions are indistinguishable from clear cell RCC on these images; the presence of intravoxel fat (ie, decreased signal intensity on OP imaging compared to IP imaging) should not be considered diagnostic of AML as clear cell RCC can also exhibit this finding on MR imaging.²⁰ AMLs with minimal fat, however, tend to be homogeneously hypointense on T2-weighted images compared to the renal parenchyma, whereas clear cell carcinomas tend to be heterogeneous hyperintense on T2-weighted images. The IP and OP phase images may also be helpful to confirm bulk fat in a lesion, which will appear as high signal on both sets of images, however, will exhibit a hypointense rim on OP images (India-ink or edge artifact) at its interface with normal renal parenchyma.⁹ Homogeneous high-signal intensity within a lesion on unenhanced T1-weighted images (without India-ink artifact at its interface with the adjacent renal parenchyma on OP images), as well as on fat-saturated T1-weighted images (Figure 1) is indicative of hemorrhagic or proteinaceous contents.

Contrast enhancement within a lesion after the administration of gadolinium is the most reliable way of differentiating solid from cystic lesions.²¹ Enhancement within a cystic lesion can differentiate debris from true solid tissue (Figure 1). Contrast-enhanced T1-weighted images are also used to characterize the degree

and pattern of enhancement, as this is a reliable differentiating factor between the three most common subtypes of RCC.²²⁻²⁴ During the corticomedullary phase, clear-cell RCC demonstrates avid enhancement, papillary RCC demonstrates relatively low grade enhancement, and chromophobe RCC demonstrates intermediate enhancement. A percentage SI change threshold of 84% in the corticomedullary phase has been shown to differentiate clear cell RCC from papillary RCC with 93% sensitivity and 96% specificity.²³

Post-contrast imaging in the coronal or oblique sagittal planes is particularly helpful to detect small peripheral enhancing components within lesions that are predominantly cystic. Although most of these lesions containing “simple” fluid and small solid components represent low-grade clear-cell RCC, cystic lesions with internal hemorrhage and peripheral-papillary nodules are more likely to be papillary RCC.¹⁹ Other features, such as a delayed enhancing central scar, may favor diagnosis of oncocytoma rather than RCC.⁹

Besides small size, other challenges in detection of enhancing elements include pre-contrast high signal within lesions, which may either mimic or mask enhancing components. Subtraction imaging allows detection of enhancement above and beyond the native pre-contrast hyperintense signal within the lesion²⁵ (Figure 1). It also allows for easier detection of low-grade enhancement in lesions, such as in papillary RCC.¹¹ On the other hand, it may reveal lack of enhancement in a lesion that is hyperintense on post-contrast images owing to inherent high T1-weighted signal. Another potential confounding factor when evaluating a renal lesion on T1 pre- and post-contrast images may be inhomogeneous fat suppression. In addition to decreasing lesion-to-background contrast, inhomogeneous fat suppression can potentially mask enhancement when seen adjacent to the lesion in question. The authors have seen much more reliable and homogeneous exclusion of the fat signal on mDIXON images compared with 3D, T1, fat-suppressed GRE images.⁷ Furthermore, mDIXON acquisition allows for reconstruction of IP, OP, water-only (used for dynamic imaging) and fat-only image

datasets. The fat-only reconstructed images may assist in detection of small amounts of intracellular lipid within lesions, not readily identified when comparing the 2-dimensional IP and OP GRE images.

Post-contrast images can help assess the renal vascular anatomy including the arterial supply to the kidney, which may have surgical implications, as well as the presence of tumor (ie, enhancing) and/or bland (ie, nonenhancing) thrombus with the renal vein and IVC.

Conclusion

MR imaging offers advantages over CT and US for characterization of renal masses and is especially attractive due to its lack of exposure to ionizing radiation, superior inherent contrast differentiation, and multiplanar capabilities. A robust high-quality MR protocol, such as the one outlined in this article, can help facilitate clinical management or provide viable options for imaging follow-up.

References

- Mourad WF, Dutcher J, Ennis RD. State-of-the-art management of renal cell carcinoma. *American Journal of Clinical Oncology*. Epub ahead of print Aug, 2012.
- Zhang J, Pedrosa I, Rofsky NM. MR techniques for renal imaging. *Radiologic Clinics of North America*. 2003;41:877-907.
- Birnbaum BA, Maki DD, Chakraborty DP, et al. Renal cyst pseudoenhancement: Evaluation with an anthropomorphic body CT phantom. *Radiology*. 2002;225:83-90.
- Maki DD, Birnbaum BA, Chakraborty DP, et al. Renal cyst pseudoenhancement: Beam-hardening effects on CT numbers. *Radiology*. 1999;213:468-472.
- Eggers H, Brendel B, Duijndam A, et al. Dual-echo Dixon imaging with flexible choice of echo times. *Magnetic resonance in medicine: Official journal of the Society of Magnetic Resonance in Medicine / Society of Magnetic Resonance in Medicine*. 2011;65:96-107.
- Perkins TG, Van Tilburg JL, Herigault G, et al. Preliminary clinical experience with a multiecho 2-point Dixon (mDixon) sequence at 3T as an efficient alternative for both the SAR-intensive acquired in- and out-of-phase chemical shift imaging as well as for 3D fat-suppressed T1-weighted sequence used for dynamic gadolinium-enhanced imaging. *Proceedings, International Society for Magnetic Resonance Medicine*. Stockholm, Sweden 2010; p. 556.
- Sims RD, Yuan Q, Khatri G, et al. Multiecho 2-point Dixon (mDixon) imaging as an alternative to separate 2D chemical shift imaging and 3D fat-suppressed T1-weighted sequences for gadolinium enhanced imaging. Poster Presentation, International Society for Magnetic Resonance in Medicine. Melbourne, Australia 2012.
- Bosniak MA. The Bosniak renal cyst classification: 25 years later. *Radiology*. 2012;262:781-785.
- Pedrosa I, Sun MR, Spencer M, et al. MR imaging of renal masses: Correlation with findings at surgery and pathologic analysis. *Radiographics: A review publication of the Radiological Society of North America, Inc*. 2008;28:985-1003.
- Bostwick DG, Murphy GP. Diagnosis and prognosis of renal cell carcinoma: Highlights from an international consensus workshop. *Seminars in Urologic Oncology*. 1998;16:46-52.
- Pedrosa I, Chou MT, Ngo L, et al. MR classification of renal masses with pathologic correlation. *European Radiology*. 2008;18:365-375.
- Eilenberg SS, Lee JK, Brown J, et al. Renal masses: Evaluation with gradient-echo Gd-DTPA-enhanced dynamic MR imaging. *Radiology*. 1990;176:333-338.
- Yamashita Y, Watanabe O, Miyazaki T, et al. Cystic renal cell carcinoma. Imaging findings with pathologic correlation. *Acta Radiol*. 1994;35:19-24.
- Leroy X, Zini L, Leteurtre E, et al. Morphologic subtyping of papillary renal cell carcinoma: Correlation with prognosis and differential expression of MUC1 between the two subtypes. *Modern Pathology: An official journal of the United States and Canadian Academy of Pathology, Inc*. 2002;15:1126-1130.
- Qayyum A. Diffusion-weighted imaging in the abdomen and pelvis: Concepts and applications. *Radiographics: A review publication of the Radiological Society of North America, Inc*. 2009;29:1797-1810.
- Taouli B, Thakur RK, Mannelli L, et al. Renal lesions: Characterization with diffusion-weighted imaging versus contrast-enhanced MR imaging. *Radiology*. 2009;251:398-407.
- Wang H, Cheng L, Zhang X, et al. Renal cell carcinoma: Diffusion-weighted MR imaging for subtype differentiation at 3.0 T. *Radiology*. 2010;257:135-43.
- Kwee TC, Takahara T, Luijten PR, et al. ADC measurements of lymph nodes: inter- and intra-observer reproducibility study and an overview of the literature. *European Journal of Radiology*. 2010;75:215-20.
- Pedrosa I, Alsop DC, Rofsky NM. Magnetic resonance imaging as a biomarker in renal cell carcinoma. *Cancer*. 2009;115(10 Suppl):2334-45.
- Hindman N, Ngo L, Genega EM, et al. Angiomyolipoma with minimal fat: Can it be distinguished from clear cell renal cell carcinoma with standard mr imaging techniques? In press *Radiology*.
- Rofsky NM, Bosniak MA. MR imaging in the evaluation of small (< or =3.0 cm) renal masses. *Magnetic Resonance Imaging Clinics of North America*. 1997;5:67-81.
- Kim JK, Kim TK, Ahn HJ, et al. Differentiation of subtypes of renal cell carcinoma on helical CT scans. *AJR American J Roentgenol*. 2002;178:1499-1506.
- Sun MR, Ngo L, Genega EM, et al. Renal cell carcinoma: Dynamic contrast-enhanced MR imaging for differentiation of tumor subtypes—correlation with pathologic findings. *Radiology*. 2009;250:793-802.
- Vargas HA, Chaim J, Lefkowitz RA, et al. Renal cortical tumors: Use of multiphasic contrast-enhanced MR imaging to differentiate benign and malignant histologic subtypes. *Radiology*. 2012;264:779-788.
- Hecht EM, Israel GM, Krinsky GA, et al. Renal masses: Quantitative analysis of enhancement with signal intensity measurements versus qualitative analysis of enhancement with image subtraction for diagnosing malignancy at MR imaging. *Radiology*. 2004;232:373-378.

Clinical Case

Metastatic workup of a morbidly obese patient with colorectal cancer

Julia Grossman, MD, Gaurav Khatri, MD, and Ivan M. Pedrosa, MD

Case summary

A 45-year-old morbidly-obese male (weight 391 lbs (177 kg), BMI >40) initially presented to an outside institution with an obstructing rectosigmoid mass in March 2009. The patient underwent an abdominoperineal resection in April 2009 (T4 lesion with 1/34 nodes positive) and was then treated with chemoradiation followed by chemotherapy until December 2009. After several follow-up computed tomography (CT) scans without evidence of metastatic disease, an outside surveillance CT in April 2012 identified 2 new liver lesions; only one was confirmed on an FDG positron emission tomography (PET) scan in May 2012. Carcinoembryonic antigen remained within normal limits before and after surgery. The patient transferred care to our institution for consideration of surgical resection of hepatic metastasis in May 2012.

Imaging findings

The patient underwent a multiphasic CT with intravenous contrast, which was limited by streak and beam hardening artifact from the patient touching the CT gantry, and identified a single heterogeneous indeterminate lesion in the right lateral hepatic lobe (Figure 1). This was the lesion that was seen on the prior PET/CT (Figure 1). Given the patient's body habitus, an magnetic resonance imaging (MRI) examination of the liver was obtained on a large-bore magnet (Philips Ingenia 1.5T, 70-cm bore), which allows for imaging of patients up to 550 lbs (250 kg). The patient was imaged with a

torso 16-element digital phased-array surface coil. A hepatobiliary contrast agent, Gadoxetate disodium (Eovist; Bayer HealthCare Pharmaceuticals), was utilized to increase conspicuity between the normal liver parenchyma and potential metastases.¹ Six hypoenhancing lesions consistent with metastatic disease were identified with MRI. While some of the lesions were identified on the T2-weighted, diffusion weighted and/or dynamic post-contrast images obtained during the arterial and portal phases, they were better depicted during the hepatobiliary phase acquired 20 minutes after administration of contrast (Figure 1).

Diagnosis

Multiple colorectal metastases to the liver

Discussion

The liver is the most common site of metastatic spread in patients with colorectal adenocarcinoma. Almost 50% of patients with colorectal cancer develop metachronous metastasis in the liver at some time after their primary resection.² New advances in chemoradiation have resulted in improved mortality in patients with metastatic colorectal cancer although surgical resection is still considered the only therapeutic option with potential long-term survival. While the indications for surgical resection of hepatic metastases continue to evolve, the number and location of metastatic lesions remain a critical aspect of the assessment of patients being considered for this therapeutic option.

Dr. Grossman is a Body MRI fellow, **Dr. Khatri** is an Assistant Professor, Body/Body MRI section, and **Dr. Pedrosa** is the Chief-of-MRI, Associate Professor, Department of Radiology, University of Texas Southwestern Medical Center, Advanced Imaging Research Center, Dallas, TX.

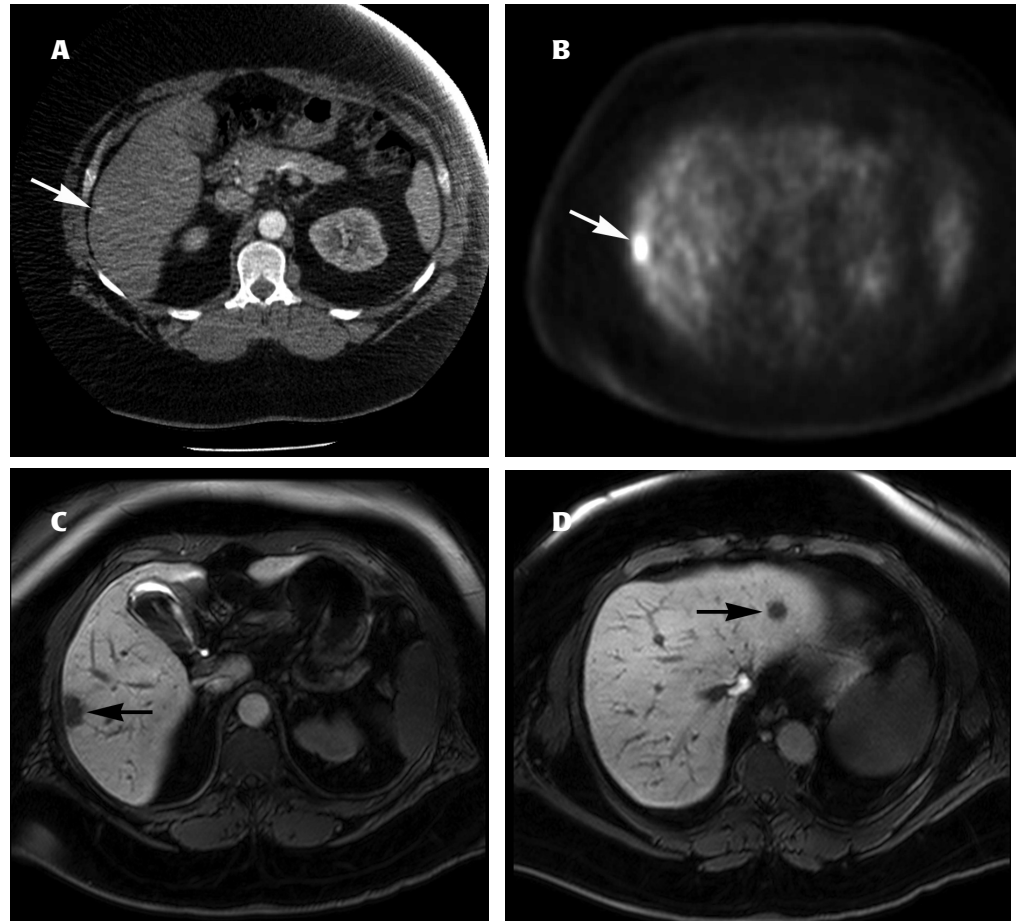


FIGURE 1. (A) An axial CT image at the level of the lower right lobe of the liver obtained during the late arterial phase after administration of intravenous iodinated contrast material demonstrates a heterogeneous focus (arrow) along the lateral margin. The remainder of the liver was unremarkable on this examination (not shown). (B) A PET image corresponding to the same anatomic level as Figure A demonstrates avid focal uptake within the lateral right hepatic lobe (arrow). (C) A 20-minute delayed hepatobiliary-phase MR image with Gadobutrol. A discrete metastatic lesion is well depicted as a focal area of hypointense signal (arrow) corresponding to the area of faint abnormality on CT. (D) A 20-minute delayed hepatobiliary-phase MR image with Gadobutrol. Another discrete metastatic lesion is depicted as focal areas of hypointense signal in the left hepatic lobe (arrow). Up to 4 additional lesions were seen within the liver consistent with metastatic disease (not shown).

Therefore, optimal imaging of the liver is crucial for pre-surgical evaluation of a patient with colorectal cancer.

Metastatic colorectal adenocarcinoma to the liver commonly presents as hypoenhancing lesions, better seen during the portal venous phase when the uninvolved liver parenchyma enhances avidly. As such, it is frequently challenging to diagnose the presence of small liver lesions, as their detection may be challenged by

normal vascular structures and/or the presence of benign incidental lesions (eg, hepatic cysts, hemangiomas). Furthermore, the detection of small hepatic metastasis may be obscured by respiratory artifacts. Additionally, the phenomenon of pseudoenhancement on CT further contributes to the difficulty in detecting small hypovascular liver metastases.³

The liver-specific contrast agent Gadobutrol disodium is transported from the extracellular

space into functioning hepatocytes, where the molecule is subsequently excreted through the hepatobiliary pathway. In patients with normal hepatorenal function, approximately 50% of the agent is excreted via the hepatobiliary pathway.⁴ Imaging in the late arterial, portal venous and early delayed phases is similar to conventional gadolinium agents, as the molecule is within the extracellular blood volume during these acquisitions. The unique 20-minute delayed phase reflects hepatobiliary excretion, as only functioning hepatocytes and bile ducts are hyperintense. Lesions within the liver composed of other cells will be hypointense relative to the background liver, which increases the conspicuity of small nonhepatocellular lesions, such as metastases. The increased sensitivity of Eovist MRI for liver metastases has been reported in the literature.^{1,5}

This case illustrates the technical challenges to adequately imaging a larger patient. The CT images obtained were noisy and demonstrated some beam hardening artifact generated due to the patient's abdominal wall contacting the CT gantry. This examination vaguely demonstrated only the largest lesion, which measured 3 cm in craniocaudal dimension. The patient also exceeded the weight and size limit on several MR magnets at the authors' institution. The ability to perform the MRI examination in a large-bore MRI scanner (70-cm wide), with up to 55-cm field-of-view, provided the opportunity to fit this larger patient comfortably and obtain images of the liver with high diagnostic quality.

Furthermore, digital surface coils, which directly digitize the MR signal before the images are sent to the magnet, provide an improved signal-to-noise ratio over standard analog surface coils, which may be essential in challenging patients, such as the one presented here. In this large patient, the combination of existing hardware, together with the homogeneous fat exclusion achieved with the optimized mDIXON

acquisition,^{6,7} and the administration of a hepatobiliary agent (Eovist) were critical to altering the therapeutic approach by demonstrating several unsuspected liver metastases.

Conclusion

The synergism of state-of-the-art MRI hardware, including a large 70-cm bore, improved signal-to-noise from digital coils, optimized fat exclusion over large fields-of-view using a Dixon-based acquisition (mDIXON), and the use of an hepatobiliary agent (Eovist) were essential in detecting very small lesions in a morbidly obese patient that were not identified on contrast-enhanced CT and PET imaging. This MRI examination was crucial in making a decision about the best treatment options for this patient.

References

1. Bluemke DA, Sahami D, Amendola M, et al. Efficacy and safety of MR imaging with liver-specific contrast agent: U.S. multicenter phase III study. *Radiology*. 2005;237:89-98.
2. Quan D, Gallinger S, Nhan C, et al. The role of liver resection for colorectal cancer metastases in an era of multimodality treatment: A systematic review. *Surgery*. 2012;151:860-870.
3. Tappouni R, Kissane J, Sarwani N, et al. Pseudoenhancement of renal cysts: Influence of lesion size, lesion location, slice thickness, and number of MDCT detectors. *AJR Am J Roentgenol*. 2012;198:133-7.
4. Ringe KI, Husarik DB, Sirlin CB, et al. Gadoteric acid-enhanced MRI of the liver: Part 1, protocol optimization and lesion appearance in the noncirrhotic liver. *AJR Am J Roentgenol*. 2010;195:13-28.
5. Huppertz A, Balzer T, Blakeborough A, et al. Improved detection of focal liver lesions at MR imaging: Multicenter comparison of gadoteric acid-enhanced MR images with intraoperative findings. *Radiology*. 2004;230:266-275.
6. Perkins TG, Van Tilburg JL, Herigault G, et al. Preliminary clinical experience with a multiecho 2-point dixon (mdixon) sequence at 3T as an efficient alternative for both the SAR-intensive acquired in- and out- of-phase chemical shift imaging as well as for 3D fat-suppressed T1-weighted sequence used for dynamic gadolinium-enhanced imaging. *Proc. Intl Soc Mag Reson Med*. Stockholm, Sweden 2010;18:556.
7. Sims RD, Yuan Q, Khatri G, et al. Multiecho 2-Point Dixon (mDIXON) imaging as an alternative to separate 2D chemical shift imaging and 3D fat-suppressed T1-weighted sequences for gadolinium enhanced imaging. Poster Presentation. *Intl Soc Mag Reson Med*. Melbourne, Australia. 2012.

IntelliSpace streamlines the continuum of care

Cristen Bolan

A multidisciplinary approach to cancer diagnosis and treatment can optimize patient care and change outcomes. Studies show that the multidisciplinary setting can be an independent predictor for improved 5-year survival compared to treatment outside of such a setting.¹

In oncology, there are many stakeholders throughout the process of image interpretation, measurement, monitoring, and reporting of cancerous lesions. This requires substantial data sharing and coordination.

At Franciscan Saint Francis Health, Indianapolis, IN, (Saint Francis) the radiology and

oncology departments initiate the process, working closely to review and analyze multi-modality oncology datasets for tumor detection and monitoring. Since they adopted the IntelliSpace Portal, a multidisciplinary data collaboration platform by Philips Healthcare, the doctors and staff at Saint Francis have found the resulting increase in consistency and accuracy key to their success in lesion surveillance and in transforming patient care.

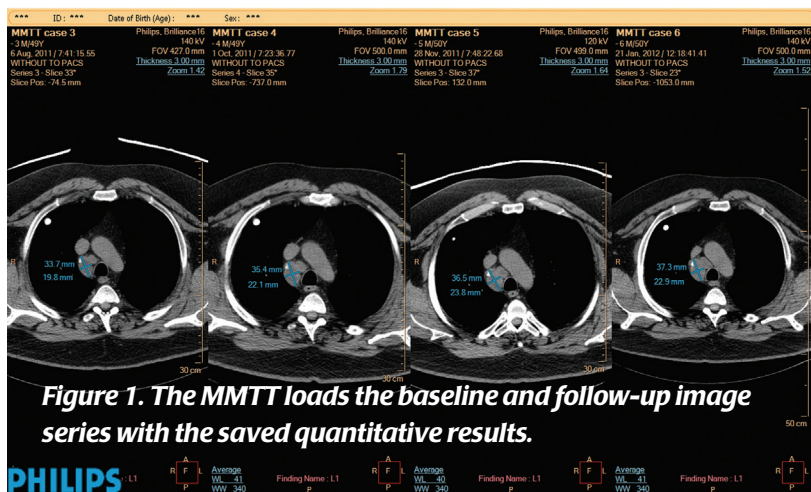
Streamlining lesion surveillance

Several time-consuming steps are involved in lesion surveillance. In many radiology departments, post-processing involves tracking down and loading multiple patient examinations to compare baseline to nadir scans, scrolling through a series of datasets to find the lesions and lymph nodes, measuring quantitative parameters, and calculating tumor burden based on Response Evaluation Criteria in Solid Tumors (RECIST) and World Health Organization (WHO) criteria.

At Saint Francis, radiologists were previously tasked with identifying lesions on a data sheet on the PACS and matching those with prior and current stacks of images before dictating the lesion measurements, explained J. Louis Rankin, RT (R)(MR) (PET), 3D Technical Coordinator, Imaging Services, at Saint Francis.

A complete transformation in workflow was ushered in with the introduction of IntelliSpace Portal, featuring the Multi-Modality Tumor Tracking application (MMTT). The IntelliSpace Portal is a thin-client solution for advanced image review and analysis, designed to share data across multispecialty, multimodality, and multivendor platforms. The MMTT application provides tools to decrease the time required to implement RECIST and supports datasets from CT, MR, PET/CT, and other modalities.

“The IntelliSpace Portal has automated many of these steps,” said Rankin. With the “Smart ROI,” the lesion volume as well as the maximum and minimum diameters can be measured semi-automatically. At the same time, the baseline and follow-up image series with the saved quantitative results are loaded into the MMTT application (Figure 1).



MMTT case 1		Lesions Summary Table			Philips, Brilliance 64
- 1 M/40Y Name	Study Date	Max. 2D diam. (mm)	Perp. 2D diam. (mm)	Max 2D diam * Perp. diam	Zoom 0.00 Contrast
18 Apr, 2011 / 16:32:09	10 Jun 2011	36.55	22.7	829.68	
WITH TO PACS	10 Jun 2011	31.56 (-13.65%)	17.97 (-20.84%)	567.13 (-31.64%)	
	06 Aug 2011	33.74 (-7.69%)	19.76 (-12.95%)	666.7 (-19.64%)	
	01 Oct 2011	35.36 (-3.26%)	22.07 (-2.78%)	780.4 (-5.94%)	
	28 Nov 2011	36.53 (-0.05%)	23.8 (+4.85%)	869.41 (+4.79%)	
	21 Jan 2012	37.28 (+2%)	22.9 (+0.88%)	853.71 (+2.9%)	
L2	18 Apr 2011	24.21	18.25	441.83	
	10 Jun 2011	20.98 (-15.87%)	15.8 (-13.47%)	329.67 (-26.2%)	
	06 Aug 2011	22.37 (-7.6%)	17.08 (-13.41%)	382.08 (-13.52%)	
	01 Oct 2011	24.92 (+9.35%)	18.24 (+0.05%)	454.54 (+2.88%)	
	28 Nov 2011	26.21 (+8.26%)	21.58 (+18.25%)	565.61 (+28.02%)	
	21 Jan 2012	27.63 (+14.13%)	21.69 (+18.85%)	599.29 (+35.64%)	
L3	18 Apr 2011	11.73	7.54	88.44	
	10 Jun 2011	9.44 (-19.52%)	6.01 (-20.29%)	56.73 (-35.85%)	
	06 Aug 2011	10.12 (-13.73%)	7.23 (-4.11%)	73.17 (-17.27%)	
	01 Oct 2011	9.55 (-18.58%)	7.72 (-12.39%)	73.73 (-16.63%)	
	28 Nov 2011	9.39 (-19.95%)	6.92 (-8.22%)	64.98 (-26.53%)	
	21 Jan 2012	11.52 (-1.79%)	7.85 (+4.11%)	90.43 (+2.95%)	
L4	18 Apr 2011	11.69	10.62	124.15	
	10 Jun 2011	12.04 (+2.99%)	8.09 (-23.87%)	97.4 (-21.55%)	
	06 Aug 2011	13.06 (+11.72%)	9.79 (-7.82%)	127.86 (+2.99%)	
	01 Oct 2011	11.7 (+0.09%)	9.2 (-13.37%)	107.64 (-13.3%)	
	28 Nov 2011	12.7 (+8.64%)	9.07 (-14.6%)	115.19 (-7.22%)	
	21 Jan 2012	12.47 (+6.67%)	11.16 (+5.08%)	139.17 (+12.1%)	
Total	18 Apr 2011	84.18	59.11	1484.1	
	10 Jun 2011	73.42 (-12.78%)	47.87 (-19.02%)	1043.26 (-29.7%)	
	06 Aug 2011	79.29 (-5.81%)	53.86 (-8.8%)	1249.81 (-15.79%)	
	01 Oct 2011	81.53 (-3.15%)	57.23 (-3.18%)	1416.31 (-4.57%)	
	28 Nov 2011	84.83 (+0.77%)	61.37 (+3.82%)	1615.19 (+8.83%)	
	21 Jan 2012	88.9 (+5.61%)	63.6 (+7.6%)	1682.6 (+13.38%)	

Figure 2. The MMTT calculates the quantitative RECIST criteria based on percentage change in lesion diameter.

IntelliSpace streamlines the continuum of care

Cristen Bolan

A multidisciplinary approach to cancer diagnosis and treatment can optimize patient care and change outcomes. Studies show that the multidisciplinary setting can be an independent predictor for improved 5-year survival compared to treatment outside of such a setting.¹

In oncology, there are many stakeholders throughout the process of image interpretation, measurement, monitoring, and reporting of cancerous lesions. This requires substantial data sharing and coordination.

At Franciscan Saint Francis Health, Indianapolis, IN, (Saint Francis) the radiology and

oncology departments initiate the process, working closely to review and analyze multi-modality oncology datasets for tumor detection and monitoring. Since they adopted the IntelliSpace Portal, a multidisciplinary data collaboration platform by Philips Healthcare, the doctors and staff at Saint Francis have found the resulting increase in consistency and accuracy key to their success in lesion surveillance and in transforming patient care.

Streamlining lesion surveillance

Several time-consuming steps are involved in lesion surveillance. In many radiology departments, post-processing involves tracking down and loading multiple patient examinations to compare baseline to nadir scans, scrolling through a series of datasets to find the lesions and lymph nodes, measuring quantitative parameters, and calculating tumor burden based on Response Evaluation Criteria in Solid Tumors (RECIST) and World Health Organization (WHO) criteria.

At Saint Francis, radiologists were previously tasked with identifying lesions on a data sheet on the PACS and matching those with prior and current stacks of images before dictating the lesion measurements, explained J. Louis Rankin, RT (R)(MR) (PET), 3D Technical Coordinator, Imaging Services, at Saint Francis.

A complete transformation in workflow was ushered in with the introduction of IntelliSpace Portal, featuring the Multi-Modality Tumor Tracking application (MMTT). The IntelliSpace Portal is a thin-client solution for advanced image review and analysis, designed to share data across multispecialty, multimodality, and multivendor platforms. The MMTT application provides tools to decrease the time required to implement RECIST and supports datasets from CT, MR, PET/CT, and other modalities.

“The IntelliSpace Portal has automated many of these steps,” said Rankin. With the “Smart ROI,” the lesion volume as well as the maximum and minimum diameters can be measured semi-automatically. At the same time, the baseline and follow-up image series with the saved quantitative results are loaded into the MMTT application (Figure 1).

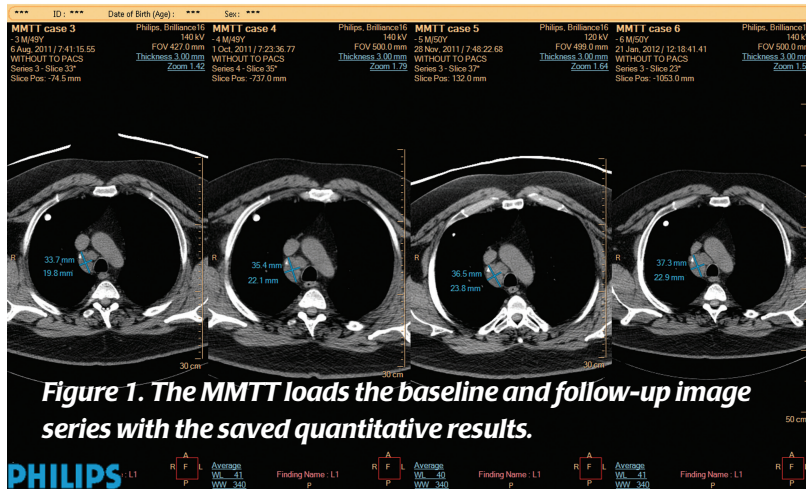


Figure 1. The MMTT loads the baseline and follow-up image series with the saved quantitative results.

MMTT case 1		Lesions Summary Table				Philips, Brilliance 64
- 1 M/49Y Name	Study Date	Max 2D diam. (mm)	Perp. 2D diam. (mm)	Max 2D diam Perp. diam	Zoortm.00 (mm)	
18 Apr. 2011 / 16:32:09	10 Jun 2011	36.55	22.7	829.68	Contrast	
WITH TO PACS	10 Jun 2011	31.56 (-13.65%)	17.97 (-20.84%)	567.13 (-31.64%)		
	06 Aug 2011	33.74 (-7.69%)	19.76 (-12.95%)	666.7 (-19.64%)		
	01 Oct 2011	35.36 (-3.26%)	22.07 (-2.78%)	780.4 (-5.94%)		
	28 Nov 2011	36.53 (-0.05%)	23.8 (+4.85%)	869.41 (+4.79%)		
	21 Jan 2012	37.28 (+2%)	22.9 (+0.88%)	853.71 (+2.9%)		
L2	18 Apr 2011	24.21	18.25	441.83		
	10 Jun 2011	20.38 (-15.82%)	15.8 (-13.42%)	322 (-27.12%)		
	06 Aug 2011	22.37 (-7.6%)	17.08 (-6.41%)	382.08 (-13.52%)		
	01 Oct 2011	24.92 (+9.3%)	18.24 (-0.05%)	454.54 (+8.88%)		
	28 Nov 2011	26.21 (+5.26%)	21.58 (+18.25%)	565.61 (+28.02%)		
L3	21 Jan 2012	27.63 (+14.13%)	21.69 (+18.85%)	599.29 (+35.64%)		
	18 Apr 2011	11.73	7.54	88.44		
	10 Jun 2011	9.44 (-19.52%)	6.01 (-20.79%)	56.73 (-35.85%)		
	06 Aug 2011	10.12 (-13.72%)	7.22 (-4.11%)	73.17 (-17.27%)		
	01 Oct 2011	9.55 (-18.58%)	7.72 (-2.39%)	73.73 (-16.62%)		
L4	28 Nov 2011	9.39 (-19.35%)	6.97 (-8.22%)	64.98 (-26.53%)		
	21 Jan 2012	11.52 (-1.79%)	7.85 (+4.11%)	90.43 (+29.25%)		
	18 Apr 2011	11.69	10.62	124.15		
	10 Jun 2011	12.04 (+2.99%)	8.09 (-23.82%)	97.4 (-21.55%)		
	06 Aug 2011	13.06 (+11.72%)	9.79 (-7.82%)	127.86 (+29.99%)		
Total	01 Oct 2011	11.7 (+0.09%)	9.2 (-13.37%)	107.64 (-13.3%)		
	28 Nov 2011	12.7 (+8.64%)	9.07 (-14.6%)	115.19 (-7.22%)		
	21 Jan 2012	12.47 (+6.67%)	11.16 (+5.08%)	139.17 (+12.1%)		
	18 Apr 2011	84.18	59.11	1484.1		
	10 Jun 2011	73.42 (-12.78%)	47.87 (-19.02%)	1043.26 (-29.7%)		
06 Aug 2011	79.29 (-5.81%)	53.86 (-8.88%)	1249.81 (-15.79%)			
01 Oct 2011	81.53 (-3.15%)	57.23 (-3.18%)	1416.31 (-4.57%)			
28 Nov 2011	84.83 (+0.77%)	61.37 (+3.82%)	1615.19 (+8.82%)			
21 Jan 2012	88.9 (+5.61%)	63.6 (+7.6%)	1682.6 (+3.38%)			

Figure 2. The MMTT calculates the quantitative RECIST criteria based on percentage change in lesion diameter.

The system calculates the quantitative RECIST criteria based on percentage change in lesion diameter (Figure 2) and posts the results on the screen, plotted on a graph over time (Figure 3). All of the quantitative results are stored with the image series, which includes a summary of the results and screen shots of the lesions with treatment response categories for the oncology team to reference.

“Instead of scrolling through the data, finding the lesion, and wondering if it’s the correct target lesion, now the application does that for you,” said Rankin.

The follow-up series is automatically sent to the IntelliSpace Portal Server, also reducing substantial amounts of time.

“Once a study is in tumor tracking, it can save 20 to 30 minutes of prep time for the physician to read,” said Rankin.

The new process also cuts reading time by 5 to 10 minutes for a 5-lesion study, indicated Andrew J. Mullinix, MD, Diagnostic Radiologist at Saint Francis. “The hassle factor that it takes away is huge because you’re no longer spending a lot of time searching for the lesions when you could be adding diagnostic information,” Dr. Mullinix said.

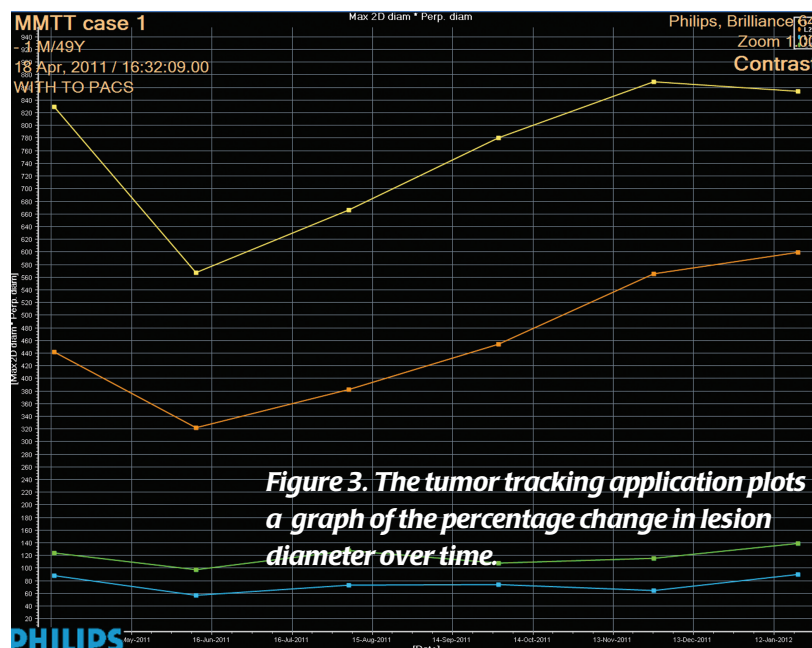
Enhanced quality in patient care

Consumers are becoming more actively involved in healthcare decisions, thanks largely to demand for more efficiency.²

The MMTT tumor tracking application increases efficiency by enabling consistency and accuracy in lesion tracking. Dr. Mullinix said one of the most useful features of MMTT is its ability to plot a graph of the lesions over time. “Because you’re comparing the lesion to 3 or 4 or 5 prior studies, you get a nice longitudinal feel for what the tumor is doing, not just a staccato sense,” he said.

Improved efficiency can enhance quality of care. A recent patient of Dr. Mullinix presented with 2 mediastinum lymph nodes and 2 lung nodules. Dr. Mullinix was able to see, on a single graph, progressive disease in the mediastinum, but not in the lung nodules—circumstances that changed the course of treatment.

Once a radiologist completes a report, the oncology group can move forward with lesion response. The graph is especially helpful with monitoring progressive disease. “If a patient has reached 20%, he has progressive disease and



must come off study,” explained Cindy Stoner, CCCP (Certified Clinical Research Professional). “With the real-time data on tumor percentage changes in tumor sizes plotted on the graph, the oncology team can better prepare patients for changes in treatments,” Stoner said.

“Today, our patients are so informed about the drugs and treatment, they call for the results right after each scan. Tumor tracking has allowed us to give them more information, and prepare patients if we have to take them off study and suggest alternatives,” she added.

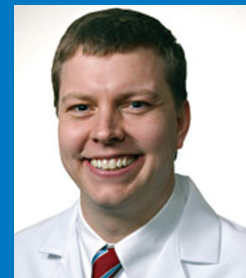
Consistency across disciplines

IntelliSpace Portal and the tumor tracking application have helped optimize oncological lesion surveillance by automating steps, saving time, and improving the presentation of the data.

“The workflow takes a team approach, and the IntelliSpace Portal has impacted my workflow,” said Dr. Mullinix. “It has made our workflow smoother, the lesions are easier to find, it’s easier to report, and it makes the referring physicians happy because it’s a more complete report.”

Ultimately, it is transforming the way doctors at Saint Francis deliver care.

“The best part about IntelliSpace,” said Rankin, “is the accuracy and consistency. The more accurate and consistent we are, the more volumes of data we can build up, which will help us be more accurate and concise with cases in the future.”



Andrew J. Mullinix, MD

Workflow takes a team approach, and the IntelliSpace Portal ... has made our workflow smoother.

References

1. Junor EJ, Hole DJ, Gillis CR. Management of ovarian cancer: Referral to a multidisciplinary team matters. *Br J Cancer*. 1994;70:363-370.
2. Moser JW, Wilcox PA, Bjork SS, et al. Pay for performance in radiology: ACR White Paper. *J Am Coll Radiol*. 2006;3:650-664.

Striking a balance in PET imaging transforms patient care

Medhat M. Osman, MD, PhD

Dr. Osman is the Program Director of the Division of Nuclear Medicine, Department of Radiology, Saint Louis University Hospital, St. Louis, MO.



Medhat M. Osman, MD, PhD

TOF PET has been shown to significantly improve lesion detection compared to non-TOF images.

One of the most significant transformations in patient care can be achieved simply by striking a balance across the continuum of care. This is especially true when managing oncology patients from diagnosis to staging to monitoring disease, where managing tradeoffs is critical to delivering the best treatment.

As the second most common cause of death in the United States, preceded only by cardiovascular disease (CVD), cancer accounts for nearly 1 of every 4 deaths.¹ In 2012, an estimated half-million Americans, or >1,500 people a day, were expected to die of cancer.¹

The use of integrated positron emission tomography and computed tomography (PET/CT) imaging with ¹⁸F fluorodeoxyglucose (FDG) is a widely established imaging technique with major indications in oncology for staging, re-staging, and monitoring response to therapy.² In fact, at leading nuclear medicine institutions, such as Saint Louis University School of Medicine, St. Louis, MO, 90% of PET studies are conducted on patients with cancer, while the other 10% is divided among neurological and cardiac PET-imaging studies. The majority of PET studies involve lymphoma and cancers of the lung, head and neck, colon, esophageal, melanoma, and breast.

One of the challenges with PET/CT imaging is respiratory motion, which can have a major degrading impact on PET-based tumor quantification and delineation,³⁻⁷ and inhibits the ability to define accurate target volumes in radiation oncology. This is particularly true for small lesions found in borders between organs, such as the lung and liver.

In lesion detection, the challenge is the difference in the resolution. In the PET world, the

accuracy of a lesion 1 cm or less in size used to be suboptimal. It was even more complicated if the same small-size lesion was in a patient with a high body-mass index (BMI). In obese patients, scatter and attenuation artifacts led to more challenges in identifying and characterizing small lesions.

Additionally, with organized industry efforts, such as ALARA (as low as reasonably achievable) and the Image Gently® Campaign, to lower the levels of radiation dose patients are exposed to during medical imaging exams, radiologists and nuclear medicine physicians have been challenged to find strategies to manage dose without degrading image quality.

The main problem we have had in PET imaging is how to balance scanner throughput without compromising image quality and without having to resort to higher radiotracer dose. Up until now, balancing image quality, dose and scan time has been the tradeoff.

The Ingenuity TF PET/CT advantage

The need for more accurate tumor quantification and delineation has led to the development of technology that enables high-quality PET/CT images to be acquired at low dose levels.

Philips Ingenuity TF PET/CT addresses the challenges of localization, specificity and low dose in oncology and neurological imaging exams, and overcomes obstacles for conducting cardiac perfusion and diagnostic CT studies. The system is equipped with Astonish TF with 4-dimensional (4D) time-of-flight (TOF) capabilities for high-speed and full-fidelity PET imaging. With 495 picoseconds (ps) timing resolution on the system, Astonish TF provides the fastest timing resolution currently

available, helping to lead to enhanced localization of events.

Astonish TF provides TOF technology designed to enhance image quality by reducing noise and providing high sensitivity. The high-quality images help to improve lesion detection and localization to increase diagnostic confidence and preserve healthy tissue during treatment. This latest generation in TOF technology leads to enhanced contrast by up to 30% compared to non-TOF images.

The 4D component of TOF is designed to provide additional image quality and standard uptake value (SUV) quantitation improvements to account for patient movement during respiratory-gated studies. In fact, Astonish TF shows up to 50% improved contrast resolution, while maintaining quantitative accuracy with up to 4 times the reconstruction speed of previous-generation systems.

Low dose techniques for quality imaging

To address the need to manage CT dose without sacrificing image quality, the system comes available with iDose⁴, a CT iterative reconstruction technique.

As an iterative reconstruction technique, iDose⁴ gives the user control of the dial, enabling clinicians to personalize image quality based on the patients' needs at low dose. iDose⁴ is designed to improve spatial resolution at low dose, reduce noise with a natural appearance, provide robust artifact prevention, and improve image quality*. In fact, iDose⁴ improves spatial resolution by up to 57% on the Ingenuity CT platform.

List mode capabilities

Another important feature of Astonish TF for improving lesion detection is list mode reconstruction capabilities. This technology records each event and timing sequentially to enhance image resolution and improve accuracy. By leveraging list-mode reconstruction, Astonish TF can provide higher accuracy in SUV values without compromising performance.

List mode reconstruction enables us to acquire all the information with a single event at a time and to process this data in a short amount

of time. It produces a more uniform picture and better tradeoff. What's unique about the Astonish TF is what's described as full fidelity, and it is the only TOF that offers a highly accurate way to reconstruct images in a very fast mode.

Clinical applications

Improving lesion detection

The clinical advantage of TOF technology for PET is that it produces sharper images that are better for lesion detection and localization. This increases diagnostic confidence for the physician and contributes to preserving healthy tissue during radiation therapy treatments.

Another advantage of the TOF is the ability to see smaller and smaller lesions that, until recently, were unable to be detected and/or characterized.

In a recent study,⁷ TOF PET yielded a significant improvement in lesion detection in oncologic studies over all contrasts and BMIs, and this improvement was greater for lower lesion contrasts. The study evaluated 100 patients with various body types and found that TOF PET scans improved the signal-to-noise ratio for both liver and lung images and resulted in improvement in lesion detection.

Fast image acquisition in TOF PET is enabling doctors to acquire head-to-toe whole-body images acquisitions in a reasonable amount of time without compromising the throughput of the scanner. We are able to see smaller lesions, get better image quality, and image head-to-toe in a reasonable amount of time.

In a recent case, a 65-year-old male presented with a history of laryngeal cancer. Chest, abdomen, and pelvic contrast-CT images revealed an esophageal lesion with no nodal or distant metastases. The PET/CT was ordered for initial treatment strategy. The PET/CT (Figure 1) images revealed a large FDG-avid esophageal mass as well as a 3-mm node FDG-avid abdominal node (Figure 2). While a 3-mm node appeared normal on a CT scan, it was very FDG-avid on PET, demonstrating the metabolic size was significantly larger than the anatomic size (Figure 2). A subsequent biopsy confirmed lymph-node metastases, which changed staging and management in this case.



Figure 1. Static MIP image showing a large FDG-avid esophageal mass and a small FDG-avid abdominal node.

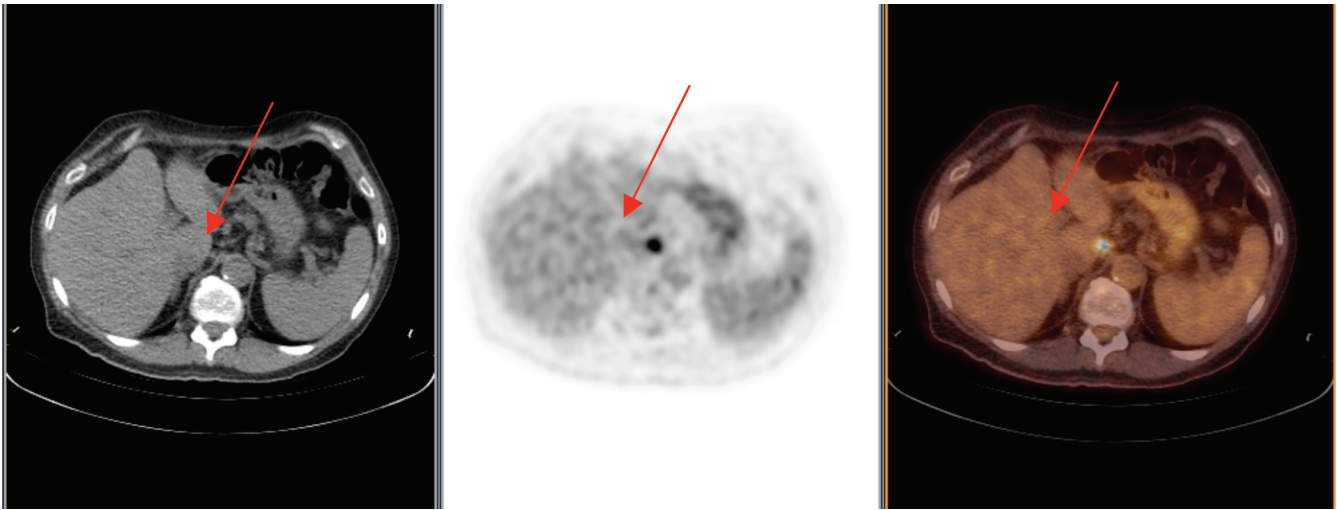


Figure 2. The presence of the 3-mm node (arrows) metastases on the PET/CT scan showed a highly suspicious abdominal node. A subsequent biopsy confirmed nodal metastases. The 3-mm abdominal metastases, which were missed on CT, changed staging and management in this case.

Expanding neuro-imaging applications

While the majority of PET/CT procedures today are geared toward oncology applications, there are a growing number of PET/CT neurological and cardiovascular imaging studies.¹⁰ Most clinical procedures for neurological imaging are for dementia, epilepsy, and brain tumors. Although FDG for brain imaging is still the most important PET/CT tracer, this may change with the recent approval of amyloid tracers for conditions, such as Alzheimer's Disease. Accordingly, neurological imaging is an area that is expected to experience tremendous growth.

The recent FDA approval of amyloid imaging agents may improve diagnostic evaluation of patients with suspected dementia.⁸ This coupled with new promising treatment agents may open the door for the routine incorporation of PET in clinical trials in patients with cognitive impairment.

Cardiovascular imaging

In managing patients with known or suspected coronary artery disease, PET/CT is increasingly used to perform tests on the patient at rest or with stress for noninvasive imaging of the perfusion of the heart.⁹

The introduction of the F-18-based cardiac tracer may present a shift in myocardial nuclear imaging from SPECT to PET. This is possible because image quality in PET is much better than

in the SPECT images and is much faster. A whole stress-rest study can be completed in one hour as opposed to 4 hours in the SPECT world.

Astonish TF and PET/CT and F-18-based cardiac tracers will change how nuclear cardiology is being utilized. It will open a whole new area in nuclear cardiology and PET utilization.

Tailored treatment in bariatrics

Another clinical condition that is transforming patient care is obesity. More than 100 million people in the U.S. are defined as obese, 12 million of whom have extreme obesity.¹⁰ Along with the increasing number of obese patients comes a growing challenge to diagnostic imaging.

A recent study¹¹ showed TOF scans can help improve lung and liver lesion detectability in heavy patients. This is critical at Saint Louis University School of Medicine, where nearly half of all patients presenting for nuclear medicine exams are obese.

Fundamental to improving image quality in patients with a high BMI is higher sensitivity. The TOF serves as a sensitivity amplifier. On average scanners, to achieve higher detectability of smaller lesions, an injection of a significantly higher dose of FDG may be necessary. But with TOF, small lesions may be detected in obese patients by adjusting imaging protocols and with minimal increase in injected dose. We therefore

have higher sensitivity due to the inherent lower signal-to-noise ratio in the TOF scanner.

With solutions like TOF, imaging patients with a large body habitus is feasible.

We use the least amount of radiation, and we are able to produce interpretable scans in patients with high BMI where at other sites these images may be of lower quality.

Transforming patient care for the future

While the adoption of PET for neurological and cardiac imaging promises to revolutionize the future of patient care, we are already seeing a significant transformation today.

We have fast image acquisition, and we are able to detect smaller lesions, produce better quality images independent of body mass index, and on this PET/CT system we can better manage radiation.

Balancing image quality, dose, and scan time no longer has to be a matter of managing tradeoffs. With Astonish TF, we can already strike that balance without compromise.

**Note: Improved image quality is defined by improvements in spatial resolution and/or noise reduction as measured in phantom studies.*

References

1. American Cancer Society: Cancer Facts and Figures 2012. Atlanta, Ga: American Cancer Society, 2012. Last accessed January 6, 2012.

2. Julianne Suhy, BS, CNMT, RT(N), Piotr J. Maniawski, MSc. Routine clinical applications of 4D TOF PET/CT. Philips Healthcare – Nuclear Medicine, Cleveland, OH. http://clinical.netforum.healthcare.philips.com/us_en/Explore/List?modalities=PetCT&documentTypes=White-Papers.

3. Lui C, Alessio A, Kinahan PH. Respiratory motion correction for quantitative PET/CT using all detected events with internal–external motion correlation. *Med Phys*. 2011;38:2715-2723.

4. Erdi YE, Nehmeh SA, Pan T, et al. The CT motion quantitation of lung lesions and its impact on PET-measured SUVs. *J Nucl Med*. 2004;45:1287-1292.

5. Thorndyke B, Schreiber E, Koong A, Xing L. Reducing respiratory motion artifacts in positron emission tomography through retrospective stacking. *Med Phys*. 2006;33:2632-2641. doi: 10.1118/1.2207367.

6. Nehmeh SA, Erdi YE. Respiratory motion in positron emission tomography/computed tomography: A review. *Semin Nucl Med*. 2008;38:167-176. doi: 10.1053/j.seminuclmed.2008.01.002.

7. Kawano T, Ohtake E, Inoue T. Deep-inspiration breath-hold PET/CT of lung cancer: Maximum standardized uptake value analysis of 108 patients. *J Nucl Med*. 2008;49:1223-1231. doi: 10.2967/jnumed.107.049296.

8. Yang L, Rieves D, Ganley C. Brain Amyloid Imaging – FDA Approval of Florbetapir F18 Injection. *N Engl J Med*. 2012;367:885-887. September 6, 2012 DOI:10.1056/NEJMp1208061.

9. Cardiac PET and PET/CT Imaging Practice Guidelines. A summary of the recommendations and practice guidelines of professional groups. SNM PET Center of Excellence. http://www.snm.org/docs/PET_PROS/CardiacPracticeGuidelinesSummary.pdf. May 2009.

10. Gordon-Larsen P, Adair LS, Nelson MC, Popkin BM. Five-year obesity incidence in the transition period between adolescence and adulthood: The National Longitudinal Study of Adolescent Health. *Am J Clin Nutr*. 2004;80:569-575.

11. El Fakhri et al. Improvement in lesion detection with whole-body oncologic time-of-flight PET. *J Nucl Med*. 2011; 52:347-353.

Astonish TF and PET/CT and F-18-based cardiac tracers will change how nuclear cardiology is being utilized.

Medhat M. Osman, MD, PhD

Clinical Case

Recurrent lymphoma in the left acetabulum

Razi Muzaffar, DO, and Medhat M. Osman, MD, PhD

Dr. Muzaffar is a Fellow and **Dr. Osman** is the Program Director of the Division of Nuclear Medicine, Department of Radiology, Saint Louis University Hospital, St. Louis, MO.

Case summary

A 75-year-old female presented to our outpatient clinic for her annual follow-up for lymphoma. She had been diagnosed 5 years prior with marginal zone lymphoma in the mediastinum with recurrent pleural-effusions status post-chemotherapy and eventually pleurodesis. Since that time, she had multiple negative positron emission tomography and computed tomography (PET/CT) scans.

Imaging findings

PET/CT demonstrated stable focal uptake in the thyroid and post-pleurodesis changes in the chest (Figure 1). A new subtle ¹⁸F-fluorodeoxyglucose (¹⁸F-FDG) focus was present in the left acetabulum with normal CT raising the suspicion for metastasis (Figure 1). Magnetic resonance imaging (MRI) demonstrated an irregular lesion within the left acetabulum with increased signal on short T1-inversion recovery (STIR) and low signal on T1 and T2, suggestive of an intraosseous vascular lesion (Figure 2). The follow-up PET/CT demonstrated significant increased size and FDG uptake in the acetabular lesion consistent with disease progression (Figure 3).

Diagnosis

Recurrent lymphoma in the left acetabulum

Discussion

Lymphoma is a malignancy of lymphocytes and is usually present as a solid tumor composed of lymphoid cells. Lymphoma can be classified into 2 groups, Hodgkin lymphoma and non-Hodgkin lymphoma (NHL). Hodgkin lymphoma derives from abnormal B cells whereas NHL can arise from abnormal B or T cells. The malignant cells accumulate in lymph nodes, but can also involve other organs, such as skin, brain, bowel, and bones. Since these lymph nodes or extranodal sites are typically subtle, they are often felt to be normal or reactive on CT. However, ¹⁸F-FDG PET/CT helps differentiate the indeterminate cases. A recent study found ¹⁸F-FDG PET/CT was more accurate than CT alone in early detection of bone metastasis and improved staging in 15% of the study population.¹

The use of ¹⁸F-FDG PET/CT has been gaining momentum in diagnosing, staging, and restaging many cancers and is often better than anatomical imaging alone.² According to the Academy of Molecular Imaging, there are more than 5,000 PET/CT systems installed worldwide, making it one of the fastest growing imaging modalities.³ The National Oncologic PET Registry (NOPR) was developed in 2006 to collect data on the clinical utility of PET. As of June 2012, it has evaluated over 280,000 PET

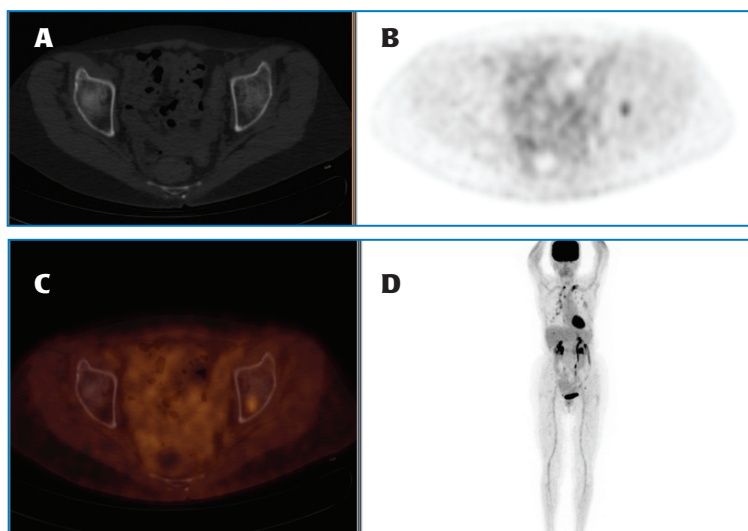


FIGURE 1. The image (B) shows subtle FDG focus on PET (top right). There is no significant abnormality on CT (A) (top left). A fused PET/CT (C) demonstrates focal FDG uptake in the left acetabulum (bottom left). There is a maximum intensity projection PET image (D) (bottom right).

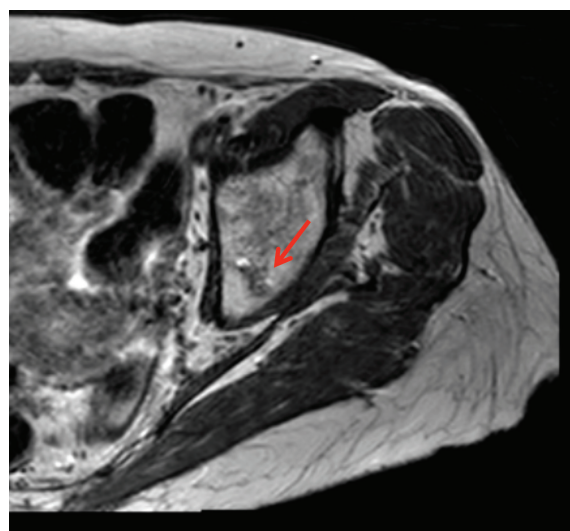


FIGURE 2. MRI demonstrates an irregular lesion in the left acetabulum suggestive of an intraosseous vascular lesion (arrow).

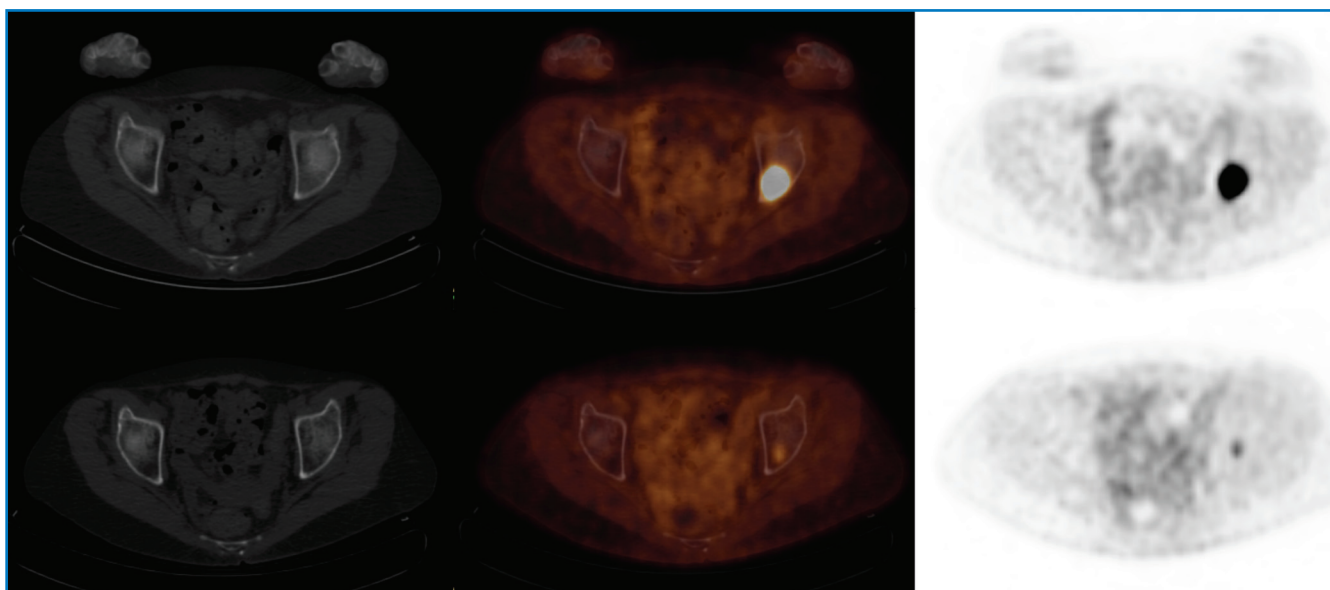


FIGURE 3. A follow-up PET/CT demonstrates significantly increased size and FDG uptake in the left acetabular lesion (top row) as compared to the prior study (bottom row).

studies performed at 1,756 centers.⁴ The fusion of functional and anatomic imaging continues to evolve and provide valuable clinical information. PET/CT provides additional informa-

tion as compared to either modality alone and has become the first-line imaging modality for tumor staging, restaging, and therapy response in various types of cancer.⁵

Another advancement of PET/CT is the use of time-of-flight (TOF) to improve lesion detection, especially in heavier patients. Conventional PET scanners detect gamma rays from radioisotopes injected in the body. However, they do not account for the time it takes to reach the detector. TOF will account for this time, resulting in an enhanced signal-to-noise ratio. TOF PET has been shown to significantly improve lesion detection compared to non-TOF images of 8.3% in the liver and 15.1% in the lungs. The greatest improvement was for lower lesion contrasts.⁶ The availability of such technology improves our ability to characterize lesions and affect treatment decisions and patient management.

Conclusion

A bone biopsy was performed and revealed metastatic lymphoma. The patient was treated with chemotherapy and is now in remission. PET/CT images can be used in the evaluation,

diagnosis, and staging of cancer. As in this case, PET/CT was both more sensitive and specific than MRI.

References

1. Evangelista L, Panunzio A, Polverosi R, et al. Early bone marrow metastasis detection: The additional value of FDG-PET/CT vs. CT imaging. *Biomed Pharmacother.* 2012. 66:448-453.
2. Czernin J, Allen-Auerback M, Schelbert HR. Improvements in cancer staging with PET/CT: Literature-based evidence as of September 2006. *J Nucl Med.* 2007;48(Supplement 1):78S-88S.
3. "International Survey of PET/CT Operations and Oncology Imaging 2010." Academy of Molecular Imaging. http://www.ami-maging.org/index.php?option=com_content&task=view&id=181. Accessed September 19, 2012.
4. "NOPR Update: Monthly Status Report." National Oncologic PET Registry. <http://www.cancerpetregistry.org/status.htm>. Accessed September 19, 2012.
5. Antoch G, Vogt FM, Freudenberg LS, et al. Whole-body dual modality PET/CT and whole-body MRI for tumor staging in oncology. *JAMA.* 2003;290:3199-3206.
6. El Fakhri G, Surti S, Trott CM, et al. Improvement in lesion detection with whole-body oncologic time-of-flight PET. *J Nucl Med.* 2011;52:347-353.

Low-dose, high-quality SPECT/CT imaging transforms patient care

Medhat M. Osman, MD, PhD

Today, more than ever, doctors are transforming patient care through the early detection and diagnosis of disease, giving patients a greater chance of survival.

The 5-year relative survival rate for all cancers diagnosed between 2001 and 2007 is 67%, up from 49% in 1975-1977. More specifically, for detection of breast cancer at the early localized stage, the 5-year survival rate is 98%,¹ for prostate cancer it is 99.6%,² and for stage 1 lung cancer it is 45% to 49%.³ The improvement in survival reflects both progress in diagnosing certain cancers at earlier stages and improvements in treatment.⁴

Much of this early detection is achieved through medical imaging technology. One imaging technology that is gaining more widespread use is the combination of single photon emission computed tomography (SPECT) and computed tomography (CT). In the nuclear medicine division at Saint Louis University School of Medicine, Saint Louis, MO, 50% of the patients referred for a nuclear medicine study receive a SPECT/CT exam. The majority are scanned for metastatic bone disease, pheochromocytoma, neuroblastoma, and cardiac imaging, and the remaining for musculoskeletal, hepatobiliary, renal, and neurological conditions.

With the recent installation of the BrightView XCT SPECT/CT system by Philips Healthcare, doctors at Saint Louis University School of Medicine are effectively changing patient management, while lowering the radiation dose in some cases and increasing the speed of image acquisition and reporting in others.

Clearing technical hurdles

Hybrid SPECT/CT imaging has been instrumental in overcoming some of the inherent shortcomings of SPECT imaging, in particular the lack of anatomic localization.

While SPECT gave us tomographic information and higher sensitivity than planar, you still had challenges with localization of lesions because there still wasn't the detailed anatomy from the CT.

Some hybrid SPECT/CT systems combine SPECT cameras with conventional diagnostic CT systems. While these dual-gantry systems resolve the localization challenges, they also introduce additional complexities of their own.

Although the addition of the CT addressed these challenges by adding the anatomy and the localization of lesions, it brought with it its own challenges, including a larger footprint, increased radiation dose, and more training for the technologists and physicians. The radiation from the CT was also an important consideration in pediatric patients.

The unique design of the BrightView XCT system overcomes many of these obstacles. This hybrid imaging system integrates a full-featured variable angle gamma camera with a flat-panel cone-beam CT component used for localization and attenuation correction of the SPECT data. The flat-panel CT component is mounted on the same rotatable gantry as the SPECT detectors. This coplanar configuration reduces room size requirements and system weight compared to hybrid systems using spatially separated SPECT and CT gantries.

Dr. Osman is the Program Director of the Division of Nuclear Medicine, Department of Radiology, Saint Louis University Hospital, St. Louis, MO.



Medhat M. Osman, MD, PhD

The flat-panel CT acquires a low dose (0.12 mSv) CT image of the entire heart volume in just one 60-second rotation while the patient is breathing normally.



FIGURE 1. A whole-body bone scan with focal uptake in the left distal femur indicates the differential diagnosis includes benign and malignant conditions.

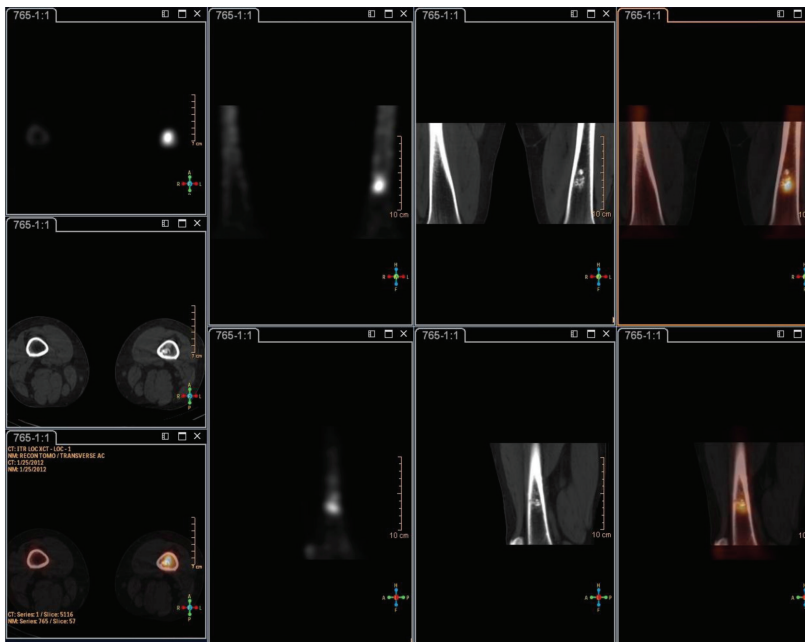


FIGURE 2. SPECT/CT of distal femurs show focal intense uptake within the bone marrow with some calcification, more likely benign.

Furthermore, it reduces the amount of table translation required between the SPECT and CT imaging position. The flat-panel localization images are acquired with a fraction of the dose compared to a diagnostic CT exam, using less power to operate and without requiring any additional dose for a scout or topogram image that conventional CT scanners require. Furthermore, the high-resolution flat-panel detector enables true isotropic voxels, which means that image resolution is maintained when the data are viewed from any angle. This is particularly important in the context of SPECT/CT imaging, since SPECT data also have isotropic voxels and are routinely reviewed in transverse, sagittal and coronal views.

A costly problem for hospitals when acquiring a new system is retrofitting an existing floor plan, which can be prohibitively expensive. However, BrightView XCT's footprint is compact and fits into rooms as small as 15' 6" × 11' 7" (4.72 meters × 3.53 meters) with minimal shielding, and, in most cases, there is no need to reinforce flooring.

The BrightView XCT was a solution that made everyone happy—the hospital and physicians. It gave us the same footprint as the dedicated SPECT camera, so we didn't have to build out a larger room. Since the system was designed entirely for nuclear medicine, the learning curve on the technology was not as steep as with other SPECT/CT scanners, and training the staff did not pose any significant concerns. We were able to overcome a lot of the limitations of SPECT/CT when we installed the BrightView XCT, and we promoted this fact to our referral network.

Hybrid imaging technology will become the gold standard for conventional scintigraphy for a number of oncology applications, including bone imaging for staging malignancy, tumor scintigraphies that visualize neoplastic foci via tumor-specific agents, such as octreotide labeled with ^{111}In or ^{131}I , and sentinel lymph node scintigraphy, where SPECT/CT fusion helps considerably in localizing the first lymph node draining a tumor.⁵

With the localization of SPECT uptake that CT provides, physicians are better able

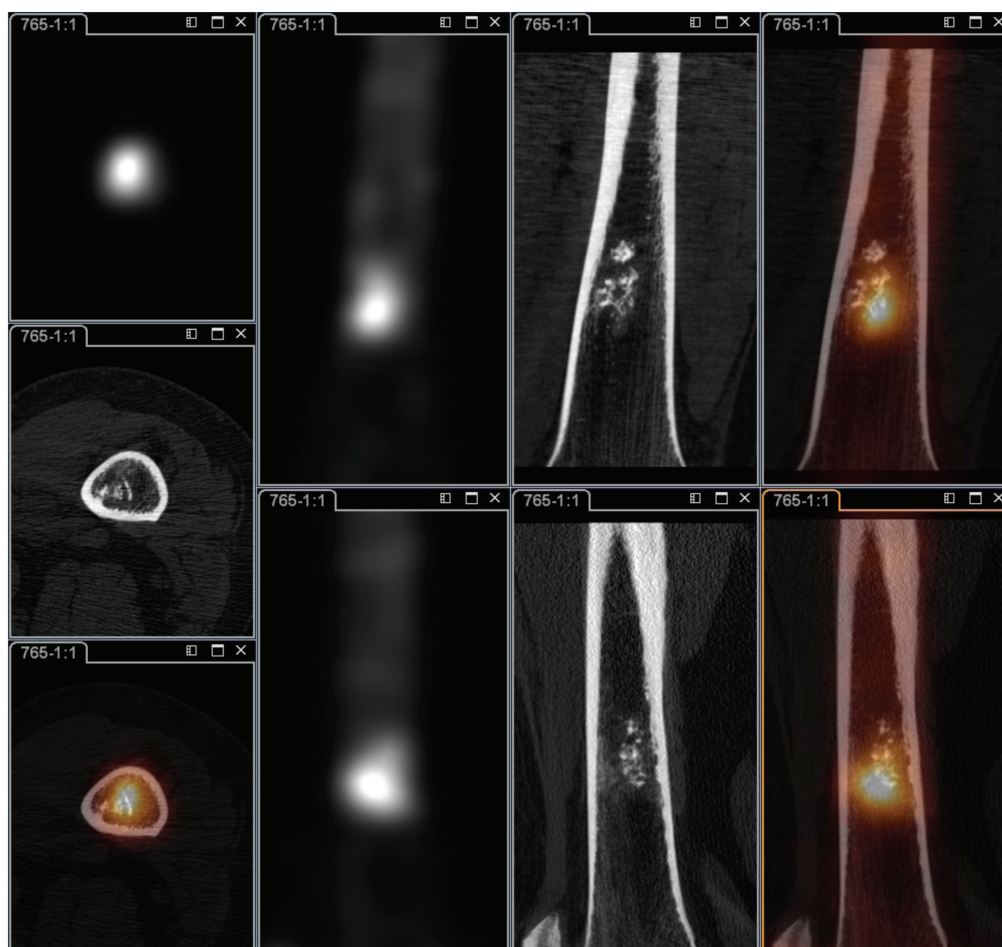


FIGURE 3. A high-resolution SPECT/CT of the left distal femur shows stippled calcifications within the distal femoral intramedullary cavity without additional aggressive features, which is highly suggestive of enchondroma.

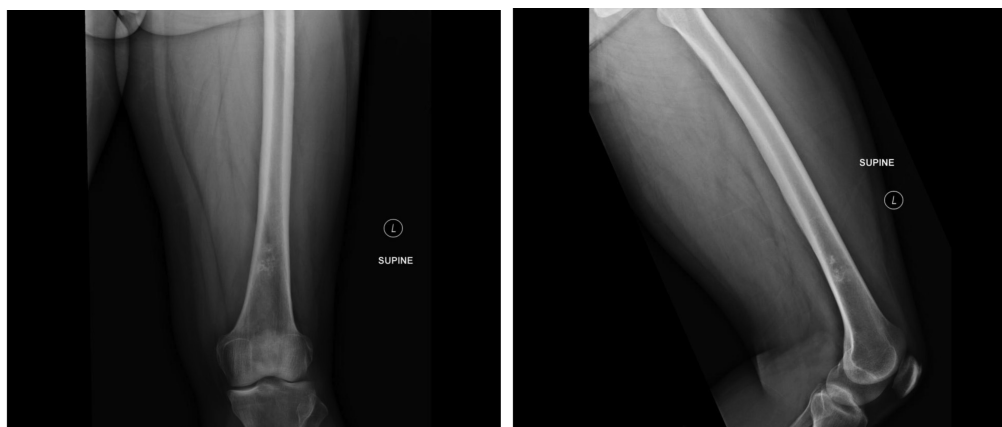


FIGURE 4. Left femur x-ray showed stippled calcifications within the distal femoral intramedullary cavity without additional aggressive features most consistent with an enchondroma. Given the information already provided by the high-resolution SPECT/CT BrightView examination, the x-ray or any additional radiologic evaluation would not be needed.

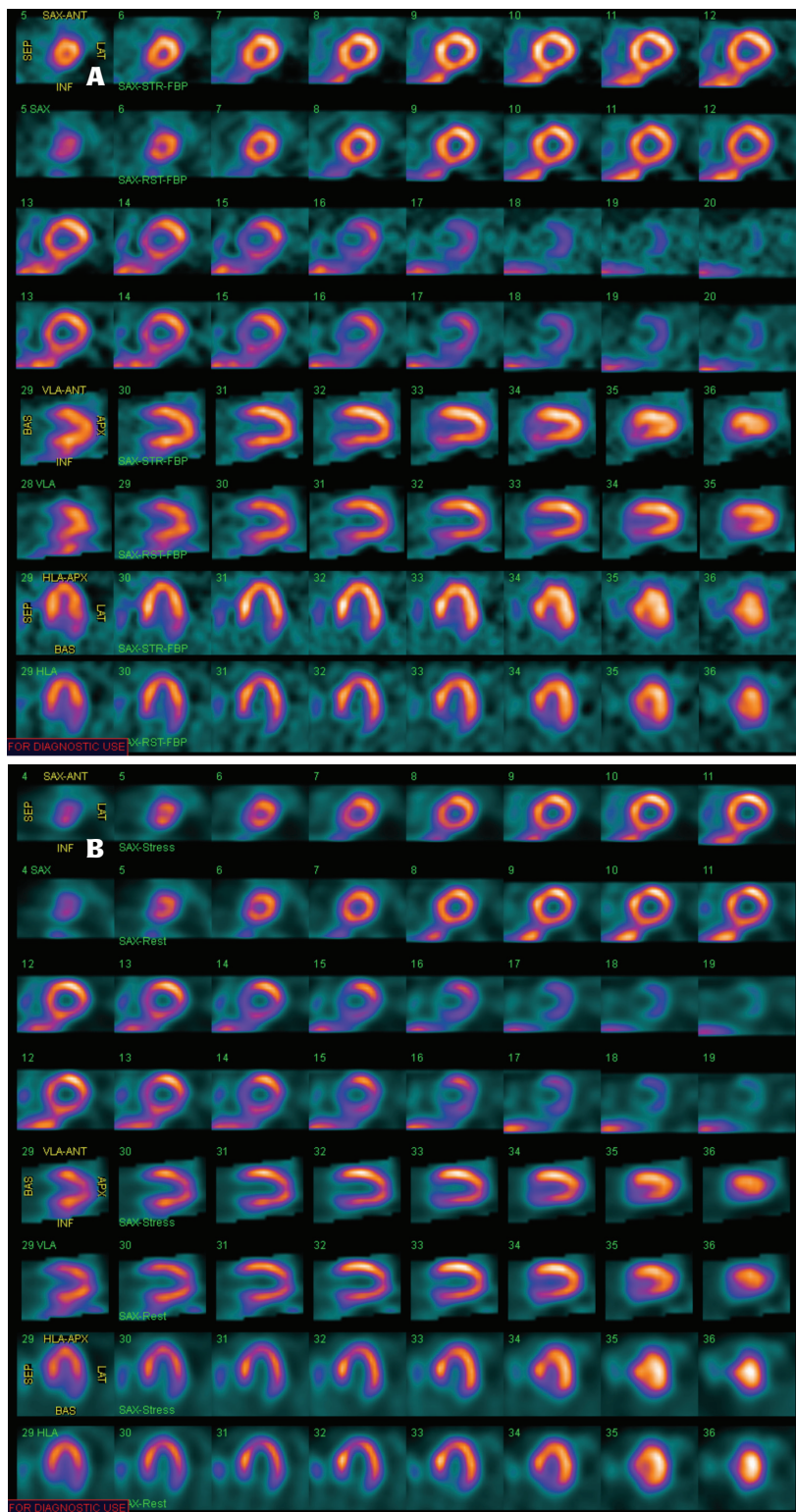


FIGURE 5. SPECT/CT images show full-time data without Astonish (A) versus half-time data with Astonish (B). Both studies were reported as normal.

to identify uptake as pathological versus normal physiological uptake. In a recent study, researchers investigated the added value of SPECT/CT for correlation of MIBG scintigraphy (planar and SPECT) and diagnostic CT in neuroblastoma and pheochromocytoma. In the small series of cases examined, the improved anatomical localization provided by SPECT/CT increased the diagnostic certainty in 89% of discordant studies.⁶

A recently published study evaluated Sentinel Lymph Node Excision (SLNE) with and without SPECT/CT. The study concluded that the use of SPECT/CT was associated with a higher rate of metastatic node detection, which subsequently prolonged the disease-free survival. The same study showed that the use of SPECT/CT changed the surgical approach for SLNE in 33/149 (22.1%) melanoma patients.⁷

Clinical advantages in musculoskeletal imaging

Concurrent imaging and the ability to acquire high-resolution CT images are two features of BrightView XCT that have helped to stimulate a renewed interest in musculoskeletal (MSK) imaging. Concurrent imaging, which allows the user to create multiple datasets from a single acquisition step, offers more flexibility in acquisition protocols and provides additional information without requiring additional imaging time. One way to make use of concurrent imaging is in dual isotope studies.

A classic example is with infection imaging in the musculoskeletal system, and with one day for the indium and one day for the bone scan. Now we can do a simultaneous acquisition for the indium and the bone scan without worrying about patient repositioning or additional image acquisitions in a single day. That is a very unique feature that is available now on the XCT.

The high-resolution imaging capabilities of the BrightView XCT system have also proved useful for MSK imaging, especially when imaging of the extremities is involved. The high-resolution acquisition on the new system has come in handy by giving us a niche in musculoskeletal imaging. The MSK applications brought life to bone scanning. We can

now produce information and give our referring physicians images that have a 0.33-mm resolution of the foot or hand where they suspect a tumor or an infection. This is compared to studies we had where magnetic resonance imaging (MRI) and x-rays were negative, the bone scan planar was negative, and even the SPECT was questionable, until we did the bone examination at high-resolution image acquisition, which showed the abnormality with high certainty. This enabled us to provide information to referring physicians that we would otherwise not be able to do.

In a recent case, a 46-year-old female presented with a history of hepatic adenoma and persistent elevated alkaline phosphatase since October 2011. There had been no history of previous fracture or trauma. A whole-body planar bone scan (Figure 1) with focal uptake in the left distal femur indicated the differential diagnosis involved benign and malignant conditions. The limited uptake of the upper-thigh SPECT/CT (Figure 2) revealed the uptake to be within the bone marrow. The differential diagnosis involved benign and malignant lesions. Yet, a high-resolution SPECT/CT of the left distal femur (Figure 3) showed stippled calcifications within the distal femoral intramedullary cavity without additional aggressive features most consistent with an enchondroma. Given the information already provided by the high-resolution SPECT/CT examination acquired on the BrightView XCT, the x-ray (Figure 4) or any additional radiologic evaluation would not be needed.

Patient management has subsequently changed by reducing the need for follow-up exams, such as MRI, or further evaluation because we now can provide functional and anatomical information without additional image acquisition. This not only reduces cost to the healthcare system and additional cost to the patient, but also speeds up throughput because there is no lag in time between exam 1 and exam 2.

Clinical advantages in cardiology

The American Society of Nuclear Cardiology and the Society of Nuclear Medicine have

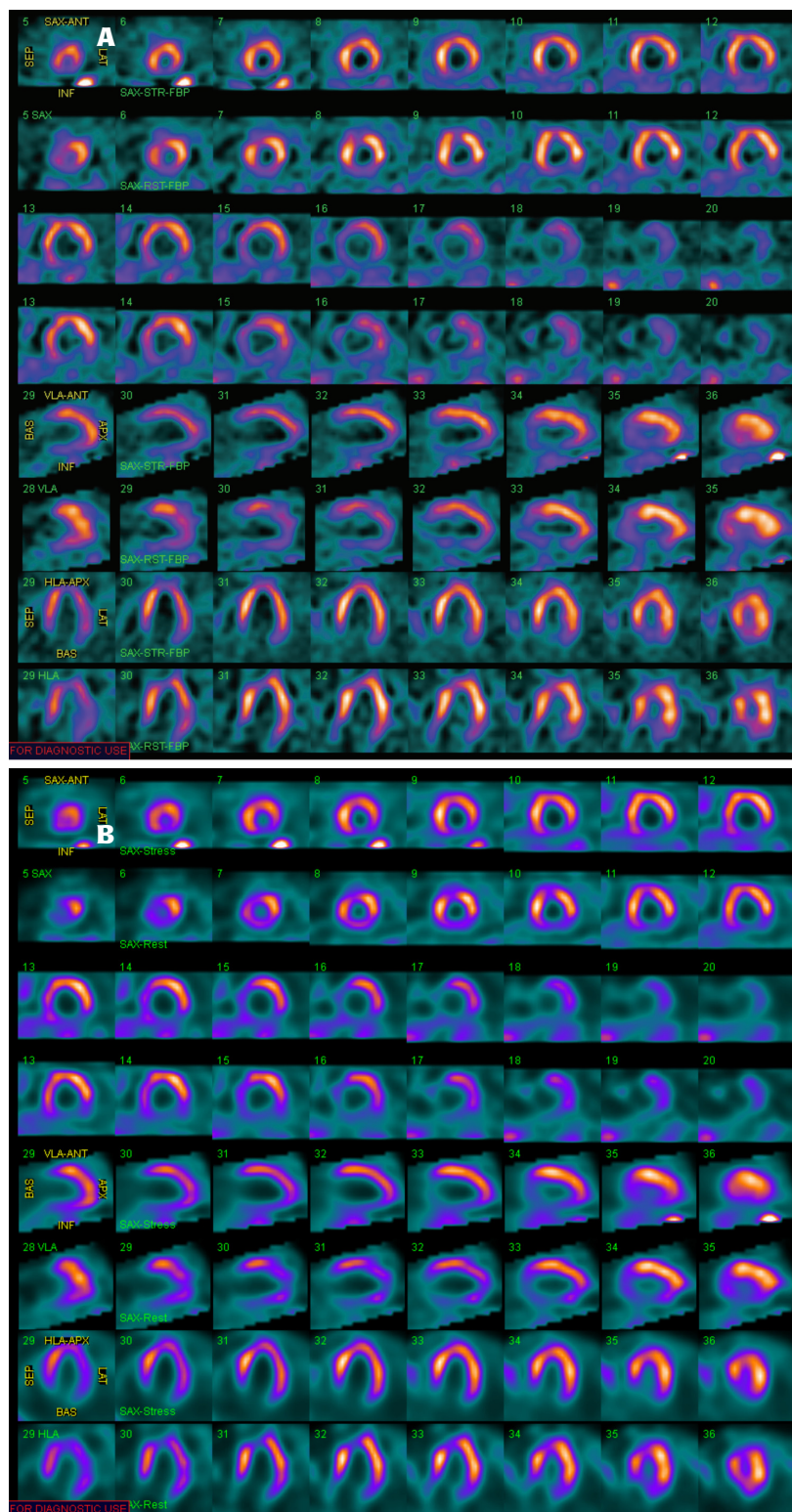


FIGURE 6. SPECT/CT images compare full-time data without Astonish (A) to half-time data with Astonish (B). Both studies reported as inferior wall infarct.

jointly recommended the use of attenuation correction in addition to ECG gating for SPECT myocardial perfusion studies.⁸ Attenuation in cardiac studies has always been a challenge, but the BrightView XCT is well-suited to attenuation correction for cardiac imaging. The flat-panel CT acquires a low-dose (0.12 mSv) CT image of the entire heart volume in just one 60-second rotation while the patient is breathing normally.

In this way, the data used for attenuation correction is averaged over multiple respiratory cycles to match the position of the heart during the SPECT acquisition.

BrightView XCT also supports the Astonish reconstruction technology, which can process half-count data without compromising image quality. This gives the nuclear physician the option of improving laboratory efficiency by reducing the acquisition time using conventional dosing protocols or reducing the patient radiation dose by injecting less radioactivity and using more conventional acquisition times. The ability to take advantage of the cardiac application has allowed us to reduce the acquisition time by half or cut the injection by half, depending on the patient population (Figure 5).

The Astonish reconstruction technology with attenuation correction can be used to further reduce patient dose and imaging time by enabling stress-only imaging (Figure 6). Historically, stress-only imaging has been underutilized, despite findings that stress-only myocardial perfusion imaging (MPI) saves time by eliminating rest imaging in some patient populations, which is important for patient throughput.⁹

If you do stress-only, you can get the answer in <1 hour instead of the 4 hours it typically takes, with one less injection, and reducing the radiation dose by 30% to 40%. Now with the SPECT/CT, we can do stress-only images, and if the stress is negative, then we don't need to do any rest-only images. If 50% of the studies are negative, then we can take advantage of stress-only, which helps with faster image acquisition and faster transfer of information to the referring physician, as well as decreasing the radiation dose to the patient.

In many cases, cardiologists need a quick answer because they are contemplating taking the patient to the cardiac cath lab. The half-time acquisition with the stress-only imaging is critical because it provides the information at a much faster rate and has the potential to significantly improve operational efficiency without sacrificing accuracy because of the CT attenuation correction.

The hospital's referring physicians acknowledged the improvement in cardiovascular studies, and the half dose is especially beneficial in pediatric patients who, by definition, are more sensitive to exposure to radiation. The referring physicians are happy that we are scanning them at faster speeds or half the radiation dose to the patient.

Patient comfort for quality imaging

Another important consideration is patient comfort, especially on SPECT/CT, where patients spend significantly longer times compared to dedicated CT or x-ray. The more comfortable the patient, the less movement there is likely to be and the fewer image artifacts. This is hugely important in cardiac imaging, where motion between the SPECT and CT image can cause misalignment between the transmission and emission data, which can lead to artifacts in the attenuation-corrected SPECT image. Controlling patient movement is also important in oncology, where accurate alignment of the two image sets is critical for localizing the SPECT uptake to the anatomy visualized in the CT image. Being able to position patients reproducibly is also important for patients who may undergo several exams over the course of their treatment. The exact positioning of these patients and alignment of lesions over a series of scans allows the physician to more accurately evaluate the response to therapy.

The BrightView XCT is designed with a large gantry aperture that provides an open patient experience during the CT scans. This provides additional comfort for all patients, especially those with a high body-mass index (BMI) or those suffering from claustrophobia. The 500-lbs (227 kg) capacity of the patient table also facilitates imaging high BMI patients. The large bore enables us to acquire SPECT/CT

We can now give our referring physicians images that have a 0.33 mm resolution of the foot or hand where they suspect to find a tumor.

Medhat M. Osman, MD, PhD

images for patients with high BMI and not have to resort to planar acquisition.

Transforming the future of care

Advances in BrightView XCT have made significant strides in low-dose, high-resolution imaging. But it is only the beginning. We foresee doctors pushing to get more with less radiation and faster scan times. We also foresee a demand for dual-tracer image acquisition techniques.

We were able to overcome a lot of the limitations of SPECT when we installed the BrightView XCT system, and we anticipate there will be a push for more types of simultaneous acquisition imaging.

The key advantages of BrightView XCT include unique features, such as the large bore for bariatric patients, improved reporting speed and accuracy, minimal training required for technologists, the small footprint for ease of installation, and lower overall cost. Yet what is truly transforming the quality of care is improved image quality, reduced dose and shorter scan times, which we expect will lead to better overall care.

References

1. Early detection plan. National Breast Cancer Foundation. <http://www.nationalbreastcancer.org/edp/>. Accessed August 24, 2012.
2. SEER Stat Fact Sheets: Prostate. National Cancer Institute's Surveillance, Epidemiology, and End Results (SEER).
3. Lung Cancer (Non-Small Cell). American Cancer Society. <http://www.cancer.org/Cancer/LungCancer-Non-SmallCell/DetailedGuide/non-small-cell-lung-cancer-survival-rates>. Last Revised on February 17, 2012. Accessed August 24, 2012.
4. American Cancer Society: *Cancer Facts and Figures 2012*. Atlanta, Ga: American Cancer Society, 2012. Last accessed January 6, 2012.
5. Bockisch A, Freudenberg LS, Schmidt D, et al. Hybrid imaging by SPECT/CT and PET/CT: Proven outcomes in cancer imaging. *Semin Nucl Med*. 2009;39:276-289.
6. Rozovsky K, Kolewitz BZ, Krausz Y, et al. Added value of SPECT/CT for correlation of MIBG scintigraphy and diagnostic CT in neuroblastoma and pheochromocytoma. *AJR Am J Roentgenol*. 2008;190:1085-1090.
7. Stoffels I, Boy C, Pöppel T, Kuhn J, Klötgen K, Dissemond J, Schadendorf D, Klode J, et al. Association between sentinel lymph node excision with or without preoperative SPECT/CT and metastatic node detection and disease-free survival in melanoma. *JAMA*. 2012;308:1007-1014.
8. Heller GV, Links J, Bateman TM, et al. American Society of Nuclear Cardiology and Society of Nuclear Medicine joint position statement: Attenuation correction of myocardial perfusion SPECT. *J Nucl Cardiol*. 2004;11:229-230.
9. Duvall WL, Wijetung MN, Klein TM. Stress-only Tc-99m myocardial perfusion imaging in an emergency department chest pain unit. *J Emerg Med*. 2012;42:642-650. Epub 2011 Aug 27.

Clinical Case

Osteomyelitis with associated fracture in the toe as seen on high-resolution SPECT/CT

Razi Muzaffar, DO, and Medhat M. Osman, MD, PhD

Dr. Muzaffar is a Fellow and **Dr. Osman** is the Program Director of the Division of Nuclear Medicine, Department of Radiology, Saint Louis University Hospital, St. Louis, MO.

Case summary

A 16-year-old female presented to our outpatient clinic with complaints of pain in the right foot, lower back, right hand, and left knee. She had a history of recurrent cellulitis of the right foot. The most recent episode of active osteomyelitis was diagnosed in the right fourth phalanx by physical exam, magnetic resonance imaging (MRI) and plain films. She presented to us after finishing her course of antibiotics with continued pain to evaluate for multifocal osteomyelitis.

Imaging findings

MRI of the right foot prior to bone scan demonstrated edematous soft tissue of the dorsal mid- to distal-foot extending to the soft tissue of the fourth toe (Figure 1). The proximal phalanx of the fourth toe as well as surrounding edema enhanced post-contrast. Findings were consistent with osteomyelitis with cellulitis. Plain films demonstrated normal bones, soft tissues, and joint spaces. A three-phase bone scan demonstrated hyperemia to the right forefoot with focal uptake on the delayed image (Figure 2). High-resolution single photon emission computed tomography and computed tomography (SPECT/CT) was then performed, demonstrating intense focal uptake in the proximal right fourth toe corresponding to a nondisplaced fracture in the distal aspect of the right fourth proximal phalanx (Figure 3).

Diagnosis

Osteomyelitis with associated nondisplaced fracture in right proximal phalanx

Discussion

Osteomyelitis is an infection of the bone and bone marrow. Pediatric osteomyelitis is generally considered rare. In the pediatric population, hematogenous route of infection is the most common route of infection.¹ Imaging this infection can be problematic, particularly in the pediatric population. Multiple imaging modalities are being used in the workup of children with known or suspected osteomyelitis. Radiographs are often negative or inconclusive early in the development of the disease.² Skeletal scintigraphy detects physiological changes as low as 5% in bone turnover, whereas x-ray requires a 30% to 50% loss of bone mineralization before morphological changes can be detected.² Furthermore, skeletal scintigraphy is positive as early as the first 24 hours after the onset of symptoms.³ MRI typically has higher sensitivity than CT in detecting osteomyelitis and has the advantage of defining the extent of infection and associated soft-tissue changes. However, CT has the advantage of providing images with high spatial resolution and superb cortical bone details.⁴ In addition, MR imaging in pediatrics has additional limitations, including increased time for imaging and susceptibility to metal artifacts.⁵



FIGURE 1. MRI of the right foot demonstrates edema in the dorsal soft tissue of the right mid to distal foot extending to the soft tissue of the fourth toe. The proximal phalanx of the fourth toe shows increased signal on T2-weighted images (A and B) and enhances post-contrast, suggestive of osteomyelitis with cellulitis. Plain film (C) of the foot shows normal bone, soft tissue, and joint spaces.

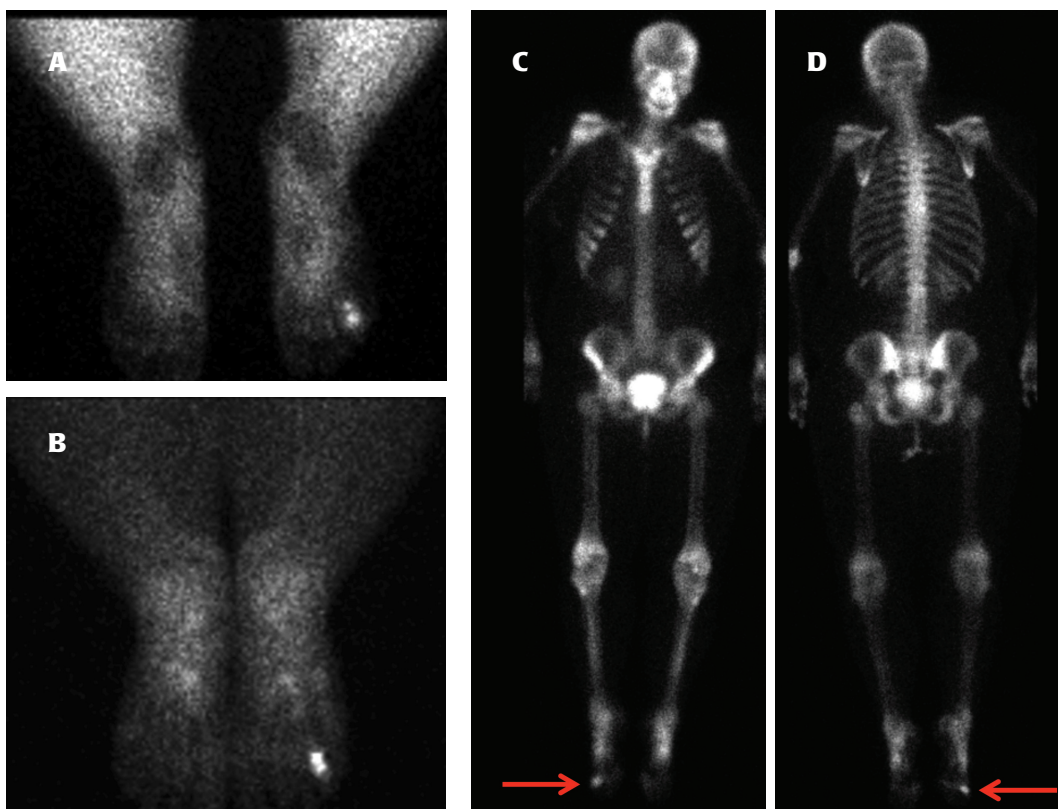


FIGURE 2. A three-phase bone scan demonstrates hyperemia in the right forefoot (A) (top left). Delayed spot view shows focal uptake in the same region (B) (bottom left). Anterior and posterior whole-body images show focal uptake in the right distal foot (C and D) (right).

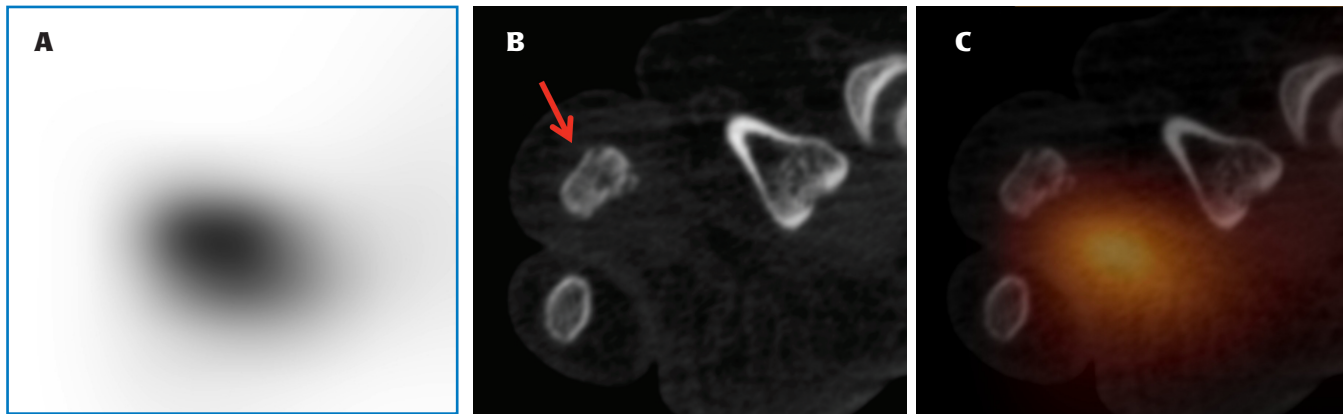


FIGURE 3. SPECT/CT images demonstrate intense focal tracer activity in the proximal right fourth toe with a nondisplaced fracture in the distal aspect of the right fourth proximal phalanx.

Chronic recurrent multifocal osteomyelitis is a rare condition that affects multiple bones.⁶ The multifocal nature of such a condition requires whole-body imaging. Skeletal scintigraphy provides a whole-body evaluation with high sensitivity, but with variable specificity. In addition to the lack of anatomic localization, there is an inherent limitation to such a technique. Employing SPECT/CT is better than employing CT or SPECT alone. The CT component of the SPECT/CT is typically used for lesion localization and for attenuation correction. The high-resolution image acquisition feature of the BrightView SPECT/CT provides a unique opportunity and value to the field of musculoskeletal imaging. It provides a superb, sub-mm (0.33 mm) evaluation of skeletal anatomy. The availability of such technology may improve our ability to characterize lesions and may affect treatment decisions and patient management.

Conclusion

High-resolution SPECT/CT provides the additional information of bone detail, which

may otherwise be unapparent in other imaging modalities. In this case, a fracture in the fourth toe was identified on SPECT/CT and not apparent on MRI or plain film. The detection of such fracture explained the patient's right foot pain.

References

1. Mader JT, Shirliff M, Calhoun JH. The host and the skeletal infection: Classification and pathogenesis of acute bacterial bone and joint sepsis. *Best Pract Res Clin Rheumatol.* 1999;13:1-20.
2. Saigal G, Azouz EM, Abdenour G. Imaging of osteomyelitis with special reference to children. *Semin Musculoskelet Radiol.* 2004;8:255-265.
3. Maurer AH, Chen DCP, Camargo EE, Wong DF, et al. Utility of three-phase skeletal scintigraphy in suspected osteomyelitis: Concise communication. *J Nucl Med.* 1981;22:941-949.
4. Pineda C, Vargas A, Rodriguez AV. Imaging of osteomyelitis: Current concepts. *Infect Dis Clin North Am.* 2006;20:789-825.
5. Vijayanathan S, Butt S, Gnanasegaran G, Groves AM. Advantages and limitations of imaging the musculoskeletal system by conventional radiological, radionuclide, and hybrid modalities. *Semin Nucl Med.* 2009;39:357-368.
6. Kothari NA, Pelchovitz DJ, Meyer JS. Imaging of musculoskeletal infections. *Radiol Clin North Am.* 2001;39:653-671.

Improving patient outcomes with ultrasound elastography

Richard G. Barr, MD, PhD, FACR

Ultrasound elastography is a new technique that generates images or quantitative data based on the stiffness of a tissue. Tissue stiffness changes in many disease states, including softening of edematous tissues or hardening of malignant lesions. Elastography has been shown to provide clinically useful information in many organs.¹⁻¹³ This article reviews clinically useful applications.

Technology

Two types of ultrasound elastography are currently available.* For the purposes of this article, we will focus on compression strain elastography.

Compression strain elastography evaluates how a tissue deforms when an external or patient-induced force is applied to the tissue. Soft tissues deform more; hard tissues deform less. For example, if a gelatin mold contains a glass marble and the mold itself is externally compressed, the gelatin would change shape while the marble would not. The algorithm analyzes the frame-to-frame differences with compression. The more a tissue deforms, the softer it is. This technique is considered qualitative and is relative to a given patient. The resulting images are displayed on a scale of the relative tissue stiffness in the field of view.⁴ Some analysis can be generated using such strain as compression strain/B-mode measurement comparison ratios and relative strain value displays and comparisons.

Clinical applications

Compression strain elastography can be performed on any tissue from which a B-mode

image can be obtained. This article concentrates on 3 primary elastography applications: breast lesion characterization, musculoskeletal assessment, and gynecologic pathology.

Breast elastography

Compression strain elastography has been shown to improve characterization of breast lesions as benign or malignant.⁶⁻¹⁰ Compression strain requires only a few minutes of additional scanning. Benign breast lesions appear smaller on compression strain imaging, while malignant lesions appear \geq in size to the same lesions on B-mode imaging. This phenomenon is unique to breast tissue. Figure 1 is a biopsy-proven fibroadenoma. Note that the lesion measures 1.03 cm on B-mode, but 0.80 cm on elastography—a strain/B-mode ratio of 0.78, suggestive of a benign lesion. Figure 2 is an ultrasound scan of a patient who presented with an abnormal screening mammogram. On B-mode imaging, the lesion has a superior portion outlined by a red circle, a central hypoechoic mass, and a finger of tissue inferiorly (green arrow). Note that on the elastogram, the superior portion is color-coded white (soft), while the central mass is color-coded black (hard) and is larger than in the B-mode image (strain/B-mode ratio of 1.5). The finger of tissue inferiorly is also color-coded black and appears larger on the B-mode image. Pathology revealed the central mass and finger of tissue to be invasive ductal carcinoma, as suggested by the increase in size. The area in the red circle was a benign fibroadenoma, as predicted benign by the elastogram. In a large multicenter trial⁷ the sensitivity and specificity of this size

Dr. Barr is a Professor of Radiology, Northeastern Ohio Medical University, and a Diagnostic Radiologist at Radiology Consultants Inc., Youngstown, OH.



Richard G. Barr, MD, PhD, FACR

With strain elastography, the “bull’s eye” artifact is extremely sensitive and specific to benign simple and complicated cysts.

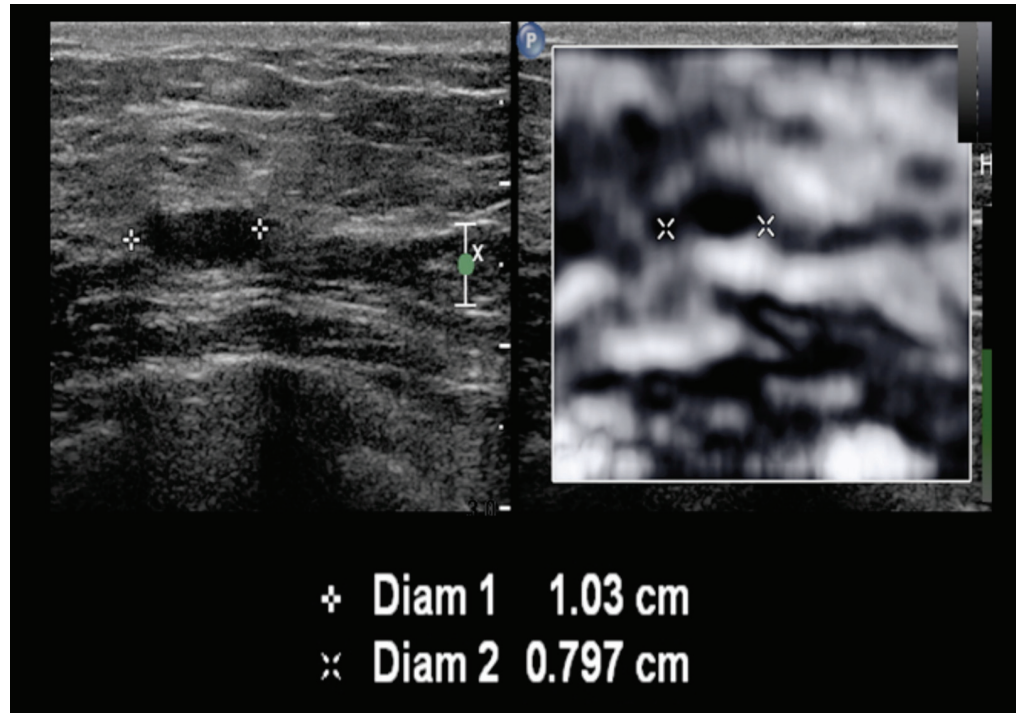


FIGURE 1. Breast fibroadenoma showing B-mode and strain measurement comparison.

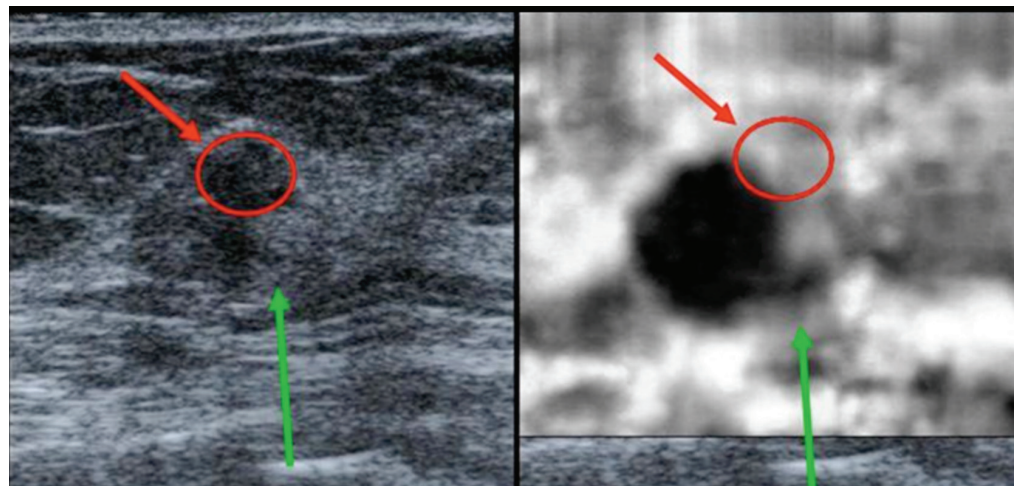


FIGURE 2. Multiple breast lesions. The green arrow indicates ductal carcinoma. The red arrow/circle indicates fibroadenoma.

change to distinguish benign from malignant lesions were 98.5% and 85%, respectively.

When cystic lesions are being evaluated with strain elastography, an artifact can be seen on some manufacturers' equipment. This "bull's eye" artifact has been described in the literature, and it occurs in both simple and complex cysts. This artifact has a unique appearance, demonstrating a white central area in a black lesion and a white area inferior to the lesion.⁸

This artifact has been shown to be extremely sensitive and specific to benign simple and complicated cysts.⁸ The presence of this artifact can potentially reduce the number of biopsies performed on benign lesions.⁸

Musculoskeletal assessment

Musculoskeletal elastography is in its infancy.¹⁴⁻¹⁷ Current studies show that tendons are one of the stiffest tissues in the body.

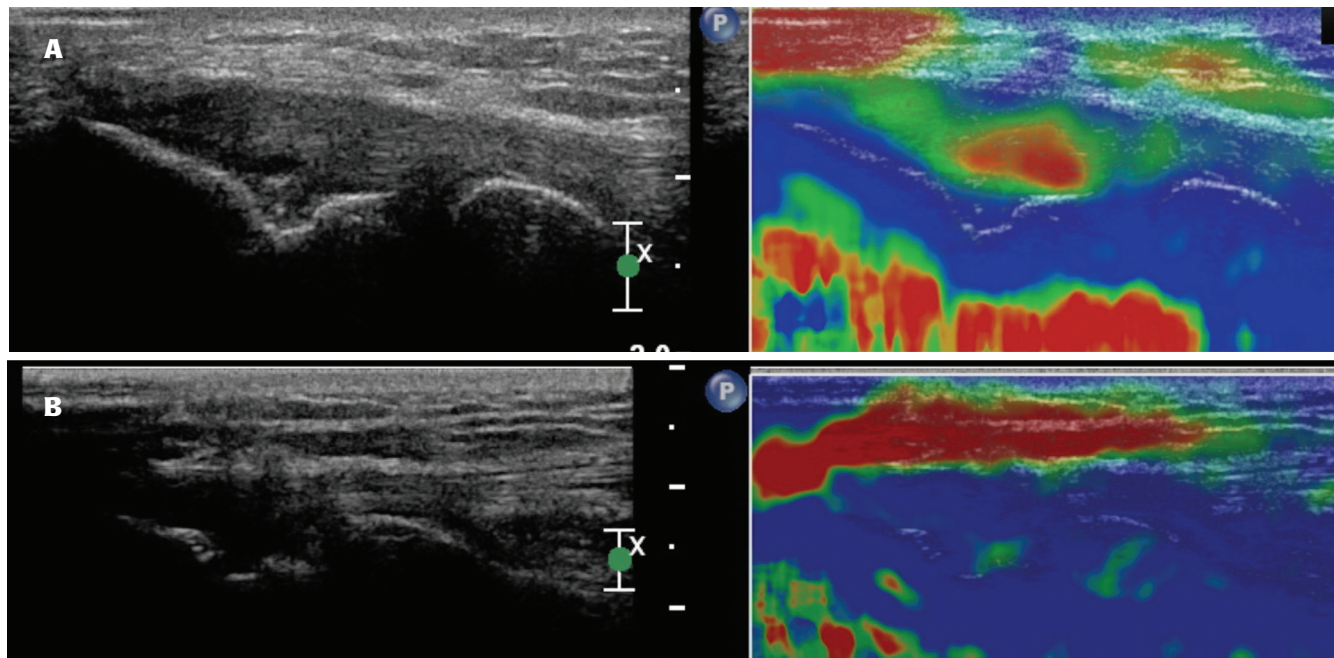


FIGURE 3. (A) The elastogram of a patient with lateral epicondylitis shows the abnormal area as red (soft) compared to the normal tendon, which is hard (blue). After conservative treatment, a repeat elastogram (B) confirms resolution of the tendinitis and the tendon is now all stiff (blue).

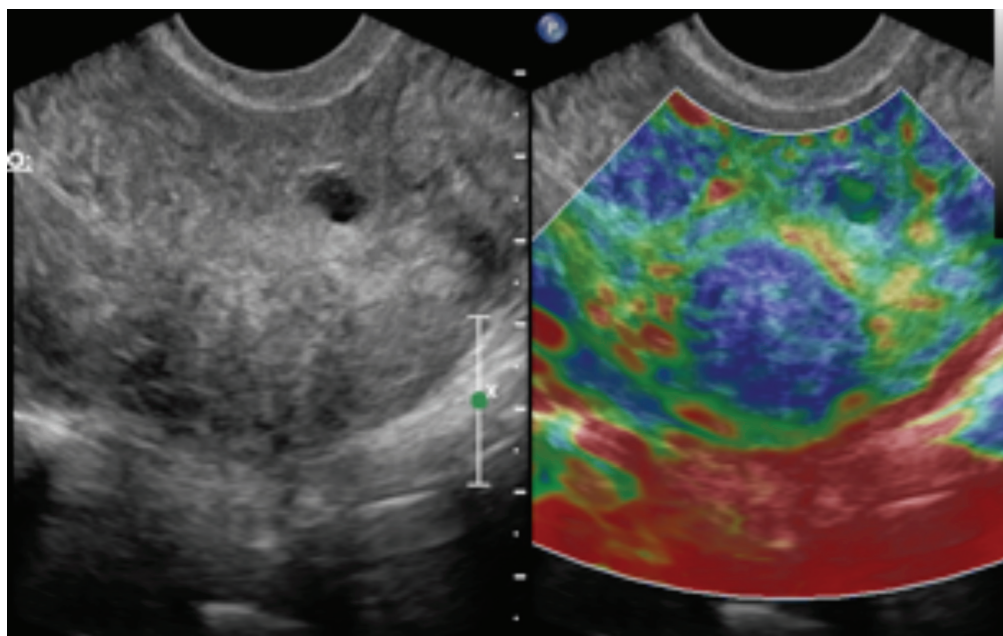


FIGURE 4. The elastogram of a uterine fibroid using the endocavity probe. Note that the fibroid is better visualized on elastography than on B-mode.

Pathologies, such as tendinitis or tears, can cause the relative stiffness to lessen. Magnetic resonance imaging (MRI) is considered the standard technique for evaluating these changes. However, ultrasound elastography may be able to

evaluate these changes at a lower cost than MRI and allow monitoring of healing. Ultrasound also has the ability to evaluate the dynamics of muscles and tendons. It is also easy to obtain the contralateral images for comparison.

Figure 3 is the elastogram from a patient with lateral epicondylitis. Soft tissue is color-coded red, while stiff tissue is color-coded blue. The normal tendon is stiff (blue), while the area of tendinitis is soft (red). In Figure 3, the area of tendinitis is identified as the red area within the tendon. After conservative treatment, the tendinitis has improved clinically, and the area which was previously abnormal has returned to a normal appearance.

Gynecologic elastography

With the addition of strain elastography to the endocavitary probe, high-quality elastograms of the uterus and ovary can now be obtained. Early studies demonstrate that uterine fibroids can be characterized by their stiffness using elastography. Some uterine fibroids can be better visualized using strain, especially if they are significantly stiffer than the adjacent uterus (Figure 4). The bull's eye artifact, which has been described in breast tissue,⁸ also occurs in ovaries. This could be helpful in classifying complicated ovarian cysts as benign, as this artifact only occurs when low-viscosity fluid is present. Since the elastograms are generated based on frame-to-frame changes in B-mode, done as post-processing, this technique can be used in fetuses without additional energy input.

Conclusion

Ultrasound elastography is a rapidly evolving technology shown to be an important adjunct to B-mode imaging in many exams, including those of the breast, thyroid, musculoskeletal system, liver, prostate, and female reproductive system. The technology has been shown to be most advanced in breast imaging, where it has demonstrated a major impact on lesion characterization. Elastography is an exciting development that has the potential to expand ultrasound into more diverse clinical roles as well as to improve clinical outcomes across many applications.

**Only qualitative strain compression elastography is available on Philips products in the U.S. and shear wave is not available on Philips products in the U.S.*

References

1. Takahashi H, Ono N, Eguchi Y, et al. Evaluation of acoustic radiation force impulse elastography for fibrosis staging of chronic liver disease: A pilot study. *Liver Int.* 2010;30:538-545.
2. Friedrich-Rust M, Wunder K, Kriener S, et al. Liver fibrosis in viral hepatitis: Noninvasive assessment with acoustic radiation force impulse imaging versus transient elastography. *Radiology.* 2009;252:595-604.
3. Seeff LB, Hoofnagle JH. National Institutes of Health Consensus Development Conference: Management of hepatitis C: 2002. *Hepatology.* 2002;36:S1-S2.
4. Barr RG. Sonographic breast elastography: A primer. *J Ultrasound Med.* 2012; 31:773-783.
5. Barr RG, Zhang Z. Effects of precompression on elasticity imaging of the breast. *J Ultrasound Med.* 2012; 31:895-902.
6. Barr RG. Real-time ultrasound elasticity of the breast: Initial clinical results. *Ultrasound Quarterly.* 2010;26:61-66.
7. Barr RG, Destounis S, Lackey, LB II, et al. Evaluation of breast lesions using ultrasound elasticity imaging: A multicenter trial. *J Ultrasound Med.* 2012; 31:281-287.
8. Barr RG, Lackey AE. Predictive value of the "bull's eye" artifact on breast elasticity imaging to characterize cysts. *Ultrasound Quarterly.* 2011;27:151-155.
9. Tanter M, Bercoff J, Athanasiou A. Quantitative assessment of breast lesion viscoelasticity: Initial clinical results using supersonic shear imaging. *Ultrasound in Med. & Biol.* 2008;34:1373-1386.
10. Berg WA, Cosgrove DO, Dore CJ, et al. Shear-wave elastography improves the specificity of breast US: The BE1 multinational study of 939 masses. *Radiology.* 2012;262:435-449.
11. Barr RG, Memo R, Schaub CR. Shear-wave ultrasound elastography of the prostate: Initial results. *Ultrasound Quarterly.* 2012;28:13-20.
12. Lyschchik A, Higashi T, Asato R, et al. Thyroid gland tumor diagnosis at US elastography. *Radiology.* 2005;237:202-211.
13. Dighe M, Bae U, Richardson ML, et al. Differential diagnosis of thyroid nodules with US elastography using carotid artery pulsation. *Radiology.* 2008;248:662-669.
14. De Zordo T, Fink C, Feuchtner GM, et al. Real-time sonoelastography findings in healthy Achilles tendons. *AJR Am J Roentgenol.* 2009;193:W134-W137.
15. Trombetti J. Sonoelastography and musculoskeletal imaging. <http://www.dotmed.com/news/story/7760/?lang=en>. Updated December 23, 2008. Accessed August 28, 2012.
16. Schreiber V, Smekal V, De Zordo T, et al. Real-time sonoelastography in rotator cuff imaging and comparison to magnetic resonance imaging as gold standard. *RSNA 2009.* http://rsna2009.rsna.org/search/event_display.cfm?em_id=8016421&printmode=Y&autoprnt=N. Updated 2009. Accessed August 29, 2012.
17. De Zordo T. Value of real-time sonoelastography in lateral epicondylitis: Comparison with clinical examination, ultrasound, and power Doppler ultrasound. *Radiological Society of North America 94th Scientific Assembly and Annual Meeting; November 30th - December 5th, 2008; Chicago, USA.* Updated 2008. Accessed August 29, 2012.

Clinical Case

Elastography in evaluation of musculoskeletal abnormalities

Richard G. Barr, MD, PhD, FACR

Dr. Barr is a Professor of Radiology, Northeastern Ohio Medical University, and a Diagnostic Radiologist at Radiology Consultants Inc., Youngstown, OH.

Case summary

A 42-year-old male who is an avid runner had an injury 2 months prior. The pain at his heel area persisted despite conservative management and was increasing when he presented. The patient had no other medical problems, but a history of 2 torn ligaments in the past. The patient underwent a magnetic resonance imaging (MRI) scan of his hind foot.

Imaging findings

The proton-density weighted MRI (Figure 1) demonstrates the presence of an abnormal signal involving the Achilles tendon. The diagnosis of Achilles tendinitis was made. There was no evidence of a significant tear, although minimal tears could not be excluded. There was no evidence of bone-marrow edema, ankle-joint effusion, or fluid surrounding the Achilles tendon.

An ultrasound (Figure 2) of the Achilles tendon was performed, including strain elastography at the same time. The B-mode ultrasound showed an area of decreased echogenicity within the tendon, which on elastography is soft (red) compared to the normal tendon, which is hard (blue).

Fusing the MRI and ultrasound images (Figure 3) shows the area of tendinitis is similarly identified on both techniques.



FIGURE 1. The tendinitis identified on the MRI with high-signal edema involving the tendon (arrow).

Diagnosis

The patient's MRI confirmed the diagnosis of Achilles tendinitis.

The patient was placed in a cast for 4 weeks with significant symptomatic improvement.

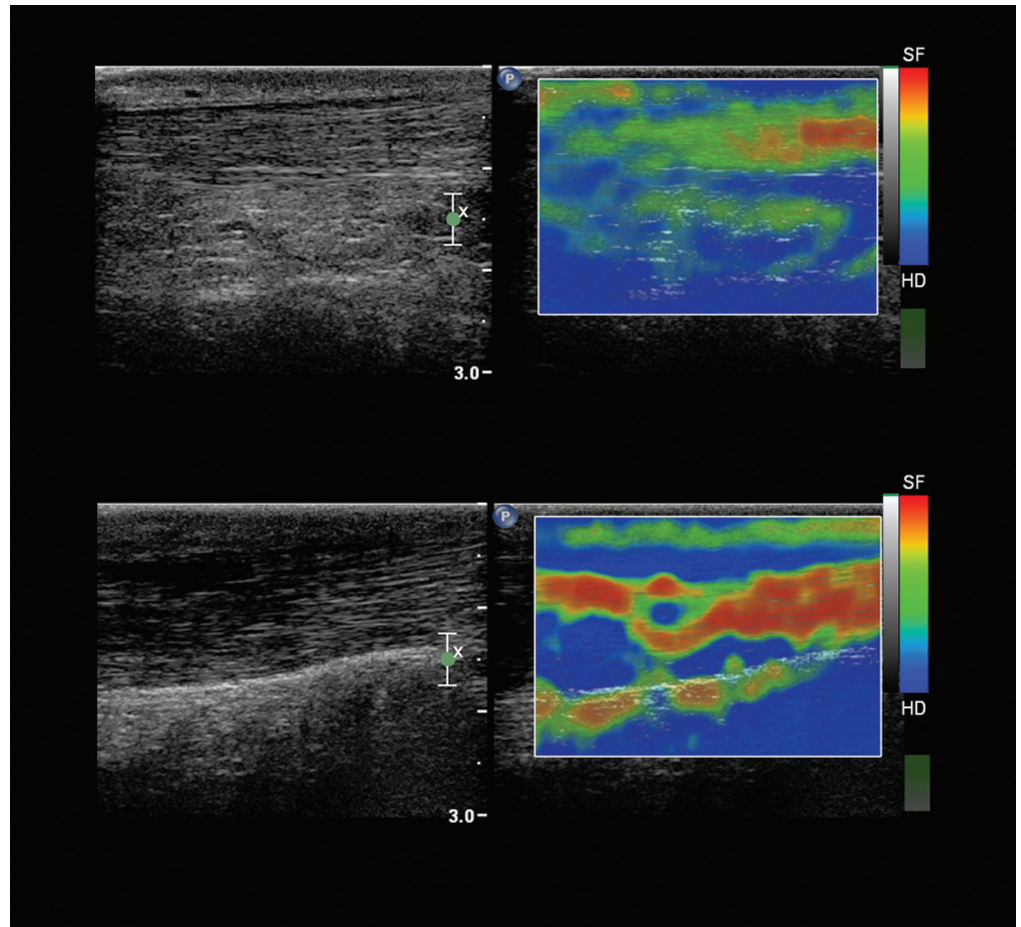


Figure 2. The strain elastogram is presented with a color map superimposed on a grayscale B-mode image. Soft tissue is color-coded red while stiff tissue is color-coded blue. The normal tendon is stiff (blue), while the area of tendinitis soft (red).

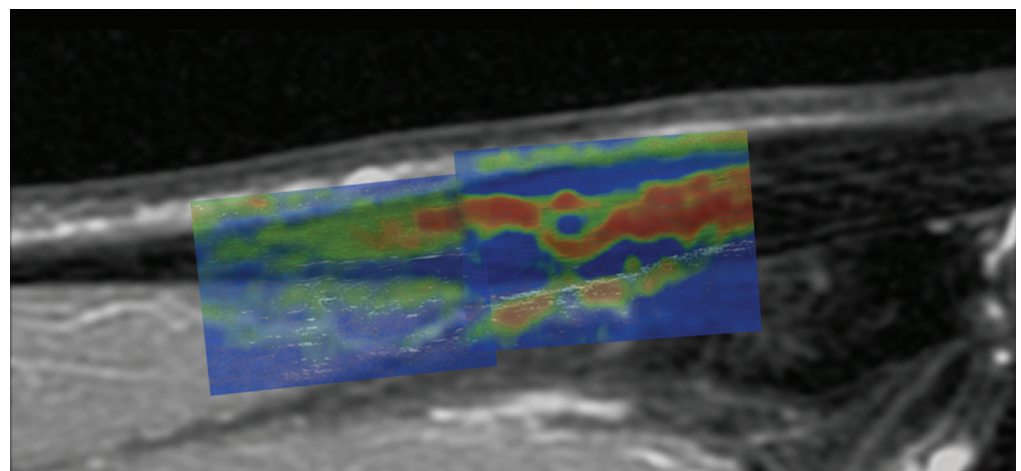


FIGURE 3. Fusion of the MRI image and elastography demonstrate that both techniques identify a similar area of tendinitis.

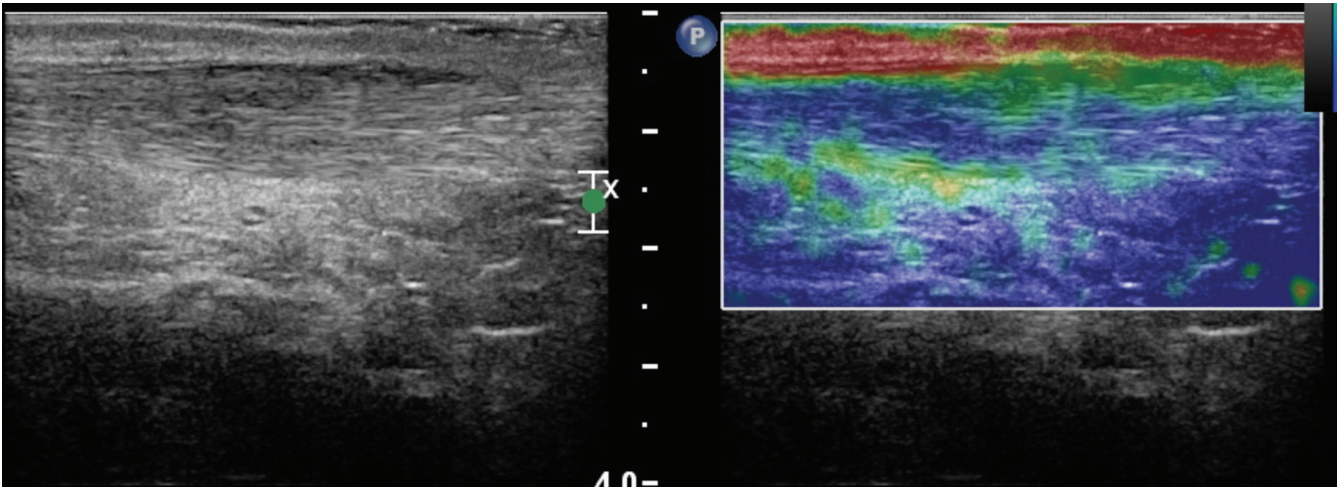


FIGURE 4. Ultrasound elastography of the same area of the Achilles tendon after treatment shows that soft (red) area of tendinitis on the initial study has resolved, and now there is a small area of green (intermediate stiffness), which may represent either scar formation or continued healing.

A follow-up ultrasound (Figure 4) shows that the area of soft (red) tendinitis has resolved and a small area of green (intermediate hardness) is present, consistent with a scar/healing area.

Discussion

Musculoskeletal elastography is in its infancy.¹⁻⁴ Current studies show that tendons are one of the stiffest tissues in the body. Pathologies, such as tendinitis or tears, can cause the relative stiffness to lessen. MRI is considered the standard technique for evaluating these changes. However, ultrasound elastography may be able to evaluate these changes at a lower cost than MRI and allows monitoring of healing. By monitoring the relative softness as well as the size of the area affected, one can monitor treatment and may be able to better tailor treatment to the patient's healing. In addition, ultrasound is useful for demonstrating dynamics of muscle and tendons. It is also easy to obtain the contralateral images for comparison.

Conclusion

Strain elastography is a promising new technology that has the potential to change the present clinical patterns in diagnosis and patient management in musculoskeletal imaging. Ongoing studies will help to define the role of strain elastography in musculoskeletal imaging.

References

1. De Zordo T, Fink C, Feuchtner GM, et al. Real-time sonoelastography findings in healthy Achilles tendons. *AJR Am J Roentgenol.* 2009;193:W134-W137.
2. Trombetti J. Sonoelastography and musculoskeletal imaging. <http://www.dotmed.com/news/story/7760/?lang=en>. Updated December 23, 2008. Accessed August 28, 2012.
3. Schreiber V, Smekal V, De Zordo T, et al. Real-time sonoelastography in rotator cuff imaging and comparison to magnetic resonance imaging as gold standard. *RSNA 2009.* http://rsna2009.rsna.org/search/event_display.cfm?em_id=8016421&printmode=Y&autoprint=N. Updated 2009. Accessed August 29, 2012.
4. De Zordo T. Value of real-time sonoelastography in lateral epicondylitis: Comparison with clinical examination, ultrasound, and power Doppler ultrasound. *Radiological Society of North America 94th Scientific Assembly and Annual Meeting; November 30th - December 5th, 2008; Chicago, USA.* Updated 2008. Accessed August 29, 2012.

Transformation from film-screen to MicroDose digital mammography: Selection challenges, opportunity, and value

Raymond Tu, MD, Riad Charafeddine, MD, Theodore Williams, MA, RT(R), and Steven Rothenberg

Digital mammography has proven its effectiveness in breast cancer detection programs for over a decade. From the patient's perspective the screening examination is quick, taking less time than prior analog film-screen technology. From the technologists' perspective, digital provides enhanced throughput, eliminating the need for film manipulation, cassettes, toxic photographic liquids, and mechanical processors. From the radiologist's perspective, the streamlined integration is intuitive with existing plain film, CT, and MRI viewing systems, with the obvious benefits familiar to any digital modality.

Until recently there was only one digital mammographic choice. Though available in Europe and Canada for years, the recent debut of MicroDose digital mammography in the United States (U.S.) market improves fundamental mammographic detector technology. MicroDose provides all the benefits of existing digital mammography with high resolution and lower dose — with 18% to 50% lower radiation dose than used on other digital mammography systems, with an average dose reduction of 40%*.¹⁻⁴ MicroDose competes with standard mammographic technology as a solution to the film-screen replacement challenge (for those sites which have yet to replace legacy film techniques). It also addresses concerns over unnecessary, nondiagnostic radiation exposure in healthy patients while providing an edge in a competitive provider market.

MicroDose: Low-dose digital mammography

The MicroDose digital mammographic system is the first to use photon counting technology, a patented technological revolution in x-ray detector development. The individual x-ray photon is counted by a 50-micrometer detector element, the smallest in the industry (as much as 4 times smaller). The single-layer detector counts individual photons, creating very low noise during the digital-to-digital data collection, and eliminating the analog to digital conversion used by other vendors. The photon counting technology is unique to MicroDose.⁵

Also unique to MicroDose is the image acquisition. By using a multi-slit pre-collimator and a matching multi-slit post-collimator, only those x-rays perfectly aligned with the detector are allowed to pass through the breast. All other x-rays are blocked, as that radiation would only increase patient dose without contributing to image quality; scatter radiation, which adds to patient dose and degrades image quality, is minimized. MicroDose reduces 97% of scatter, enabling the system to achieve excellent image quality at low radiation.⁶

Radiation exposure

The measurement of breast radiation exposure was published by the Irish Breast Screening Program. The purpose of the study was to compare radiation dose to the breast per exposure and per exam among the digital mammography systems of 3 common vendors: Philips MicroDose,



Raymond Tu, MD

Patients request MicroDose realizing the added benefit of 18% to 50% less dose than other breast imaging practices.

Table 1. Radiation dose per exposure* (mean glandular dose, mGy)

	CC	MLO	2 view FFDM
Philips MicroDose	0.90	0.88	1.86
Hologic Selenia	1.36	1.44	2.91
General Electric Essential	1.39	1.52	3.03

*Irish Breast Screening program
FFDM = full-field digital mammogram



Figure 1. Full-field digital MicroDose mammogram. Screening study. Craniocaudal projection. Mildly opaque glandular tissue with opacities and calcification.

Hologic Selenia, and General Electric Essential. The lowest to highest craniocaudal (CC) doses (mGy per exposure) were 0.90 (Philips Healthcare (Philips)), 1.36 (Hologic), and 1.39 (General Electric (GE)). The lowest to highest mediolateral oblique (MLO) doses (mGy per exposure) were 0.88 (Philips), 1.44 (Hologic) and 1.52 (GE). The mean glandular doses for a complete examination (MLO and CC) from lowest to highest radiation dose (mGy per breast) were 1.86 (Philips), 2.91 (Hologic) and 3.03 (GE). The study found that the Philips MicroDose system had the lowest mean glandular dose per image and per exam among the 3 vendors (Table 1).⁷

Price vs value

Considering differences in price vs value, not all mammograms are created equal. Price

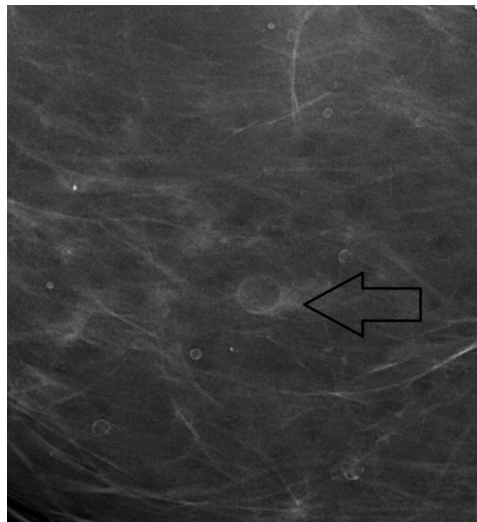


Figure 2. Enlarged view of medial quadrant of craniocaudal projection with lucency medially (open arrow) with well-circumscribed borders consistent with fat necrosis. This finding was seen on both craniocaudal and medial lateral oblique views on MicroDose, but seen only in retrospect on prior film screen mammogram.

(the financial investment) and value (the weighted multifactorial health benefit) are not synonymous. The various costs of digital mammography equipment (standard and MicroDose) are fairly similar. The vendor add-ons, such as viewing software, workstations, phantoms, service contracts, financing options, and accessories, can vary.

On the other hand, differences in *value* are striking. As healthy people are being screened, the consumer's perception of harm from radiation exposure cannot be underestimated. As customers select a provider, variation in price and value are not necessarily concordant. The patient calculates value—physician recommendation, geographic proximity, familiarity of the provider, reputation, and personal communication—and weighs it

Dr. Tu is Chairman, Department of Radiology, Not-For-Profit Hospital Corporation dba United Medical Center, Washington, DC; Partner at Progressive Radiology, Falls Church, VA; and Clinical Associate Professor of Radiology, The George Washington University School of Medicine and Health Sciences, Washington, DC.

Dr. Charafeddine is a Staff Radiologist, Department of Radiology, Not-For-Profit Hospital Corporation dba United Medical Center, Washington, DC; and Radiologist at Progressive Radiology, Falls Church, VA.

Mr. Williams is Director, Department of Radiology and Cardiology Services, Department of Radiology, Not-For-Profit Hospital Corporation dba United Medical Center, Washington, DC.

Mr. Rothenberg is a third-year medical student at The George Washington University School of Medicine and Health Sciences, Washington, DC.

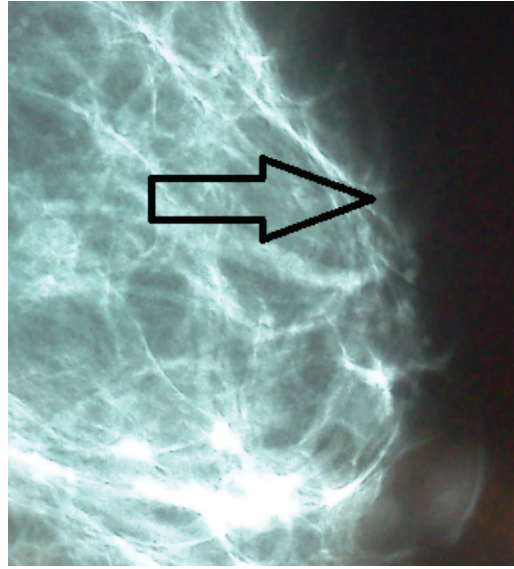


Figure 3. Analog film-screen mammogram illustrating appearance of skin (open arrow), photographically enhanced to illustrate finding.



Figure 4. Same patient one year later with full-field digital MicroDose screening study. Mediolateral oblique projection. Mildly opaque glandular tissue with very clear skin detail.

against out-of-pocket cost. Mammography providers are accredited by the American College of Radiology (ACR) and the U.S. Food and Drug Administration (FDA), removing much of the variability among various sites.

Coverage and reimbursement are usually driven by third-party payers and local carrier determination, and are not a factor unless a non-covered service, such as tomosynthesis, is added on. A customer will weigh value against cost: time, distance, money, and radiation. The radiation savings will attract informed customers to the lower-radiation option. An analogous exploited marketing benefit of lower radiation was used to promote digital mammography during the analog film-screen to digital transition. The lower-radiation advantage of MicroDose provides similar value to an imaging business seeking to enter or expand its digital mammographic service.

Clinical experience

Patient commentary

Patients are pleased with the brevity of the MicroDose exam. The breasts are compressed on a curved MicroDose patient support assembly warmed above room temperature rather than to the typical flat, cold ergonomic plate. The warmed support and compression device provide comfort and reduce the shock of having

one's breast placed on a cold tray.⁸ Patients who have returned from other mammogram studies have been complimentary of their experience on MicroDose. They request MicroDose realizing the added benefit of 18% to 50% less dose than other breast imaging practices. Many patients are fearful of radiation; offering a lower radiation option enhances patient emotional comfort with the study.

Referring providers

MicroDose mammography can elevate the reputation of the department and hospital. The perception of providing cutting-edge technology and lower radiation dose at the high resolution results in more referrals from healthcare providers. Lower radiation dose breast cancer detection with the high resolution provides cache and exclusivity to a facility's portfolio of imaging services. Patient feedback to referring providers will attract more patients to a low dose exam.

Technologist experience

Positioning a patient in the MicroDose machine is similar to placing her in standard mammography machines. Adjustment controls for the patient support tray are easy to access and operate with ergonomic foot control paddles. The computer interface is similar to that of any other computer data entry system. The elimina-

tion of film cassettes, film handling, and the processor streamlines the exam.

Radiologist experience

Installation of the MicroDose machine is simple; the system's footprint is similar to that of other vendors. Elimination of the analog film-screen dark room, processor, and chemicals does not necessarily enlarge the clinical space, as a power conditioner and cooling system is needed for the buildout. The cooling and power conditioner system must be constructed as a separate, self-contained room to maintain a quiet environment for the patient. Though not as obtrusive as a magnetic resonance computer room, there are added installation details for electronic components. Radiologist image interpretation of the digital mammogram is very satisfying, commensurate with the recent 2012 study by Cole et al, which concluded that photon-counting, full field digital mammography is not inferior to conventional digital mammography. The 50-micron resolution provides incredible diagnostic-quality images (Figures 1 and 2). The full-field digital mammograms provide exceptional image quality so that focal asymmetries are easy to identify, whereas on prior examinations the opacities were perhaps seen only on one view in prior years (Figures 3 and 4). The detail in dense breast tissue is superb, as well. Border delineation, microcalcifications, and architectural distortion are easy to identify with MicroDose. Post-procedure architectural distortion and fat necrosis, while subtle on prior studies, are very obvious with the MicroDose 50-micrometer resolution.⁹

Conclusion

MicroDose improves digital mammography technology by providing high image quality at low radiation dose. In analog-to-digital conversion, MicroDose full-field digital mammography is an excellent solution in replacing a legacy film program, decreasing unnecessary radiation exposure to otherwise healthy patients while providing market share advantage in a consumer-driven examination.

The lower dose and high resolution of MicroDose will be the standard of digital mammography as imaging centers add more units and replace older equipment with new technology.

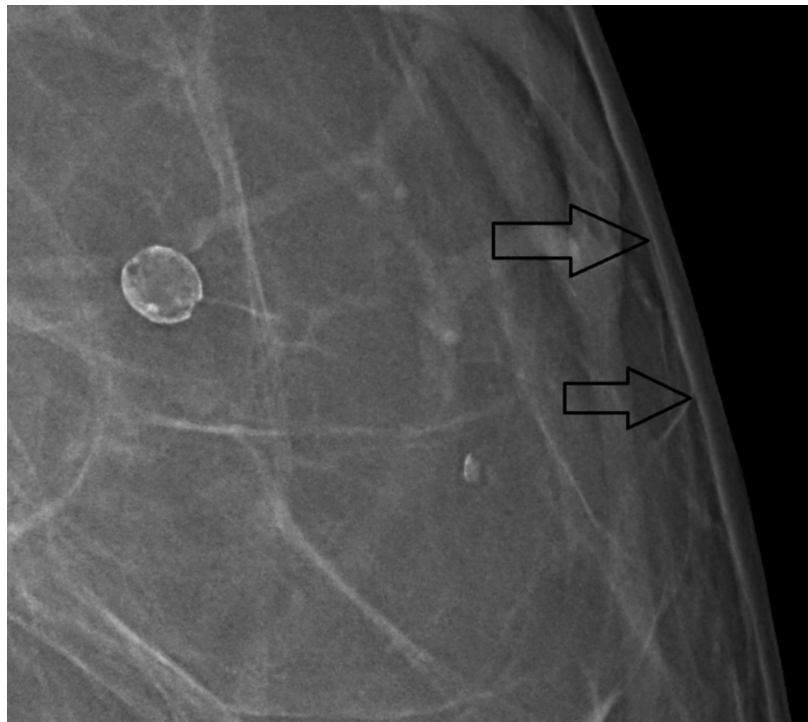


Figure 5. Enlarged view of mediolateral quadrant of breast showing very clear and discernible normal skin (open arrow). Skin detail, an important indicator of a high-quality study, is clearly imaged. The digital mammogram breast-air interface is a common site of artifacts from post-processing edge enhancement. The skin-air-glandular tissue interface is sharp and distinct, and lacks the India-ink artifact of post-processing.

References

1. Oduko, J.M. Young, K.C., Burch, A.,: A Survey of Patient Doses from Digital Mammography Systems in the UK in 2007 to 2009. *Digital Mammogr.* 2010;2:365-370.
2. Baldelli P, et al, Comprehensive dose survey of breast screening in Ireland. *Radiation Protection Dosimetry.* 2010;145:52-60.
3. Leitz W, Almén A. Patientdoser från röntgenundersökningar i Sverige – utveckling från 2005 till 2008. Strålsäkerhetsmyndigheten. <http://www.stralsakerhetsmyndigheten.se/publikationer/rapport/stralskydd/2010/201014/>. SSM 2010-14, ISSN 2000-0456. Accessed October 9, 2012.
4. White paper. Comparison of Dose Levels in a National Mammography Screening Program, Philips Healthcare.
5. Sectra microdose mammography. Highest image quality, Half the radiation. 2010.
6. Åslund M, Cederström B, Lundqvist M, Danielsson M. Scatter rejection in multi-slit digital mammography. *Medical Physics.* 2006;33:933-940.
7. Baldelli P, McCullagh J, Phelan, N, Flanagan F. Comprehensive dose survey of breast screening in Ireland. *Radiation Protection Dosimetry.* 2012;145:52-60.
8. Philips MicroDose mammography system, technical data sheet, US/Canada. 2012.
9. Cole EG, Toledano AY, Lundqvist M, Pisano ED. Comparison of radiologist performance with photon-counting full-field digital mammography to conventional full-field digital mammography. *Acad Radiol.* 2012;19:916-922.

* The actual result of the average dose reduction will vary based on variations of digital mammography systems.¹

Clinical Case

Breast cyst and dermal calcification

Raymond Tu, MD

Dr. Tu is Chairman, Department of Radiology, Not-For-Profit Hospital Corporation dba United Medical Center, Washington, DC; Partner at Progressive Radiology, Falls Church, VA; and Clinical Associate Professor of Radiology, The George Washington University School of Medicine and Health Sciences, Washington, DC.

Case summary

A 46-year-old woman presented for evaluation of a breast mass.

Diagnosis

Breast cyst and dermal calcification

Imaging findings

The initial mammogram (Figure 1) identified a focal asymmetry, which was evaluated by sonography and determined to be a cyst. Calcifications at the inferomedial quadrant were compressed and a repeat tangential view (Figure 2) identified the calcifications to be benign, with no evidence of malignancy BI-RADS 2 (arrows).

Discussion

Small dermal calcifications may be confused with malignant calcifications. Their location on

the skin surface rather than within the breast is key to proper diagnosis.¹ Dermal calcifications are benign and should not be confused with malignancy.

Conclusion

Despite findings of a focal asymmetry in the initial mammogram, a repeat tangential view, acquired on a MicroDose digital mammographic system, identified the calcification as a dermal calcification and, therefore, benign, concluding that there was no evidence of malignancy BI-RADS 2.

Reference

1. Geiss CS, Raza S, Birdwell RL. Continuing medical education: Distinguishing breast skin lesions from superficial breast parenchymal lesions: Diagnostic criteria, imaging characteristics, and pitfalls. *Radiographics*. 2011;31:1959-1972; doi:10.1148/rg.317115116.

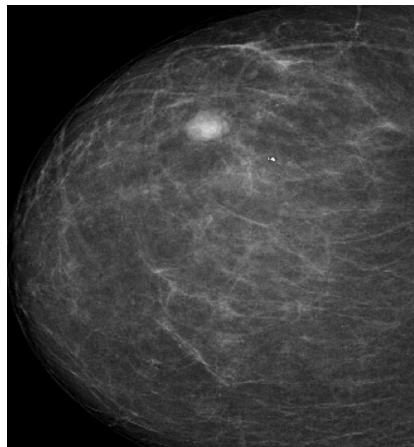


FIGURE 1. An initial mammogram identified a focal asymmetry. Sonography later determined it to be a cyst.

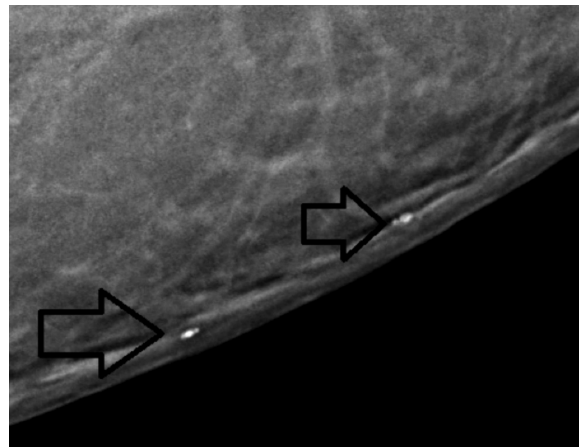
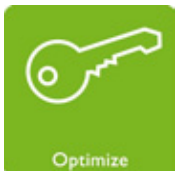


FIGURE 2. A repeat tangential view mammogram showed the calcifications to be benign.



Optimize



Enhance



Transform

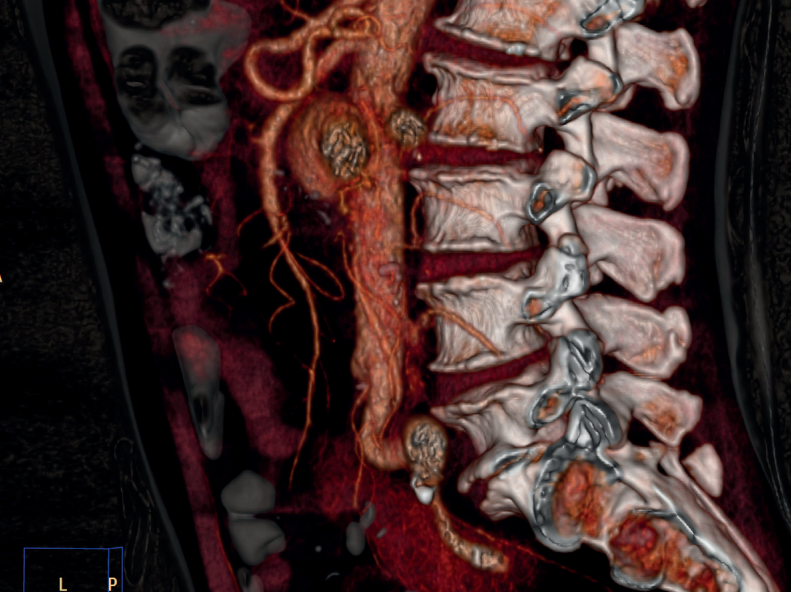
Optimize, enhance, transform.

At Philips Healthcare, we want to collaborate with you throughout the life of your system, from initial investment through replacement. Philips SmartPath provides you with solutions and innovations for your medical imaging, so you can boost your clinical and operational potential and achieve your organizational goals.

Maintain optimal performance over the long term.
Enhance your clinical capabilities and ways of working.
Transform your facility with next-generation solutions.
Let us help you.

Visit www.philips.com/smartpath

PHILIPS
sense and simplicity



Imaging 2.0 – Transforming care, together.

At Philips, we recognize that radiology is the cornerstone of diagnosis and treatment. And that clinical integration and collaboration are key to more personal care, better patient outcomes, and lower costs. Imaging 2.0 signals our endless quest to raise the bar on clinical excellence – by working with you to develop innovations that enable you to collaborate freely, diagnose confidently, and care passionately. Together, we will continue to spark a revolution in imaging science with advanced technologies designed to deliver greater collaboration and integration, increased patient focus, and improved economic value. Learn more at www.philips.com/imaging2.0

PHILIPS